

Dissertation
submitted to the
Combined Faculties for the Natural Sciences and for Mathematics
of the Ruperto-Carola University of Heidelberg, Germany
for the degree of
Doctor of Natural Sciences

presented by

Diplom-Physicist Michael Frewer
born in Windhoek

Oral examination: 17.12.2003

**On a Renormalized QCD-inspired Model
in the Light-cone Formulation**

Referees: Prof. Dr. Hans-Christian Pauli
Prof. Dr. Heinz-Jürgen Rothe

Zusammenfassung

In dem Hamiltonischen Lichtkegelzugang zur QCD wird eine effektive Ein-Teilchengleichung zur Beschreibung von Mesonen mit verschiedenen Quark- und Antiquark-flavor auf ein stark vereinfachtes Modell heruntergebrochen. Dieses Modell dient als Ausgangspunkt, eine explizite Renormierung in einem nicht-perturbativen Rahmen zu studieren. In numerischer, sowie in konzeptioneller Hinsicht, wird dies anhand von zwei grundverschiedenen Renormierungsverfahren demonstriert, die beide letztendlich dieselben physikalischen Ergebnisse liefern. Das entsprechende renormierte Quarkpotential kann für kleine relative Distanzen dahingehend beliebig gewählt werden, dass eine gewisse Freiheit in der Auswahl der Regulierungsfunktion für grosse Impulse existiert. Fernab dieses Bereiches zeigt das Potential ein universelles Coulombverhalten. Benutzt man diese Freiheit bei kleinen Distanzen in dem man fordert, dass es zum Beispiel wie ein harmonisches Potential beginnen soll, so bleibt ihm keine andere Wahl, als eine Barriere in der Streuregion zu formen, um dem asymptotischen Coulombteil des Quarkpotentials folgen zu können. Dieser Mechanismus ermöglicht es Confinement zu sehen. Das renormierte Modell wird anschliessend im Impulsraum gelöst. Das dadurch berechnete Massenspektrum der Mesonen wird dann mit den experimentell gemessenen Werten verglichen.

Ein grosser Teil dieser Arbeit befasst sich mit der Berechnung von Resonanzen im stationären Bild, sowie der Coulombstreuung im Impulsraum. Diese Problematik wird als eigenständiges Kapitel im Anhang dargestellt.

Abstract

In the Hamiltonian light-cone approach to QCD an effective one-body equation for describing mesons with different quark and anti-quark flavor is broken down to an oversimplified model. This model serves as a platform to study explicit renormalization in a non-perturbative context. Two numerically and conceptually totally different renormalization schemes are used to demonstrate this, where at the end, both yield the same physical results. The corresponding renormalized quark potential is arbitrary for small relative distances, in the sense that there is a freedom in choosing the regulating functions for large momenta. Far beyond this region the potential is showing a universal Coulomb behaviour. Using the arbitrariness at small distances, by requiring it for example to start off as a pure harmonic oscillator potential, it inevitably forms a barrier in the scattering region in order to catch up with the asymptotic Coulomb part of the quark potential. This mechanism allows to see confinement. The renormalized model is then solved in momentum space by calculating its mass spectrum. These are then compared with the experimental measured values.

A large part of this thesis is dedicated to the calculation of resonances in the stationary picture, as well as Coulomb scattering in the troublesome representation of momentum space. This difficulty is represented as a stand-alone section in the appendix.

CONTENTS

Contents

| | | |
|----------|--|-----------|
| 1 | Introduction | 3 |
| 2 | Basics | 9 |
| 2.1 | Instant frame | 10 |
| 2.2 | Light-cone frame | 11 |
| 2.2.1 | Boost transformations | 13 |
| 2.2.2 | Vacuum | 14 |
| 2.2.3 | Bound states and Light-cone wave functions | 15 |
| 3 | The QCD-inspired Model | 19 |
| 4 | Explicit Renormalization | 25 |
| 4.1 | Renormalization by a counterterm | 25 |
| 4.2 | T-matrix renormalization | 28 |
| 4.3 | Numerical evaluation | 32 |
| 4.4 | Comparing renormalization schemes | 33 |
| 5 | The Renormalized Singlet-Triplet (ST)-model | 35 |
| 5.1 | Triplet potential | 36 |
| 5.2 | Singlet potential | 39 |
| 5.3 | Numerical solution | 39 |
| 5.4 | Comparing with experiment | 44 |
| 6 | Summary and Discussion | 51 |
| A | Relativistic Dynamics | 53 |
| B | Light-front QCD | 61 |
| B.1 | Effective Hamiltonian | 66 |
| B.2 | Regularization | 76 |
| C | Spinor Matrix | 79 |
| D | Potential Scattering | 81 |
| D.1 | Potentials of finite range | 82 |
| D.1.1 | Formal stationary scattering solution | 82 |
| D.1.2 | Stationary scattering in the coordinate space picture | 87 |
| D.1.3 | S-wave scattering on potentials with a strict range R | 93 |
| D.1.3.1 | Square-well potential | 102 |
| D.1.3.2 | Oscillator-well potential | 105 |
| D.1.3.3 | Coulomb-well potential | 106 |
| D.1.3.4 | Step-well potential | 107 |
| D.1.3.5 | Step+Coulomb-well potential | 110 |
| D.1.4 | S-wave scattering on potentials with an effective range R_{eff} | 111 |

CONTENTS

| | | |
|----------|---|------------|
| D.2 | Coulomb scattering | 113 |
| D.2.1 | Pure Coulomb potential | 113 |
| D.2.2 | Coulomb-like potentials | 116 |
| D.2.3 | Step-well plus attractive Coulomb potential | 119 |
| E | Numerics in Momentum Space | 123 |
| E.1 | Bound state domain | 123 |
| E.2 | Scattering domain | 129 |
| F | Meson Summary Tables | 133 |

1 Introduction

The nature of elementary particles calls for a synthesis of relativity and quantum mechanics. The necessity of a quantum treatment is quite evident in view of the microscopic scales involved which are several orders of magnitude smaller than in atomic physics. These very scales, however, also require a relativistic formulation. A typical hadronic scale of 1fm, for instance, corresponds to momenta of $p \sim \hbar c/1\text{fm} \sim 200\text{MeV}$. For particles with masses $M < 1\text{GeV}$, this implies sizeable velocities $v \sim p/M > 0.2c$. It turns out that the task of unifying the principles of quantum mechanics and relativity is not a straightforward one (Appendix A). A natural solution is provided by covariant quantum field theory.

As we well know, there are two distinct ways of how to approach a quantum field theory. On the one hand, there is Feynmans action based path-integral method which is a manifestly covariant formulation. On the other hand, we have the Hamiltonian method, which obviously from the outset is not a manifestly covariant formulation, as it singles out a time t or an energy E , respectively. The concept of *relativistic Hamiltonian dynamics* needs to be properly defined. This leads to the famous paper by Dirac [1], where he introduced three distinct forms of Hamiltonian dynamics. Later two more forms of dynamics were described by Leutwyler and Stern [2], bringing the total number to five. So, there is a fivefold ambiguity to relativistic Hamiltonian dynamics.

Hamiltonian formulations of field theory are not immediately recognized as equivalent to the Feynman way. They rather have to be seen as complementary approaches. After more than a half century of development it is clear that the Feynman approach has many advantages if one deals with problems that may be solved by perturbative methods, while the Hamiltonian formulation represents a more natural approach towards bound-states, which need to be described in a non-perturbative context. Also, the questions concerning the regulation of divergent integrals appearing in the naive application of the Feynman rules have been answered in various ways and the program of renormalization was successfully carried out for almost all interesting field theories, while non-perturbative problems that are to be solved by diagonalization of the Hamiltonian, make the renormalization program a very hard issue to deal with.

The main question we face in the Hamiltonian approach is, which of the five forms of dynamics mentioned above is more suited to describe the problem of bound-states. One consideration comes to mind immediately: the Fock-state expansion is in principle different for the various forms of dynamics, as its terms are not invariant. Therefore the investigation of an expansion in Fock space must be an issue. The ones mostly used in practice is the usual instant form and the front form. The latter is argued to be the most suitable as the vacuum is particularly simple in this form. (Section 2) will investigate further details, in order see the advantages and disadvantages of each form respectively.

This thesis will deal with the fundamental gauge field theory of QCD, the theory of strong interactions, which has the hadrons as its physical degrees of freedom.

Like its older relative QED, QCD is a renormalizable relativistic quantum field theory. Any infinities arising from the point-like (local) nature of the interaction can therefore

1. Introduction

be consistently absorbed into a redefinition of the physical parameters like masses and couplings. As a result, the strong coupling parameter α_s is not a constant but is running with the typical momentum scale of the physical process under consideration. The microscopic reason for this are vacuum polarization effects: quarks screen and therefore weaken the color charge (analogous to QED), whereas the self-interacting gluons anti-screen the color charge which is the dominating effect. Unlike QED, therefore, the running coupling $\alpha_s(Q)$ of QCD is weak for high momentum transfer Q (small distances). This is the realm of ‘asymptotic freedom’ where perturbative methods work. For small momentum transfer Q (large distances), the coupling is large, perturbation theory breaks down, and one has to utilize non-perturbative methods. A typical and well-established value [3] for α_s is

$$\alpha_s(M_Z) = \alpha_s(91.2\text{GeV}) = 0.118, \quad (1.1)$$

where M_Z is the mass of the Z-Boson. The non-perturbative domain is generally accepted at a maximum momentum scale of approximately 1GeV. In some loose sense one can therefore speak of two relevant phases of QCD, the weak coupling phase or perturbative QCD at $Q > 1\text{GeV}$, and the strong coupling phase or non-perturbative QCD at $Q < 1\text{GeV}$.

Let us now focus on the hadrons. In principle, it is quite clear, what a hadron is in QCD: it is an eigenstate of the QCD Hamiltonian,

$$H_{\text{QCD}}|\text{Hadron}\rangle = M|\text{Hadron}\rangle, \quad (1.2)$$

where M denotes the hadron mass. The question, of course, is, whether this ‘QCD Schrödinger equation’ can be solved. If we consider a typical hadronic scale like the nucleon radius of 1fm, the associated energy is of about 200MeV. This number tells us that we are in the low-energy regime which implies that the binding of the quarks into hadrons is a non-perturbative phenomenon. In other words, a perturbative solution of the ‘QCD Schrödinger equation’ will make no sense in general.

There are two main routes out of this dilemma. Firstly, one can try to perform brute-force calculations which involve sophisticated computer simulations on the largest machines available. Technically, one can make use of a space-time discretization leading to lattice gauge theory in the Hamiltonian instant form, or of 3-momentum discretization leading to DLCQ (Discretized Light Cone Quantization) in the Hamiltonian front form. Secondly, one can rely on a reputable tradition of physics, namely model building. There is an abundance of hadron models on the market, the most popular one being the constituent quark model of [4] and variants thereof. There one mostly starts with a non-relativistic phenomenological Hamiltonian of the form

$$H = H_0 + V_{\text{conf}}, \quad (1.3)$$

with an ad-hoc confining potential V_{conf} which typically is proportional to the inter-quark distance r or sometimes even to r^2 . The Hamiltonian describes the dynamics of two or three constituent quarks with their effective masses being treated as parameters. The main virtue of the model consists in its rather accurate reproduction of the hadron

1. Introduction

masses ('spectroscopy'). However, the model has severe shortcomings. Firstly, nearly all hadrons are relativistic bound-states and therefore a non-relativistic treatment is not appropriate. Secondly, the relation of the model with QCD is rather unclear. In other words, it is unclear how a constituent picture can arise in a relativistic quantum field theory such as QCD. There one expects a bound state, like for example the pion, to be of the form

$$|\pi\rangle \sim \psi_1|q\bar{q}\rangle + \psi_2|q\bar{q}g\rangle + \psi_3|q\bar{q}q\bar{q}\rangle + \dots . \quad (1.4)$$

This means that hadrons are states containing an infinite number of quarks and gluons, which is consistent with the results of DIS (Deep Inelastic Scattering) experiments where, with growing resolution Q^2 , an increasing number of partons is observed. This confirms that there are non-vanishing amplitudes ψ_1, ψ_2, \dots to find two quarks, two quarks and a gluon, in general to find an arbitrary number of quarks and gluons in a hadron.

Our basic motivation is to do better, to construct a model which can avoid these shortcomings. In this thesis it leads us to the Singlet-Triplet (ST)-model [5] or to the more simplified $\uparrow\downarrow$ -model [6] of (Section 3). They are designed to describe only flavor off-diagonal mesons — mesons with different flavor for quark and anti-quark. Its derivation in (Appendix B) can be summarized as follows: Outgoing from the QCD-Lagrangian in light-cone coordinates, it is possible to construct a frame-independent bound-state equation for the invariant mass-squared M^2 of a meson. To solve this equation, one is confronted, as already mentioned, with the primer difficulties of every field theory, the many-body problem and the divergencies to be regulated and then to be renormalized. The first problem is attacked by constructing an effective bound-state equation having the same eigenvalue spectrum as its original equation — the simplest one is an effective one-body equation, where its Hamiltonian is acting only in the lowest Fock-space component, that between one quark and one anti-quark via an effective one gluon exchange. The technique used for the derivation is called iterated resolvents [7], which does not truncate the relevant Fock space but rather is a compact notation for resumming perturbative diagrams to all orders without double counting, and thus maintaining all symmetries of the QCD-Lagrangian. The effect is a projection of higher Fock-space sectors to lower ones, where at the end all sectors can be systematically retrieved by iteration from the lowest one. The second problem is solved by multiplying each matrix element of the Hamiltonian with a convergence enforcing vertex function, which has to drop faster than $1/Q^2$. This will regulate the ultraviolet divergencies caused by the transverse momenta. Light front dynamics contain additional singularities, so called 'longitudinal' ones, caused by longitudinal momenta close to zero. These infrared singularities are controlled by giving the gauge boson a small regulator mass. The result is a regulated effective one-body equation [7] carrying unphysical parameters. As usual, these have to be renormalized.

The renormalization program is one of the main topics of this thesis (Section 4). Breaking this effective one-body equation down to the $\uparrow\downarrow$ -model, by simplifying the spin-interaction as well as by making a non-relativistic simplification, it is, to our knowledge, for the first time possible to explicitly see how renormalization works in a Hamiltonian

1. Introduction

formulation. This will be done by comparing two drastically different renormalization schemes, both conceptually and numerically, and verify that they agree. This strong statement stands at the very basis of renormalization ideas, that no matter the intermediate steps one performs to mathematically define the initial undefined theory, after renormalization all of them produce the same physics. Since both renormalization schemes have been implemented in momentum space, the generalization to the full relativistic case can be easily performed. Also going from the $\uparrow\downarrow$ -model to the ST-model is a trivial task.

Subject of (Section 5) is now to solve this renormalized ST-model in momentum space. The corresponding equation has the structure of a local non-relativistic Schrödinger equation. With the appropriate tools at hand, it is possible to solve this equation numerically and to fit the data according to the experimental mass spectrum of flavor-off diagonal mesons. No other good reason than simplicity we will only focus on spherical s-wave solutions. Since the solutions are calculated in momentum space, the generalization to get the full relativistic solutions is not accompanied with conceptual problems, except maybe for some numerical difficulties.

If we look more closely at the renormalized quark potential of the ST-model, it is possible to see confinement. It came as a big surprise to us, that not the renormalized coupling constant $\bar{\alpha}_s(Q)$ accounts for confinement, but rather the arbitrariness of the external vertex regulator. Since the potential is of local nature we can make us a picture in coordinate space by Fourier transformation. The arbitrariness of the potential then only lies within small distances r , while asymptotically it always behaves as $-1/r$. This behaviour is universal and applies to all possible regulators. It is fully in accord with the regularization scheme given in momentum space: the arbitrariness of regularizing a systems high momenta or energies leads to an arbitrariness in the behaviour at small distances. Inspired by [8], which again was inspired by the work of [9], we use this arbitrariness in the potential for small r , by requiring it to behave as a pure harmonic oscillator potential. The connection between the oscillator behaviour for small r and the Coulomb behaviour for large r is accomplished by a barrier as it is known from nuclear physics. The potential is thus able not only to create pure bound-states but also resonances. When fixing the parameters to a physical example, the quark potential develops a barrier of such an extraordinary height and width, that possible resonances can be well treated as bound-states. This justifies to see the barrier as part of a confining potential.

A rather large part of this thesis is dedicated to Coulomb scattering and the calculation of resonances in the stationary picture. The motivation was to solve the scattering region and with it the resonance part of the above ST-potential. Furthermore, the aim was to solve the scattering problem in momentum space, in order to establish an easy generalization to the full relativistic case. But this inevitably leads to the problem of having Coulomb scattering in momentum space, which is far more difficult to realize than in coordinate space. There one knows how to treat the logarithmic divergent phase-shift: one consistently changes the boundary conditions from pure plain waves to distorted waves, leading then to a well defined space independent phase-shift. In

1. Introduction

momentum space such a construction is not straightforward, or even impossible to implement. Also a simple Fourier transformation from coordinate space to momentum space does not do the work, since the Coulomb scattering wave functions in momentum space are not functions in the usual sense, they behave more like distributions [10]. Furthermore, the Coulomb T-matrix in momentum space is not well defined, it can lead to anomalies [11].

To solve the full problem, one has to search for alternatives, which still is a subject of research [10]. On the other hand, I can show within s-wave scattering, that if the Coulomb part of any potential is changed to a more well defined scattering potential in the asymptotic region, with the rest of the potential being kept unchanged, it only has an effect on the global background but not on the local resonance structure in the cross-section of a scattering experiment. And since we are at first only interested in the calculation of resonances and since asymptotical Coulomb shielding is easy tractable in momentum space, this technique serves as a partial solution to the full Coulomb scattering problem in momentum space.

Regrettably, these ideas could not be studied at a physical example of the ST-model. As already mentioned, the corresponding potential produces resonances of an extreme small width, making it impossible to resolve them in a numerical scattering calculation. One thus has to content oneself with more or less academic potentials. Nevertheless, since these potentials allow for an analytical calculation of all relevant scattering quantities, they serve as test potentials for investigating the correctness and the stability of our numerical codes, which have been worked out in momentum space. These examples were also chosen such, that they resemble the basic structures of any potential like that of the ST-potential.

All this is represented consistently and apart from the main text in (Appendix D).

2 Basics

The usual way to describe a physical system is to take a snapshot at a certain time $t = t_0$ and see how the system evolves as time goes by. Quite in general we have seen in (Appendix A) that the Hamiltonian or energy operator $H = P_0$ is the operator which propagates the system in time

$$H|\Psi(t)\rangle = i\frac{\partial}{\partial t}|\Psi(t)\rangle. \quad (2.1)$$

Requiring a trivial time dependence

$$|\Psi(t)\rangle = e^{-iEt}|\Psi\rangle, \quad (2.2)$$

is asking for a *stationary state*

$$H|\Psi\rangle = E|\Psi\rangle, \quad (2.3)$$

which is the solution of an eigenvalue problem to the energy eigenvalue E , which again is a number. Thus, the Hamiltonian method seems to be a promising method for calculating bound states within a quantum field theory, having infinitely many degrees of freedom. From a covariant point of view, where the four space-time coordinates are treated on an equal footing, it seems a little bit artificial to choose the time axis as the zeroth component $t = x^0$ from the four space-time dimensions as the axis which defines the direction of evolution. One could as well choose one of the three space axes to play this role, or even some other direction. In general one can define ‘space’ as that hypersphere in four-space on which one chooses the initial conditions. The remaining fourth coordinate can be understood as ‘time’. These concepts of space-time parametrizations can be grasped more formally by introducing some general coordinate transformation $\tilde{x}(x)$. However, one should exclude those which are accessible through Poincaré transformations, that means pure Lorentz boosts, spatial rotations and translations. Since any coordinate transformation conserves the geometrical arc-length $ds^2 = g_{\mu\nu}dx^\mu dx^\nu = \tilde{g}_{\kappa\lambda}d\tilde{x}^\kappa d\tilde{x}^\lambda$, the metric tensors for two parametrizations are then related by

$$\tilde{g}_{\kappa\lambda} = \left(\frac{\partial x^\mu}{\partial \tilde{x}^\kappa}\right) g_{\mu\nu} \left(\frac{\partial x^\nu}{\partial \tilde{x}^\lambda}\right). \quad (2.4)$$

Three things are important to note. First, the physical content of a theory can not depend on such re-parametrizations of space-time, after all we are just dealing with different coordinate systems. Second, in generalized coordinates the covariant and contravariant indices can have rather different interpretations, and one has to be careful with the lowering and rising of Lorentz indices. Third, following Dirac [1] and Leutwyler [2] there are no more than five different parametrizations of space-time. Each of them thus have different ‘times’ and different ‘Hamiltonians’. Interesting for us are only the following two forms of Hamiltonian dynamics: the usual instant form, with its hypersphere given by $t = 0$, and the front form, where the hypersphere is a tangent plane to the light cone.

2. Basics

2.1 Instant frame

If the Hamiltonian $H = P_0$ was derived from a covariant quantum field theory, as we now always want to assume, it must represent a constant of motion in that system. Not only the Hamiltonian, but all 10 independent Poincaré generators (Appendix A) must be constants of motion:

$$M_{\mu\nu} = \begin{pmatrix} 0 & -K_1 & -K_2 & -K_3 \\ K_1 & 0 & -J_3 & J_2 \\ K_2 & J_3 & 0 & -J_1 \\ K_3 & -J_2 & J_1 & 0 \end{pmatrix} ; \quad P_\mu = \begin{pmatrix} H \\ -\vec{P} \end{pmatrix}, \quad (2.5)$$

where P_i are momentum, K_i the pure Lorentz boost and J_i the spatial rotation operators. All these operators satisfy the Poincaré algebra. Since the Hamiltonian formulation of a quantum field theory fixes its description on the energy operator H , a special role will be played by those operators which commute with H . Such operators are said to be kinematical operators. They are conserved in the sense that they map the initial condition hypersurface onto itself, that means the system stays in its initial state. The other operators which do not commute with the Hamiltonian will map a given hypersurface into another hypersurface, meaning that the initial state of a system is changed and thus are said to be dynamical operators. The commutation relations between the Hamiltonian $H = P_0$ and the remaining Poincaré operators are

$$\begin{aligned} [H, P_1] &= 0, & [H, J_1] &= 0, & [H, K_1] &= iP_1, \\ [H, P_2] &= 0, & [H, J_2] &= 0, & [H, K_2] &= iP_2, \\ [H, P_3] &= 0, & [H, J_3] &= 0, & [H, K_3] &= iP_3. \end{aligned} \quad (2.6)$$

We see that six operators, the spatial translation and rotation operators are kinematic operators. While the Lorentz boosts are of dynamical nature. They are part of the interaction. Since $P^\mu P_\mu = M^2$ is a Casimir operator commuting with all generators of the Poincaré group, the stationary state condition (2.3) in the instant form can also be written as

$$H|\Psi\rangle = \sqrt{M^2 + \vec{P}^2}|\Psi\rangle, \quad (2.7)$$

where M^2 is the invariant mass of the system. Lets say the stationary state was fixed by some initial condition $|\Psi\rangle = |\Psi(t_0)\rangle$ and has been determined in its rest system ($\vec{P} = 0$). Translating or rotating this eigensolution would not have any effect on the previous fixed initial condition of the state, it still represents the same stationary state. But if we try to boost the eigensolution into a frame where $\vec{P} \neq 0$, the state is changed in the sense that it now represents a different stationary state corresponding to a new initial condition $|\Psi'\rangle = |\Psi(t_1)\rangle$. Thus determining the boosted wavefunction is as complicated as diagonalizing H itself. This is also the reason, why we do not denote quantum states in the instant form by the eigenvalues of boost operators.

2. Basics

2.2 Light-cone frame

In the light-cone frame we use the new time $t = x^+ = x^0 + x^3$ in the Lepage-Brodsky (LB) convention [12] as the coordinate which evolves the physical system to the future. The other coordinates are chosen to ensure orthogonality. The transformation from the instant to the light-cone coordinates

$$(x^0, x^1, x^2, x^3) \longrightarrow (x^+, \vec{x}_\perp, x^-), \quad (2.8)$$

is then given by

$$x^+ = x^0 + x^3, \quad \vec{x}_\perp = (x^1, x^2), \quad x^- = x^0 - x^3. \quad (2.9)$$

This transformation can also be written as

$$\tilde{x}^\mu = C^\mu_\nu x^\nu, \quad \text{with} \quad C^\mu_\nu = \left(\frac{\partial \tilde{x}^\mu}{\partial x^\nu} \right) = \begin{pmatrix} 1 & 0 & 0 & 1 \\ 0 & 1 & 0 & 0 \\ 0 & 0 & 1 & 0 \\ 1 & 0 & 0 & -1 \end{pmatrix}. \quad (2.10)$$

The metric tensor (2.4) then becomes

$$\tilde{g}_{\mu\nu} = \begin{pmatrix} 0 & 0 & 0 & \frac{1}{2} \\ 0 & -1 & 0 & 0 \\ 0 & 0 & -1 & 0 \\ \frac{1}{2} & 0 & 0 & 0 \end{pmatrix} = (C^{-1})^T \cdot g \cdot C^{-1}, \quad (2.11)$$

with its inverse given by

$$\tilde{g}^{\mu\nu} = \begin{pmatrix} 0 & 0 & 0 & 2 \\ 0 & -1 & 0 & 0 \\ 0 & 0 & -1 & 0 \\ 2 & 0 & 0 & 0 \end{pmatrix} = C \cdot g \cdot C^T. \quad (2.12)$$

The covariant components of any light-cone 4-vector are then defined by $\tilde{x}_\mu = \tilde{g}_{\mu\nu} \tilde{x}^\nu$. The entries 1/2 in the off-diagonal part of the metric tensor imply a slightly unusual scalar product

$$a \cdot b = \tilde{g}_{\mu\nu} a^\mu b^\nu = \frac{1}{2} a^+ b^- + \frac{1}{2} a^- b^+ - a^i b^i. \quad (2.13)$$

The contravariant Poincaré generators on the light-cone can be determined as

$$(\tilde{P}^\mu) = C \cdot (P^\mu), \quad (\tilde{M}^{\mu\nu}) = C \cdot (M^{\mu\nu}) \cdot C^T, \quad (2.14)$$

which give the covariant ones as

$$(\tilde{P}_\mu) = \tilde{g} \cdot (\tilde{P}^\mu) \quad (\tilde{M}_{\mu\nu}) = \tilde{g} \cdot (\tilde{M}^{\mu\nu}) \cdot \tilde{g}^T \quad (2.15)$$

$$= (C^{-1})^T \cdot (P_\mu), \quad = (C^{-1})^T \cdot M_{\mu\nu} \cdot C^{-1}. \quad (2.16)$$

Since all relevant quantities on the light-cone have been determined, we can suppress the tilde-symbol and simply refer to them as light-cone objects.

2. Basics

In this sense the covariant Poincaré generators on the light-cone are explicitly given as

$$M_{\mu\nu} = \begin{pmatrix} 0 & -B_1 & -B_2 & \frac{1}{2}K_3 \\ B_1 & 0 & -J_3 & S_1 \\ B_2 & J_3 & 0 & S_2 \\ -\frac{1}{2}K_3 & -S_1 & -S_2 & 0 \end{pmatrix} ; \quad P_\mu = \begin{pmatrix} \frac{1}{2}(P^0 - P^3) \\ -\vec{P}_\perp \\ \frac{1}{2}(P^0 + P^3) \end{pmatrix}, \quad (2.17)$$

where we defined

$$B_1 = \frac{1}{2}(K_1 + J_2), \quad B_2 = \frac{1}{2}(K_2 - J_1), \quad S_1 = \frac{1}{2}(K_1 - J_2), \quad \text{and} \quad S_2 = \frac{1}{2}(K_2 + J_1).$$

In analogy to the definition of the Hamiltonian H in the instant frame we define the Hamiltonian H in the light-cone frame as that operator whose action on the state $|\Psi(t)\rangle$ has the same effect as taking the partial derivative with respect to the light-cone time $t = x^+$

$$H|\Psi(x^+)\rangle = i\frac{\partial}{\partial x^+}|\Psi(x^+)\rangle. \quad (2.18)$$

Therefore in the light-cone frame the Hamiltonian is given by

$$H = P_+ = \frac{1}{2}P^-. \quad (2.19)$$

Using the Poincaré algebra (Appendix A), we can derive the commutation relations between this Hamiltonian and the remaining generators

$$\begin{aligned} [H, P_1] &= 0, & [H, S_1] &= iP_1, & [H, B_1] &= 0, \\ [H, P_2] &= 0, & [H, S_2] &= iP_2, & [H, B_2] &= 0, \\ [H, P_-] &= 0, & [H, J_3] &= 0, & [H, K_3] &= iH. \end{aligned} \quad (2.20)$$

The obvious kinematical operators are the three light-cone momenta P_1, P_2, P_- , the longitudinal rotation J_3 and the light-cone boosts B_1, B_2 . However, although K_3 does not commute with the Hamiltonian, its behaviour is special because the commutator $[H, K_3]$ is proportional to H . This has consequences. Suppose we boost the Hamiltonian H in the longitudinal direction

$$H \longrightarrow e^{i\eta K_3} H e^{-i\eta K_3}, \quad (2.21)$$

then the Baker-Campbell-Hausdorff relation can be used to derive

$$\begin{aligned} e^{i\eta K_3} H e^{-i\eta K_3} &= H + i\eta[K_3, H] + \frac{1}{2}(i\eta)^2[K_3, [K_3, H]] + \dots \\ &= H + \eta H + \frac{1}{2}\eta^2 H + \dots = e^\eta H. \end{aligned} \quad (2.22)$$

Obviously, application of the operator K_3 changes H only by a factor. Or, in other words, if we boost the system in the longitudinal direction, the energy eigenvalues are just multiplied by a constant scaling factor e^η . Because of this special behaviour, K_3 is usually called kinematical instead of dynamical. As a result the light-cone frame offers 7 out of 10 kinematical Poincaré generators, compared to 6 kinematical generators in the instant frame. The only dynamical operators besides the Hamiltonian are the two transverse rotations S_1 and S_2 . Therefore, by going from the instant to the light-cone frame, the problem of dynamical operators is shifted from boost to transverse rotation.

2. Basics

2.2.1 Boost transformations

Two of the most important kinematic symmetries in light-front field theory are the longitudinal and transverse boost symmetries. For this, we want to have a closer look into the boost transformation properties of the longitudinal P^+ and transverse \vec{P}_\perp momenta. As we will show, the longitudinal boost corresponds to a rescaling on the light-front whereas the transverse boosts simply are Galilean boosts in two dimensions in non-relativistic dynamics. The relevant commutation relations are given by

$$[B^i, P^j] = -i\delta^{ij}P^+ \quad ; \quad [K^3, P^+] = -iP^+. \quad (2.23)$$

If we boost as follows

$$P^+ \rightarrow e^{i\eta_3 K^3} P^+ e^{-i\eta_3 K^3} \quad ; \quad \vec{P}_\perp \rightarrow e^{i\eta_i B^i} \vec{P}_\perp e^{-i\eta_i B^i}, \quad (2.24)$$

and use the relation as in (2.22), we obtain the fundamental result

$$P^+ \rightarrow e^{\eta_3} P^+ \quad ; \quad \vec{P}_\perp \rightarrow \vec{P}_\perp + \vec{\eta}_\perp P^+. \quad (2.25)$$

We see that a general boost $B_\perp = \eta_1 B^1 + \eta_2 B^2$ in the transverse plane acts just like a two dimensional Galilean boost in non-relativistic dynamics. P^+ can be interpreted as a variable Galilei mass.

One thus expects that light-cone kinematics will partly show a non-relativistic behaviour. This expectation is indeed realized and leads, for instance, to a separation of center-of-mass and relative dynamics as in non-relativistic many-body systems. This is important for constructing a proper scattering theory within a quantum field theory, which is impossible to do in the instant frame. But also for the calculation of bound states, this decoupling of center-of-mass and internal motion is of tremendous help.

We can now ask the question how to boost from one momentum set (\vec{P}_\perp, P^+) to another set (\vec{Q}_\perp, Q^+) . This can be done by fixing the boost parameters η_3 and $\vec{\eta}_\perp$ as

$$\eta_3 = \ln \frac{Q^+}{P^+} \quad ; \quad \vec{\eta}_\perp = \frac{\vec{Q}_\perp - \vec{P}_\perp}{P^+}. \quad (2.26)$$

Obviously, this is only possible for $P^+ \neq 0$. We emphasize that in this construction there is no dynamics involved. This means that we can build states of arbitrary light-cone momenta with very little effort. All we have to do is applying some kinematical boost operators. The simple behavior of light-cone momenta under boosts will be important for the discussion of bound states. For instance they lead to frame independence in the Fock state wave functions.

2. Basics

2.2.2 Vacuum

Here is another advantage of light-front dynamics: the simplicity of the vacuum. The physical vacuum is defined as that Hilbert space state $|0\rangle$ which is invariant under Poincaré transformations (Appendix A)

$$U(\Lambda, a)|0\rangle = |0\rangle, \quad (2.27)$$

implying

$$P^\mu|0\rangle = 0 \quad \text{and} \quad M^{\mu\nu}|0\rangle = 0. \quad (2.28)$$

In other words $|0\rangle$ is that state for which the eigenvalues of the *conserved* operators P^μ and $M^{\mu\nu}$ are zero. Focusing only on positive energy states, that means on *massive physical* systems with $(P^2, P^-) > 0$ the above fixing of the physical vacuum turns into

$$P^+|0\rangle = 0 \quad ; \quad \vec{P}_\perp|0\rangle = 0 \quad \text{and} \quad M^{\mu\nu}|0\rangle = 0. \quad (2.29)$$

Since the Hamiltonian $H \sim P^- > 0$ is chosen to be a positive operator of having only positive eigenvalues, it immediately follows from the invariant mass condition $M^2 = P^2$, which on the light cone can be written as $P^-P^+ = M^2 + \vec{P}_\perp^2$, that the longitudinal momentum $P^+ > 0$ must be a positive operator too. Furthermore, this positivity is guaranteed for all times, since P^+ represents a conserved quantity. Then if we exclude $P^+ = 0$, the above condition $P^+|0\rangle = 0$ forces the physical vacuum to be trivial because it is the only state with $P^+ = 0$. In this case the physical vacuum is identical with the free Fock-space vacuum. But if include the so called zero modes with $P^+ = 0$, which can only exist if the system allows for $M = 0$, the light-cone vacuum starts to get complicated again.

Nevertheless, the overall dynamical behaviour of the physical light-cone vacuum is far more simpler than its counter part in the instant form. Only particles with mass zero can be created from the light-cone vacuum, unlike the instant-form vacuum that can create particles with non-vanishing masses, if their momenta sum up to zero. The vacuum in light-front interferes with the dynamic structure to a much lesser extent than in the instant form. In this form, there will exist zero total momentum states with arbitrary constituents which will mix with zero-constituent states to build up the ground state, the physical vacuum in the instant-frame.

So, if we are able to eliminate possible zero modes from a given system, we can say that the physical vacuum state in the light-cone representation is the simple Fock vacuum without any constituents. This is a tremendous simplification. For example, it allows a Fock expansion on this vacuum state which can be used as a basis for representing a general physical state as that of the bound state $|\Psi\rangle$. In other words it immediately allows for a constituent picture in a field theory with infinitely many degrees of freedom.

2. Basics

2.2.3 Bound states and Light-cone wave functions

Since the invariant operator $M^2 = P^\mu P_\mu$ on the light-cone is given as $M^2 = P^- P^+ - \vec{P}_\perp^2$ the stationary state condition (2.3) can be written as

$$H|\Psi\rangle = \frac{M^2 + \vec{P}_\perp^2}{2P^+}|\Psi\rangle. \quad (2.30)$$

Furthermore, since the boost on the light-front only depends on kinematics, we can consider the bound state in the rest frame $(\vec{P}_\perp, P^+) = (\vec{0}_\perp, M)$. Thus, the eigenstate equation simply becomes

$$H|\Psi\rangle = E|\Psi\rangle, \quad (2.31)$$

which is the familiar Schrödinger equation in ordinary quantum mechanics with the eigenvalues $E = M/2$. On the light-front, boosting a bound state from the rest frame to any other frame is dynamically independent and quite simple, as we have shown in (Section 2.2.1). Thus, once we find the bound state in the rest frame, we can completely understand it in any frame. The eigensolutions of the Hamiltonian thus describe bound states of arbitrary four-momentum, allowing the computation of possible scattering amplitudes and other dynamical quantities. As we know, this does not hold in the instant form. Although the bound state equation in the instant rest frame has the same form, the solutions in the rest frame are not easily boosted to other Lorentz frames due to the dynamical dependence of the boost transformations. Therefore, in each different Lorentz frame one needs to solve the bound state equation of P_0 to obtain the corresponding wave functions. This is the reason why one can not establish a reliable approach to construct relativistic wave functions in instant field theory in terms of the Schrödinger picture. This obstacle is obviously removed on the light-front.

As already mentioned in (Appendix A), in both the instant and the front-form the eigenfunctions can be labeled by the eigenvalues of all commuting observables given from space-time symmetry. These are the systems invariant mass M , the three space-like momenta P^+ , \vec{P}_\perp , the total spin-squared S^2 and its longitudinal projection S_z or alternatively its helicity Λ :

$$|\Psi\rangle = |M, P^+, \vec{P}_\perp, S^2, \Lambda, \alpha\rangle. \quad (2.32)$$

In addition, the eigenfunctions can be labeled by quantum numbers α which are not related to any space-time symmetry, like charge or baryon number of the system. In the following we will only maintain the momentum labels and suppress all other quantum numbers. We already know that if possible zero modes can be excluded from the system, the bare Fock vacuum is an eigenstate of the full interacting Hamiltonian. It thus serves as an appropriate ground state on top of which we can build a reasonable Fock expansion. One constructs the complete basis of Fock states $|\mu_n\rangle$ in the usual way by applying products of all possible free field creation operators to the vacuum state $|0\rangle$. All these created particles of the system are on-shell $(p^\mu p_\mu)_i = m_i^2$.

2. Basics

The number of particles is denoted by the index i , while the various Fock-space classes are conveniently labeled with a running index n . Each Fock-state $|\mu_n\rangle = |n : p_i^+, \vec{p}_{\perp i}\rangle$ is an eigenstate of P^+ , \vec{P}_{\perp} and the *free* part of the energy P_0^- , with eigenvalues

$$P^+ = \sum_i p_i^+, \quad \vec{P}_{\perp} = \sum_i \vec{p}_{\perp i}, \quad P_0^- = \sum_i \frac{m_i^2 + p_{\perp i}^2}{p_i^+}. \quad (2.33)$$

To set the stage for the definition of light-cone wave functions, we first introduce some relevant kinematical variables, the *relative* momentum coordinates x_i and $\vec{k}_{\perp i}$ via

$$p_i^+ \equiv x_i P^+, \quad \vec{p}_{\perp i} \equiv x_i \vec{P}_{\perp} + \vec{k}_{\perp i}. \quad (2.34)$$

Thus x_i is the fraction of the total longitudinal momentum that the i -th constituent carries, and $k_{\perp i}$ is its relative transverse momentum with respect to the center-of-mass frame. Comparing with (2.33) we note that these variables have to obey the constraints

$$\sum_i x_i = 1 \quad \text{and} \quad \sum_i \vec{k}_{\perp i} = 0. \quad (2.35)$$

A particularly important property of the relative momenta is their boost invariance. Using (2.25) we easily see that x_i is invariant towards a boost in the longitudinal direction

$$x'_i = e^{\eta_3} p_i^+ / e^{\eta_3} P^+ = x_i, \quad (2.36)$$

while $\vec{k}_{\perp i}$ is invariant towards a general boost in the transverse plane

$$\vec{k}'_{\perp i} = \vec{p}'_{\perp i} - x_i \vec{P}'_{\perp} = \vec{p}_{\perp i} + \vec{\eta}_{\perp} p_i^+ - x_i (\vec{P}_{\perp} + \vec{\eta}_{\perp} P^+) = \vec{k}_{\perp i}, \quad (2.37)$$

which indeed proves the frame independence of x_i and $\vec{k}_{\perp i}$.

Let us now calculate the total free light-cone energy in terms of the relative coordinates. Making use of the constraints (2.35), we obtain

$$\begin{aligned} P_0^- &= \sum_i p_i^- = \sum_i \frac{p_{\perp i}^2 + m_i^2}{p_i^+} = \sum_i \frac{(x_i \vec{P}_{\perp} + \vec{k}_{\perp i})^2 + m_i^2}{x_i P^+} \\ &= \frac{1}{P^+} \left(P_{\perp}^2 + \sum_i \frac{k_{\perp i}^2 + m_i^2}{x_i} \right) \equiv (P_0^-)_{\text{cm}} + (P_0^-)_{\text{r}}. \end{aligned} \quad (2.38)$$

This is another important result: the free light-cone Hamiltonian P_0^- separates into a center-of-mass term,

$$(P_0^-)_{\text{cm}} = P_{\perp}^2 / P^+, \quad (2.39)$$

and a term containing only the relative coordinates,

$$(P_0^-)_{\text{r}} = \frac{1}{P^+} \left(\sum_i \frac{k_{\perp i}^2 + m_i^2}{x_i} \right) = \frac{M_0^2}{P^+}. \quad (2.40)$$

2. Basics

The last identity, which states that $(P_0^-)_r$ is essentially the free invariant mass squared, follows upon multiplying (2.38) by P^+ . This decoupling of center-of-mass and internal motion is associated with the transverse dimensions, and is an indirect consequence of the non-relativistic transformation behaviour of the transverse boosts. These results are in complete contrast to instant form kinematics, where the appearance of the notorious square root in the energy prohibits a similar separation of variables.

Since the Fock states $|\mu_n\rangle$ form a complete set in the sense that

$$\sum_n \int d[\mu_n] |\mu_n\rangle \langle \mu_n| = \mathbb{1}, \quad (2.41)$$

every general state $|\Psi\rangle$ with momentum $\vec{P} = (P^+, \vec{P}_\perp)$ can be calculated in terms of these Fock states via the expansion

$$|\Psi(\vec{P})\rangle = \sum_n \int d[\mu_n] \psi_n(x_i, \vec{k}_{\perp i}) \left| n : x_i P^+, x_i \vec{P}_\perp + \vec{k}_{\perp i} \right\rangle. \quad (2.42)$$

Up to a normalization constant the phase-space differential is given as

$$d[\mu_n] = \prod_i dx_i d^2 k_{\perp i} \delta\left(1 - \sum_j x_j\right) \delta^2\left(\sum_j \vec{k}_{\perp j}\right). \quad (2.43)$$

The most important quantities in (2.42) are the light-cone wave functions

$$\psi_n(x_i, \vec{k}_{\perp i}) := \langle n : x_i P^+, x_i \vec{P}_\perp + \vec{k}_{\perp i} | \psi(\vec{P}) \rangle, \quad (2.44)$$

which are the amplitudes to find bare constituents with momenta $(x_i P^+, x_i \vec{P}_\perp + \vec{k}_{\perp i})$ in the state $|\Psi(P^+, \vec{P}_\perp)\rangle$. They are only functions of the frame-independent variables x_i and $\vec{k}_{\perp i}$ and therefore can not depend on the total momentum \vec{P} of the system. Thus light-cone quantization offers the special feature of specifying wave functions simultaneously in any frame. This property makes light-cone wave functions ideal for probing the internal structure of a system [12].

To simplify things even more, we will in this thesis always go to the ‘transverse rest frame’ where $\vec{P}_\perp = 0$, implying a vanishing free center-of-mass Hamiltonian $(P_0^-)_{\text{cm}}$. In this frame the helicity of the system is given as the total spin along the longitudinal direction. The transformation to an arbitrary frame with finite transverse momenta \vec{P}_\perp is then trivially performed.

3 The QCD-inspired Model

We address to the following effective one-body equation

$$M^2 \psi_{\lambda_1 \lambda_2}(x, \vec{k}_\perp) = \left[\frac{\bar{m}_1(\Lambda) + \vec{k}_\perp^2}{x} + \frac{\bar{m}_2(\Lambda) + \vec{k}_\perp^2}{1-x} \right] \psi_{\lambda_1 \lambda_2}(x, \vec{k}_\perp) + \sum_{\lambda'_1, \lambda'_2} \int dx' d^2 \vec{k}'_\perp U_{\lambda_1 \lambda_2; \lambda'_1 \lambda'_2}(x, \vec{k}_\perp; x', \vec{k}'_\perp; \Lambda) \psi_{\lambda'_1 \lambda'_2}(x', \vec{k}'_\perp), \quad (3.1)$$

being an integral equation with the kernel

$$U_{\lambda_1 \lambda_2; \lambda'_1 \lambda'_2} = -\frac{1}{3\pi^2} \frac{\bar{\alpha}(Q, \Lambda)}{Q^2} R(Q, \Lambda) \frac{S_{\lambda_1 \lambda_2; \lambda'_1 \lambda'_2}(x, \vec{k}_\perp; x', \vec{k}'_\perp)}{\sqrt{x(1-x)x'(1-x')}}. \quad (3.2)$$

We will now summarize the basic ingredients of this equation, for more background information one has to refer to (Appendix B).

First of all, it's an effective light-cone equation acting only in the lowest $q\bar{q}$ Fock space sector via a simple one gluon exchange between effective vertices. It's designed to describe flavor off-diagonal mesons, that means for mesons having a different flavor for quark and anti-quark — we don't have to deal with any annihilation amplitudes. By construction this effective equation has the same eigenvalue spectrum as the full light-cone Hamiltonian. The eigenvalue is the invariant mass squared M^2 . The associated eigenfunction $\psi = \langle x, \vec{k}_\perp; \lambda_1, \lambda_2 | \Psi_{q\bar{q}} \rangle$ is the probability amplitude for finding a quark with longitudinal momentum fraction x , relative transversal momentum \vec{k}_\perp and helicity λ_1 , and correspondingly the anti-quark with $1-x$, \vec{k}_\perp and λ_2 . It is convenient to see $Q^2 = Q^2(x, \vec{k}_\perp; x', \vec{k}'_\perp)$ as the mean Feynman-momentum transfer of the quarks

$$Q^2 = -\frac{1}{2} [(k_1 - k'_1)^2 + (k_2 - k'_2)^2]. \quad (3.3)$$

The spinor factor $S = S(x, \vec{k}_\perp; x', \vec{k}'_\perp)$ is the usual current-current coupling

$$S_{\lambda_1 \lambda_2; \lambda'_1 \lambda'_2} = [\bar{u}(k_1, \lambda_1) \gamma^\mu u(k'_1, \lambda'_1)] [\bar{v}(k'_2, \lambda'_2) \gamma_\mu v(k_2, \lambda_2)], \quad (3.4)$$

which will account for all fine and hyperfine interactions. It's defined in terms of Lepage-Brodsky spinors [12] with the matrix elements tabulated explicitly in (Appendix C). Due to these helicity indices the above one-body equation is a set of four coupled integral equations in the three momentum components x and \vec{k}_\perp . Finally the parameters of the equation are the physical effective quark masses \bar{m}_1 and \bar{m}_2 , and the physical effective coupling constant $\bar{\alpha}$. They implicitly depend on some unphysical cut-off scale Λ which in turn demands a renormalization of these parameters. The same holds for the regulating function $R(Q, \Lambda)$ which gives the equation an explicit dependence on the mass scale Λ for having a well-defined integral equation, since the kernel is not vanishing sufficiently fast enough for $\vec{k}_\perp \rightarrow \infty$.

Important to note is that (3.1) is a fully relativistic and frame-independent bound-state equation and we will consider it as the 'master equation'. The equation was derived

3. The QCD-inspired Model

in an non-perturbative way from the QCD-Lagrangian \mathcal{L}_{QCD} by making a few but well specified assumptions. It was derived by the method of iterated resolvents [7], that is by systematically projecting the higher Fock-space wave functions onto lower ones. In doing so the Fock-space was not truncated and all Lagrangian symmetries were preserved. If the $q\bar{q}$ -projection ψ in (3.1) is known, all higher Fock-space wave functions can be retrieved from it automatically.

The main task of this thesis is not to solve equation (3.1). This was done in full glory by Trittman et al. [13], who showed how the equation can be solved numerically with high precision. We rather want to address the problem of renormalization. To attack this problem in a more or less analytical way, we will simplify the ‘master equation’ (3.1) down to a workable model equation, the $\uparrow\downarrow$ -model [6]. This model is very important in understanding how renormalization works in a non-perturbative context.

Before we start constructing the model, we first look again at the unphysical Λ -dependence of equation (3.1). We see that its effective Hamiltonian depends on this regulator scale through three quantities. First, it *implicitly* depends on Λ through the physical quark masses $\bar{m}_f = \bar{m}_f(\Lambda)$. Second, it also *implicitly* depends on Λ through the physical effective coupling $\bar{\alpha}(Q) = \bar{\alpha}(Q, \Lambda)$. Third, the Hamiltonian *explicitly* depends on Λ through the unphysical regularization function $R(Q, \Lambda)$. The dependence on the parameter Λ must be removed

$$\frac{d}{d\Lambda} H_{\text{LC}}^{\text{eff}}[\bar{m}(\Lambda), \bar{\alpha}(\Lambda), R(\Lambda)] = 0, \quad (3.5)$$

as required by renormalization theory, but how? The above condition can be rewritten as a functional variation

$$\frac{\delta H_{\text{LC}}^{\text{eff}}}{\delta \bar{m}} \frac{\delta \bar{m}}{\delta \Lambda} + \frac{\delta H_{\text{LC}}^{\text{eff}}}{\delta \bar{\alpha}} \frac{\delta \bar{\alpha}}{\delta \Lambda} + \frac{\delta H_{\text{LC}}^{\text{eff}}}{\delta R} \frac{\delta R}{\delta \Lambda} = 0. \quad (3.6)$$

It is not in conflict with renormalization theory to vary the three terms independently

$$\frac{\delta \bar{m}}{\delta \Lambda} = 0, \quad \frac{\delta \bar{\alpha}}{\delta \Lambda} = 0, \quad \frac{\delta R}{\delta \Lambda} = 0. \quad (3.7)$$

The independent renormalization of $\bar{m}_f(\Lambda)$ can be achieved by interpreting the \bar{m}_f as parameters of the theory to be determined by experiment. The independent renormalization of $\bar{\alpha}(Q, \Lambda)$ has been performed in [7] or recently in [14], in terms of the QCD-scale κ , to be determined by experiment. Since there the renormalized effective coupling $\bar{\alpha}(Q)$ varies only little for relatively small momentum transfers, like in a typical bound system, the scale κ will be replaced by the dimensionless and Q -independent number $\bar{\alpha}$. Without avoiding to much confusion, we will from now on drop the ‘bar’-notation on the renormalized physical coupling constant $\bar{\alpha} \rightarrow \alpha$, as well as on all renormalized physical quark masses $\bar{m}_f \rightarrow m_f$. So, the full problem of renormalization can essentially be reduced to the problem of removing the explicit dependence of Λ from the bound-state equation (3.1). This will be attacked in detail in the next section.

3. The QCD-inspired Model

The next stage towards the $\uparrow\downarrow$ -model is the simplification of the spinor factor S . Two constituents are at relative rest when $\vec{k}_\perp = 0$ and $x = \bar{x} = m_1/(m_1+m_2)$. An inspection of the spinor matrix elements (Appendix C) reveals that if the relative motion between the quarks are of a small deviation from these equilibrium values, the spinor matrix is proportional to the unit matrix

$$\langle \lambda_1, \lambda_2 | S | \lambda'_1, \lambda'_2 \rangle \sim 4m_1 m_2 \delta_{\lambda_1 \lambda'_1} \delta_{\lambda_2 \lambda'_2}. \quad (3.8)$$

The values of the helicity indices λ_i will be denoted by $(+, -)$ or by (\uparrow, \downarrow) . For large deviations in the transverse plane $\vec{k}'_\perp \gg \vec{k}_\perp^2$ all matrix elements are vanishingly small compared to the only surviving element of

$$\langle \uparrow\downarrow | S | \uparrow\downarrow \rangle \sim 2\vec{k}'_\perp. \quad (3.9)$$

Since in this far-off equilibrium state the momentum transfer behaves as $Q^2 \sim \vec{k}'_\perp^2$, it's possible to combine these two extremes in the *Singlet-Triplet (ST)-model*:

$$\langle \lambda_1, \lambda_2 | S | \lambda'_1, \lambda'_2 \rangle = \delta_{\lambda_1 \lambda'_1} \delta_{\lambda_2 \lambda'_2} \langle \lambda_1, \lambda_2 | S | \lambda_1, \lambda_2 \rangle,$$

with

$$\frac{\langle \lambda_1, \lambda_2 | S | \lambda_1, \lambda_2 \rangle}{Q^2} = \begin{cases} \frac{4m_1 m_2}{Q^2} + 2 & \text{for } \lambda_1 = -\lambda_2 \text{ (singlet),} \\ \frac{4m_1 m_2}{Q^2} & \text{for } \lambda_1 = \lambda_2 \text{ (triplet).} \end{cases} \quad (3.10)$$

For singlets the model interpolates between two extremes: for small momentum transfer Q^2 the '2' is unimportant and the dominantly Coulomb aspects of the first term prevail. For large momentum transfers the Coulomb aspects become unimportant and the hyperfine interaction is dominant. The '2' carries the singlet triplet mass difference. For the triplets the model reduces to the plain Coulomb kernel. The big advantage of this model is its simplicity in dropping the helicity summations, which technically simplifies the problem enormously.

The model we will focus on, is the $\uparrow\downarrow$ -model of [6] which reduces the kernel even further

$$\frac{\langle \lambda_1, \lambda_2 | S | \lambda_1, \lambda_2 \rangle}{Q^2} R(Q, \Lambda) = \left(\frac{4m_1 m_2}{Q^2} + 2 \right) R(Q, \Lambda) \longrightarrow \frac{4m_1 m_2}{Q^2} + 2R(Q, \Lambda). \quad (3.11)$$

This model emphasizes the point that the '2', or any other constant in the kernel of an integral equation, leads to numerically undefined equations and thus singularities. Certainly this model can not be justified in the sense of an approximation. It overemphasizes many aspects of the original interaction. Nevertheless, it's remarkable how the $\uparrow\downarrow$ -model is able to predict the mass spectrum for pseudoscalar and vector mesons within less than 5% error [6]. In this sense it serves as a reliable model to do fast calculations. As we will see, this model offers a nice platform for solving the explicit renormalization problem.

Next, a rather dramatic technical simplification is achieved by a transformation of the longitudinal integration variable in (3.1) — if done correctly, such a step is no approximation but exact. After all we are just substituting the integration variable $x \in [0, 1]$ by an other integration variable $k_z \in (-\infty, \infty)$ which, as will be shown below, can be interpreted as the z-component of a usual 3-momentum vector $\vec{k} = (\vec{k}_\perp, k_z)$.

3. The QCD-inspired Model

The integration variables are changed from x to k_z by the following Sawicki transformation [15]

$$x(k_z) = \frac{E_1 + k_z}{E_1 + E_2}, \quad \text{with} \quad E_{1,2} = \sqrt{m_{1,2} + \vec{k}_\perp^2 + k_z^2}. \quad (3.12)$$

The Jacobian is

$$\frac{dx}{x(1-x)} = \frac{1}{A(k_z, \vec{k}_\perp)} \frac{dk_z}{m_r}, \quad (3.13)$$

with the dimensionless function

$$A(k_z, \vec{k}_\perp) = \frac{1}{m_r} \frac{E_1 E_2}{E_1 + E_2}. \quad (3.14)$$

If we define a new wave function ϕ which is related by the original frame-independent light-cone wave function ψ by

$$\phi(k_z, \vec{k}_\perp) = \sqrt{\frac{x(1-x)}{A(k_z, \vec{k}_\perp)}} \psi(x, \vec{k}_\perp), \quad (3.15)$$

the ‘master equation’ (3.1) within the $\uparrow\downarrow$ -model can be converted into the following integral equation

$$\left[M^2 - m_s^2 - C(k) \vec{k}^2 \right] \phi(\vec{k}) = -\frac{1}{3\pi^2} \frac{\alpha}{m_r} \int \frac{d^3 k'}{\sqrt{A(k)A(k')}} \left[\frac{4m_1 m_2}{Q^2} + 2R(Q, \Lambda) \right] \phi(\vec{k}'), \quad (3.16)$$

with the dimensionless kinematical function

$$C(k) = (E_1 + m_1 + E_2 + m_2) \left(\frac{1}{E_1 + m_1} + \frac{1}{E_2 + m_2} \right), \quad (3.17)$$

and finally with the mass parameters

$$\frac{1}{m_r} = \frac{1}{m_1} + \frac{1}{m_2}, \quad m_s = m_1 + m_2, \quad (3.18)$$

being the reduced mass and the sum mass respectively. Important to note is that the above variable transformation ($x \leftrightarrow k_z$) has a physical meaning. Since the transformation from front form to instant form is given by $p_i^+ = p_i^0 + p_i^3$ with $p_i^+ = P^+ x_i$ the longitudinal momentum fractions for the two constituents can be written as

$$x_i = \frac{p_i^0 + p_i^3}{P^+} = \frac{p_i^0 + p_i^3}{p_1^+ + p_2^+} = \frac{E_i + k_{zi}}{E_1 + k_{z1} + E_2 + k_{z2}}, \quad (3.19)$$

which immediately yields the transformation rule (3.12), if we choose a special frame in which the total momentum of the z-component vanishes: $P_z = k_{z1} + k_{z2} = 0$. Since we are already in a frame where the total transversal momentum \vec{P}_\perp is zero, the integral equation as written in (3.16) can be interpreted as an instant form equation in the center-of-mass frame.

3. The QCD-inspired Model

Furthermore, this justifies that the transformation variable k_z can be seen as the z-component of a usual 3-momentum vector. Although there is not a single trace of light-cone variables in equation (3.16), its still a genuine front form equation designed to calculate frame-independent light-cone wave functions (3.15). After all, a substitution of integration variables does not change physics.

We continue to simplify the integral equation (3.16) by constructing a more or less *non-relativistic* situation with $\vec{k}_i^2 \ll m_i^2$, thus

$$C(k) \sim m_s/m_r, \quad A(k) \sim 1, \quad Q^2 \sim (\vec{k} - \vec{k}')^2. \quad (3.20)$$

To substitute $A(k') \sim 1$ in the kernel is certainly not justified, since the integration variable has $\vec{k}' \rightarrow \infty$ at the upper limit. But if one does it anyway in the sense of a non-relativistic *simplification*, one gets

$$\left[M^2 - m_s^2 - \frac{m_s}{m_r} \vec{k}^2 \right] \phi(\vec{k}) = -\frac{1}{3\pi^2} \frac{\alpha}{m_r} \int d^3k' \left[\frac{4m_s m_r}{(\vec{k} - \vec{k}')^2} + 2R(Q, \Lambda) \right] \phi(\vec{k}'), \quad (3.21)$$

with the connection to the light-cone wave function given as

$$\psi(x, \vec{k}_\perp) = \frac{\phi(k_z, \vec{k}_\perp)}{\sqrt{x(1-x)}}. \quad (3.22)$$

The only reason why we apply the non-relativistic simplification is that (3.21) has a local Fourier transform, which allows us to have a simple picture of the underlying interaction potential. Defining the new energy variable $E = (M^2 - m_s^2)/2m_s$, which will behave as the conventional non-relativistic binding energy, turns equation (3.21) into the usual momentum space Schrödinger equation

$$\begin{aligned} E\phi(\vec{k}) &= \frac{\vec{k}^2}{2m_r} + \int d^3k' U(q^2, \Lambda) \phi(\vec{k}') \\ \text{with } U(q^2, \Lambda) &= -\frac{1}{6\pi^2} \frac{\alpha}{m_s m_r} \left[\frac{4m_s m_r}{q^2} + 2R(q^2, \Lambda) \right]. \end{aligned} \quad (3.23)$$

Fourier transforming gives

$$\begin{aligned} E\psi(\vec{r}) &= \left[\frac{\vec{k}^2}{2m_r} + V(r, \Lambda) \right] \psi(\vec{r}) \\ \text{with } V(r, \Lambda) &= \int d^3q e^{-i\vec{q}\cdot\vec{r}} U(q^2, \Lambda), \end{aligned} \quad (3.24)$$

the local Schrödinger equation in coordinate space. On the other hand, the Fourier transform of (3.16) is non-local and mathematically difficult.

4 Explicit Renormalization

In this section we are going to address solely to the $\uparrow\downarrow$ -model equation (3.21). We first look at it in the limit of $\Lambda \rightarrow \infty$

$$\left[M^2 - 4m^2 - 4\vec{k}^2 \right] \phi(\vec{k}) = -\frac{4}{3\pi^2} \frac{\alpha}{m} \int d^3k' \left[\frac{2m^2}{(\vec{k} - \vec{k}')^2} + 1 \right] \phi(\vec{k}'). \quad (4.1)$$

It is a robust physical equation to model flavor off-diagonal mesons with equal quark and anti-quark masses, as for example the pion ($m_u \sim m_d$). This is done by fixing the parameters α and m to the experimentally available mass spectrum M . The generalization to different quark and anti-quark masses is performed trivially. We deliberately wrote equation (3.21) in the form of (4.1) to suggest the reader that, due to its pure physical content, the equation is ready to be solved for and to be fitted to experiment. But unfortunately this is not possible, since equation (4.1) is mathematically not defined. It is the number ‘1’ in the kernel, which generates all the well known trouble. The aim of this section is to give (4.1) a physical meaning by renormalization. This will be done by comparing two drastically different renormalization schemes, both conceptually and numerically, and verify that they agree. This strong statement stands at the very basis of renormalization ideas, that no matter the intermediate steps one performs to mathematically define the initial equation (4.1), after renormalization all of them produce the same physics.

One scheme is to renormalize directly at the basis of the Schrödinger equation (4.1) by the method of using counter terms in a regularized interaction kernel. The other scheme is to renormalize at the basis of the complementary Lippmann-Schwinger equation (Appendix D), by applying a well specified subtraction method to the equivalent T -matrix equation. It was first developed by the authors of [16] to handle singular interactions in non-relativistic quantum mechanics. But before going there, we first want to investigate the former renormalization scheme.

4.1 Renormalization by a counterterm

If one Fourier transforms the Schrödinger equation (4.1) to coordinate space, the interaction potential consists of a long-ranged Coulomb interaction and a short-ranged Dirac-delta interaction. It is this latter part which generates trouble. In order to get reasonable solutions one has to regulate the short-range region, which implies the regularization of high momentum transfers $Q^2 = (\vec{k} - \vec{k}')^2$. As expected, we have to restore (4.1) to its original well-defined integral equation (3.21) by substituting the number 1 by a regulating function $1 \rightarrow R(Q, \Lambda)$, for which the soft cut-off (B.57) is chosen

$$\left[M^2 - 4m^2 - 4\vec{k}^2 \right] \phi(\vec{k}) = -\frac{4}{3\pi^2} \frac{\alpha}{m} \int d^3k' \left[\frac{2m^2}{(\vec{k} - \vec{k}')^2} + \frac{\Lambda^2}{\Lambda^2 + (\vec{k} - \vec{k}')^2} \right] \phi(\vec{k}'). \quad (4.2)$$

In coordinate space the short-ranged delta is now smeared out to a Yukawa interaction. Since the regulator Λ is an additional but unphysical parameter, one has to renormalize the equation in order to restore the original problem in the limit $\Lambda \rightarrow \infty$.

4. Explicit Renormalization

Here is a general but abstract procedure how the explicit Λ -dependence can be removed: suppose we have solved equation (4.2) for a fixed value of the parameters $\alpha = \alpha_0$ and $m = m_0$, and for a fixed value of $\Lambda = \Lambda_0$. Suppose further that these parameters are chosen such, that the calculated eigenvalues M_i^2 agree with experiment. Next, we change the unphysical cut-off $\Lambda = \Lambda_0 + \delta\Lambda$ by a small amount $\delta\Lambda$. Then all calculated eigenvalues will change by a small amount δM_i^2 .

Renormalization theory is then the attempt to reformulate the underlying theory, in our case equation (4.2), such, that all these changes vanishes identically. The fundamental renormalization group equation is thus

$$\frac{d}{d\Lambda} M_i^2(\Lambda) = 0, \quad \text{for all eigenstates } i. \quad (4.3)$$

No other reason than simplicity we will restrict the solutions of (4.2) to those of s-waves: $\phi(\vec{k}) = \phi(|\vec{k}|)$ and fix the mass parameter at the value of $m = 406$ MeV. Being only a function of α and Λ the spectrum of the bound-state mass squares $M_i^2(\alpha, \Lambda)$ are then calculated numerically — on numerical details see (Section 4.3) and (Appendix E). For the ground state ($i=0$) this is displayed as a contour plot in (Fig1a). A similar graph could have also be given for the first excited state ($i=1$) or for any other eigenstate. It goes without saying that such plots can be generated easily only for a sufficiently simple model, such as the $\uparrow\downarrow$ -model.

According to the general outline mentioned above, one must make sure that the mass squared spectrum stays invariant, $\delta M_i^2(\alpha, \Lambda) = 0$ for infinitesimal variations $\delta\Lambda$. This can be achieved by the following construction, by introducing a new function

$$\bar{R}(Q, \Lambda) = R(Q, \Lambda) + C(Q, \Lambda). \quad (4.4)$$

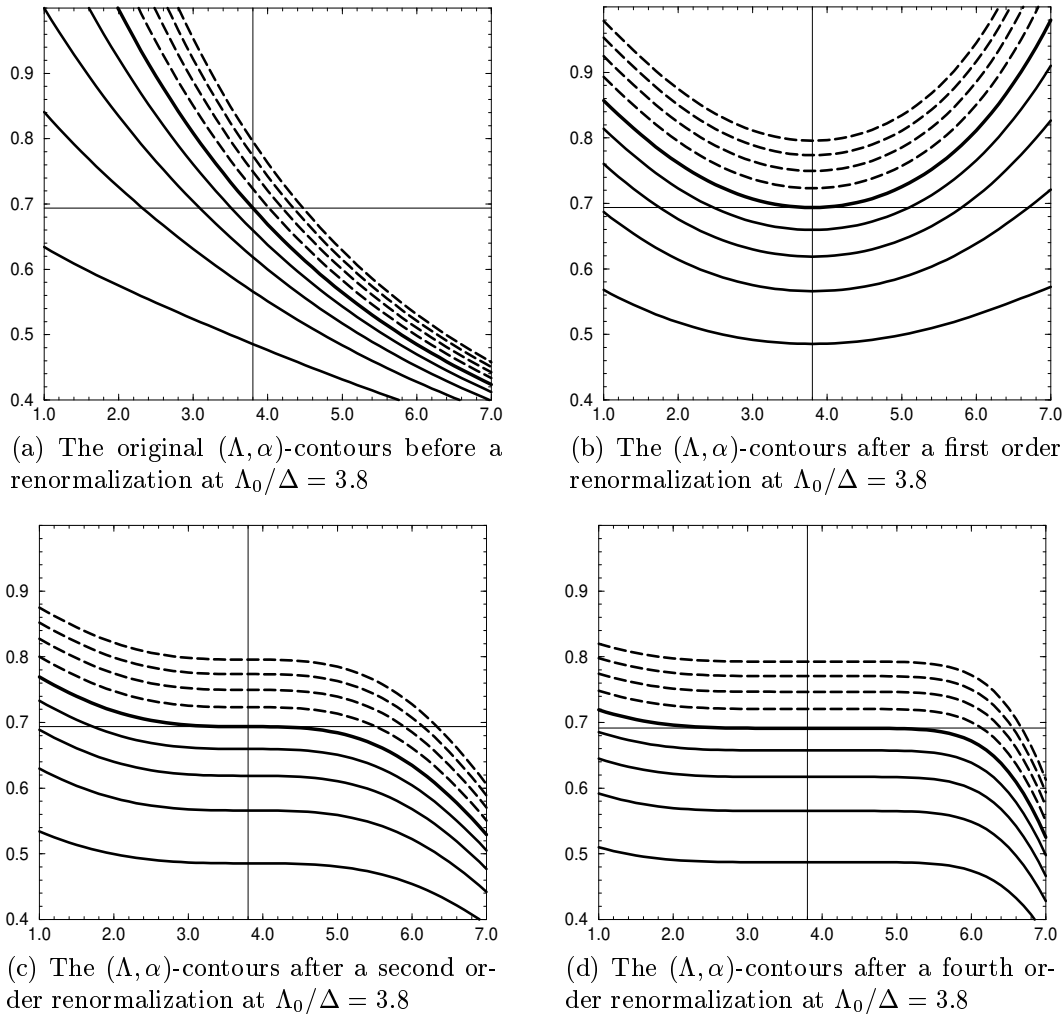
We extend the model interaction by adding to the regulator function R a counter term C . We choose this counter term according to three criteria. First, the new function \bar{R} must again be a regulator in the sense of (Appendix B.2). Second, we require that a zero is added for a particular value of Λ , say for $\Lambda = \Lambda_0$. Thus adding a counter term at $\Lambda = \Lambda_0$ will not change the original interaction at that point. Third, we require the first Λ -derivative of \bar{R} to vanish at $\Lambda = \Lambda_0$. Because a vanishing derivative of \bar{R} at $\Lambda = \Lambda_0$ implies vanishing derivatives of the eigenvalues M_i^2 with respect to Λ at this very same point. The argument is based on the Hellmann-Feynman theorem, which states that an external parameter variation in the Hamiltonian has no effect on the corresponding wavefunctions but only on its eigenvalue spectrum. All three conditions are met by

$$C(Q, \Lambda^2) = -(\Lambda^2 - \Lambda_0^2) \frac{\partial R(Q, \Lambda^2)}{\partial \Lambda^2}, \quad (4.5)$$

where the derivative is to be taken at $\Lambda = \Lambda_0$. The numerical results in (Fig1b) illustrate this very convincingly that the Hamiltonian is partially renormalized $\delta M_i^2(\alpha, \Lambda) = 0$ in the vicinity of $\Lambda \sim \Lambda_0$ for all α .

4. Explicit Renormalization

Figure 1: Nine contours $0.4 \leq \alpha_n(\Lambda) \leq 1.0$ are plotted versus $1.0 \leq \Lambda/\Delta \leq 7.0$ from bottom to top with $n = 4, 3, \dots, -3, -4$. The contours are obtained by plotting the ground state of the invariant mass-squared $M_0^2(\Lambda, \alpha) = n\Delta^2 + M_\pi^2$. The thick contour $n = 0$ describes the pion with $M_0^2 = M_\pi^2$. Masses are given in units of $\Delta = 350$ MeV.



One can carry on the procedure to the next higher order

$$\bar{R}(Q, \Lambda) = R(Q, \Lambda) - (\Lambda^2 - \Lambda_0^2) \frac{\partial R(Q, \Lambda_0^2)}{\partial \Lambda^2} - \frac{(\Lambda^2 - \Lambda_0^2)^2}{2!} \frac{\partial^2 R(Q, \Lambda_0^2)}{\partial \Lambda^4}, \quad (4.6)$$

with the result that the contours as shown in (Fig1c) become broader. And so on. In the limit of large order the contours become flat, since the renormalized regulator

$$\bar{R}(Q, \Lambda) = R(Q, \Lambda) - [R(Q, \Lambda) - R(Q, \Lambda_0)] = R(Q, \Lambda_0), \quad (4.7)$$

is *manifestly independent* of Λ . One has realized the fundamental renormalization group equation: $dM_i^2(\Lambda) = 0$ for all eigenstates, since the choice of the above counter terms are universal and apply for every i . The above results represent thus a beautiful and pedagogic example for how renormalization group works.

4. Explicit Renormalization

The result sounds incredible: invent a regulator function $R(Q, \Lambda)$ to be a function of the cut-off scale Λ . The same function but for $\Lambda = \Lambda_0$ is the *renormalized regulator*, and the parameter Λ_0 is to be determined from experiment. Important to note is that this result is only valid for regulating functions which have well defined derivatives with respect to Λ . The sharp cut-off (B.57), however, is a step function with ill defined derivatives.

With Λ_0 we thus have one more parameter than the 7 bare parameters of the QCD-Lagrangian: 6 flavor quark masses and the coupling constant. This is in full accord with renormalization theory, since whatever the model is, one has a scale at which one experiments.

4.2 T-matrix renormalization

For the purpose of presenting the subtraction method of [16], its convenient to convert the Schrödinger equation (4.1) into the abstract Dirac-notation of quantum mechanics:

$$(M_0^2 + V^c + V^\delta)|\phi\rangle = M^2|\phi\rangle, \quad (4.8)$$

where the matrix elements in momentum space of the free mass operator M_0^2 , the Coulomb potential V^c and the Dirac-delta interaction V^δ are identified as

$$\begin{aligned} \langle \vec{k} | M_0^2 | \vec{k}' \rangle &= (4m^2 + 4\vec{k}^2) \cdot \delta(\vec{k} - \vec{k}'), \\ \langle \vec{k} | V^c | \vec{k}' \rangle &= -\frac{8m}{3\pi^2} \frac{\alpha}{(\vec{k} - \vec{k}')^2}, \quad \langle \vec{k} | V^\delta | \vec{k}' \rangle = \lambda, \end{aligned} \quad (4.9)$$

where λ is to be seen as an additional *independent* parameter of equation (4.1), representing the bare strength of the Dirac-delta interaction. Its inverse carries the dimension of energy, as it was the case of Λ in the previous subsection. The drastic difference between these two additional parameters is that Λ served as a regulating parameter, while here, λ will simulate arbitrary strenghts of the trouble making delta interaction.

Next, we briefly want to supply the essence of the subtraction method, which is performed in the complementary scattering picture of the Lippmann-Schwinger equation. For this, let us solve equation (4.8) only with a pure delta interaction, i.e. $V^c = 0$, which, as said, makes (4.1) not well defined.

The relevant self-consistent T -matrix equation for a scattering state of mass M is given by

$$T(M^2) = V^\delta + V^\delta G_0^+(M^2)T(M^2), \quad (4.10)$$

with

$$G_0^+(M^2) = \frac{1}{M^2 - M_0^2 + i\epsilon}, \quad (4.11)$$

as the Green function of the free mass operator equation with a outgoing wave boundary condition. The solution of the operator equation (4.10) in this simple case is determined by iteration and the subsequent summation of the corresponding geometrical series.

4. Explicit Renormalization

As a result, the solution in the form of the matrix elements $\langle \vec{k} | T(M^2) | \vec{k}' \rangle$ only depend on the invariant mass squared M^2 :

$$\langle \vec{k} | T(M^2) | \vec{k}' \rangle = \frac{1}{\lambda^{-1} - I(M^2)} \equiv \tau(M^2), \quad (4.12)$$

with the function

$$I(M^2) = \int d^3k \frac{1}{M^2 - 4m^2 - 4k^2 + i\epsilon}, \quad (4.13)$$

which diverges linearly! From a different perspective we see again that this is the mathematical problem in (4.1) of having a delta interaction in the kernel. How to give meaning to $\tau(M^2)$? We use the renormalization idea. Suppose $\tau(\mu^2)$ is known from experiment, then we rewrite $\tau(M^2)$ using this piece of data:

$$\tau(M^2) = [\tau^{-1}(\mu^2) + I(\mu^2) - I(M^2)]^{-1}, \quad (4.14)$$

and now the subtraction of the divergence appears! A closer look to

$$I(\mu^2) - I(M^2) = (M^2 - \mu^2) \int d^3k \frac{1}{(\mu^2 - 4m^2 - 4k^2 + i\epsilon)(M^2 - 4m^2 - 4k^2 + i\epsilon)}, \quad (4.15)$$

shows that it is finite with μ being the subtraction point. Substituting (4.14) into (4.12) the bare strength λ can be written as a function

$$\lambda(\mu^2) = \frac{1}{\tau^{-1}(\mu^2) + I(\mu^2)} = \frac{1}{1 + \tau(\mu^2)I(\mu^2)} \tau(\mu^2), \quad (4.16)$$

in which the physical input and the counter terms that subtract all the infinities in the scattering matrix at the mass scale μ are present. This is the essence of the subtraction method: the renormalized delta interaction which formally can be written as

$$V_{\mathcal{R}}^{\delta}(\mu^2) = T(\mu^2) [1 + G_0^+(\mu^2)T(\mu^2)]^{-1}, \quad (4.17)$$

with its matrix elements $\langle \vec{k} | V_{\mathcal{R}}^{\delta}(\mu^2) | \vec{k}' \rangle = \lambda(\mu^2)$ results in a finite T-matrix obtained by solving the corresponding renormalized equation

$$T_{\mathcal{R}}(M^2, \mu^2) = V_{\mathcal{R}}^{\delta}(\mu^2) + V_{\mathcal{R}}^{\delta}(\mu^2)G_0^+(M^2)T_{\mathcal{R}}(M^2, \mu^2). \quad (4.18)$$

Next, the physical input $\tau(\mu^2) = \langle \vec{k} | T(\mu^2) | \vec{k}' \rangle$ can be interpreted as a renormalized Dirac-delta strength $\lambda_{\mathcal{R}}(\mu^2)$. To see this, we rewrite the above renormalized T-matrix equation as

$$\begin{aligned} T_{\mathcal{R}}(M^2, \mu^2) &= V_{\mathcal{R}}^{\delta}(\mu^2) [1 + G_0^+(M^2)T_{\mathcal{R}}(M^2, \mu^2)] \\ &= [T_{\mathcal{R}}(M^2, \mu^2)G_0^+(M^2) + 1] V_{\mathcal{R}}^{\delta}(\mu^2). \end{aligned} \quad (4.19)$$

Substituting (4.17) into the last equation, we now obtain the renormalized T-matrix equation in the form of

$$T_{\mathcal{R}}(M^2, \mu^2) = T(\mu^2) + T(\mu^2) [G_0^+(M^2) - G_0(\mu^2)] T_{\mathcal{R}}(M^2, \mu^2). \quad (4.20)$$

4. Explicit Renormalization

We observe that this equation has the same operatorial form as the original renormalized T-matrix equation (4.18), with the interaction $V_{\mathcal{R}}^{\delta}$ replaced by the physical input at the mass scale μ , and the original propagator replaced by a propagator which has a subtraction at such mass scale. The former allows to see the physical input as a renormalized Dirac-delta strength $\langle \vec{k} | T(\mu^2) | \vec{k}' \rangle = \lambda_{\mathcal{R}}(\mu^2)$, while the latter manifestly shows how the scattering equation (4.18) with the renormalized interaction appears in a subtracted form, in which all divergent momentum integrals are explicitly removed. Important to note is that, instead of working formally with the operator $V_{\mathcal{R}}^{\delta}$, one could have also used an ultraviolet momentum cutoff Λ by defining in this way a regularized interaction. However, after the construction of the regularized T-matrix equation one can perform the limit $\Lambda \rightarrow \infty$, arriving at the same results as the ones obtained directly with the use of the renormalized interaction.

To complete the renormalization scheme we have to think about the renormalization point itself, which in this context is given by a subtraction point μ . As we know, the subtraction point is the scale at which the scattering amplitude is known. But this point is arbitrary in the definition of the renormalized interaction and in principle it can be moved. On the other hand, a sensible theory of a singular interaction, as here for the delta interaction exists only if the subtraction point slides without affecting the physics of the renormalized theory. That means a Hamiltonian should have the property to be stationary in the parametric space of the subtraction point. The renormalization group method can be used to realize the invariance of physics under dislocations of the subtraction point. This condition demands the renormalized potential $V_{\mathcal{R}}^{\delta}$ to be independent on the subtraction point. When applied on (4.17) the renormalization group equation can be written as

$$\frac{d}{d\mu^2} V_{\mathcal{R}}^{\delta}(\mu^2) = 0 \quad \iff \quad \frac{d}{d\mu^2} T(\mu^2) = -T(\mu^2) G_0^+(\mu^2)^2 T(\mu^2), \quad (4.21)$$

and is a prescription how the renormalized coupling constant $\lambda_{\mathcal{R}}(\mu^2)$ has to change as the subtraction point μ moves. As long as the first order differential equation (4.21) is satisfied, it automatically follows from (4.18) that the renormalized T-matrix also does not depend on the subtraction point $T_{\mathcal{R}}(M^2, \mu^2) \equiv T_{\mathcal{R}}(M^2)$.

The subtraction method as exemplified above for the pure delta interaction, is now applied to the effective model defined by the full mass operator of equation (4.8). The corresponding scattering matrix comes from the solution of the scattering equation

$$T_{\mathcal{R}}(M^2) = V_{\mathcal{R}} + V_{\mathcal{R}} G_0^+(M^2) T_{\mathcal{R}}(M^2), \quad (4.22)$$

with the renormalized potential $V_{\mathcal{R}} = V^c + V_{\mathcal{R}}^{\delta}$, where the Coulomb interaction is a regular interaction which need not to be renormalized. In finding the solution, we will make use of the 2-potential formula as given in (D.126), where $T_{\mathcal{R}}(M^2)$ becomes

$$T_{\mathcal{R}}(M^2) = T^c(M^2) + [1 + T^c(M^2) G_0^+(M^2)] \cdot V_{\mathcal{R}}^{\delta} \cdot [G_0^+(M^2) T_{\mathcal{R}}(M^2) + 1]. \quad (4.23)$$

The regular Coulomb T-matrix $T^c(M^2)$ is the solution of the scattering equation (4.22) for the pure Coulomb potential V^c . Important to note is that the Coulomb T-matrix

4. Explicit Renormalization

only shows its anomalous behaviour [11] in the calculation of scattering quantities, as for example in the scattering amplitude or phase-shift, but not in its bound state region, as we are interested in. We will see that the general procedure of identifying bound states as poles of a T-matrix leads here to well-defined results.

We manipulate (4.23) further by multiplying on both sides with $G_0^+(M^2)$ and solving it we get

$$G_0^+(M^2)T_{\mathcal{R}}(M^2) = \frac{G_0^+(M^2)T^c(M^2) + G^+(M^2)V_{\mathcal{R}}^\delta}{1 - G^+(M^2)V_{\mathcal{R}}^\delta}, \quad (4.24)$$

with the interacting Green function defined as

$$G^+(M^2) = G_0^+(M^2) + G_0^+(M^2)T^c(M^2)G_0^+(M^2). \quad (4.25)$$

Substituting (4.24) back into (4.23) one finally finds the formal solution of the renormalized T-matrix as

$$T_{\mathcal{R}}(M^2) = T^c(M^2) + [1 + T^c(M^2)G_0^+(M^2)] \cdot t_{\mathcal{R}}(M^2) \cdot [G_0^+(M^2)T^c(M^2) + 1], \quad (4.26)$$

with the reduced matrix elements

$$\langle \vec{k} | t_{\mathcal{R}}^{-1}(M^2) | \vec{k}' \rangle = \langle \vec{k} | (V_{\mathcal{R}}^\delta)^{-1} - G^+(M^2) | \vec{k}' \rangle \equiv \lambda_{\mathcal{R}}^{-1}(\mu^2) + \langle \vec{k} | G_0^+(\mu^2) - G^+(M^2) | \vec{k}' \rangle,$$

where in the last identity (4.17) has been used. Instead of using $\lambda_{\mathcal{R}}^{-1}(\mu^2)$ as the physical input, its convenient to introduce a new input variable

$$\bar{\lambda}_{\mathcal{R}}^{-1}(\mu^2) = \lambda_{\mathcal{R}}^{-1}(\mu^2) - \langle \vec{k} | G_0^+(\mu^2)T^c(\mu^2)G_0^+(\mu^2) | \vec{k}' \rangle, \quad (4.27)$$

which leads to the more symmetrical expression of

$$\langle \vec{k} | t_{\mathcal{R}}^{-1}(M^2) | \vec{k}' \rangle = \bar{\lambda}_{\mathcal{R}}^{-1}(\mu^2) - \langle \vec{k} | G^+(M^2) - G^+(\mu^2) | \vec{k}' \rangle. \quad (4.28)$$

The physical input is constructed as follows: if for example we take the pion mass at $M = m_\pi \sim 140$ MeV the T-matrix (4.26) should have a bound-state pole; consequently

$$t_{\mathcal{R}}^{-1}(m_\pi^2) = 0, \quad (4.29)$$

and choosing the subtraction point for convenience as $\mu = m_\pi$, implies

$$\bar{\lambda}_{\mathcal{R}}^{-1}(m_\pi^2) = 0. \quad (4.30)$$

Finally, the invariance of the renormalized T-matrix (4.26) under dislocation of the subtraction point just reads as

$$\frac{d}{d\mu^2} t_{\mathcal{R}}(M^2) = 0 \quad \iff \quad \frac{d}{d\mu^2} \bar{\lambda}_{\mathcal{R}}^{-1}(\mu^2) = \frac{d}{d\mu^2} \langle \vec{k} | G^+(\mu^2) | \vec{k}' \rangle. \quad (4.31)$$

The solution of this differential equation gives the dependence of the physical input $\bar{\lambda}_{\mathcal{R}}$ on the subtraction point μ , which must run as

$$\bar{\lambda}_{\mathcal{R}}^{-1}(\mu'^2) = \bar{\lambda}_{\mathcal{R}}^{-1}(\mu^2) + \langle \vec{k} | G^+(\mu'^2) - G^+(\mu^2) | \vec{k}' \rangle. \quad (4.32)$$

4. Explicit Renormalization

4.3 Numerical evaluation

To find all s-wave bound-states M_n of the counter-term renormalized Schrödinger equation (4.2), we have to solve the following s-wave projected integral equation

$$[M_n^2 - 4m^2 - 4k^2] \phi_n(k) = 2\pi \cdot \int_0^\infty dk' k'^2 \cdot U(k, k') \cdot \phi_n(k'), \quad (4.33)$$

with the attractive kernel

$$U(k, k') = -\frac{4}{3\pi^2} \frac{\alpha}{m} \int_{-1}^1 d\cos\vartheta \left(\frac{2m^2}{(\vec{k} - \vec{k}')^2} + \frac{\Lambda_0^2}{\Lambda_0^2 + (\vec{k} - \vec{k}')^2} \right). \quad (4.34)$$

The unique fixing of the three unknown parameters to experiment will be done in the next section. For further numerical details on how an equation as above is solved correctly, especially how the trouble making momentum space Coulomb singularity at $k = k'$ in (4.34) is properly treated, one should consult (Appendix E).

On the other hand, in order to find all s-wave bound-states M_n of the subtraction renormalized Lippmann-Schwinger equation, we have to determine the zeros of (4.28)

$$0 = G^+(M_n^2) - G^+(\mathcal{M}^2), \quad (4.35)$$

where \mathcal{M} represents the physical input, which will be fixed in the next section as well. According to (4.25) this equation explicitly reads as

$$0 = \int_0^\infty dk k^2 \cdot \left[\frac{1}{M_n^2 - M_0^2(k)} - \frac{1}{\mathcal{M}^2 - M_0^2(k)} \right] + \int_0^\infty dk \int_0^\infty dk' k^2 k'^2 \cdot \left[\frac{T^c(k, k'; M_n^2)}{(M_n^2 - M_0^2(k)) \cdot (M_n^2 - M_0^2(k'))} - \frac{T^c(k, k'; \mathcal{M}^2)}{(\mathcal{M}^2 - M_0^2(k)) \cdot (\mathcal{M}^2 - M_0^2(k'))} \right]. \quad (4.36)$$

The free invariant mass for the two quark system of equal masses is $M_0(k) = 4m^4 + 4k^2$, whereas the s-wave projected T-matrix of the pure Coulomb potential in (4.36) is the solution of the integral equation

$$T^c(k, k'; M^2) = V^c(k, k') + \int_0^\infty dq q^2 V^c(k, q) \frac{1}{M^2 - M_0^2(q)} T^c(q, k'; M^2), \quad (4.37)$$

with $V^c(k, k')$ as the s-wave projected Coulomb potential

$$V^c(k, k') = 2\pi \cdot \int_{-1}^1 d\cos\vartheta \langle \vec{k}' | V^c | \vec{k} \rangle = -\frac{16m\alpha}{3\pi} \int_{-1}^1 dx \frac{1}{k^2 + k'^2 - 2kk' \cdot x}. \quad (4.38)$$

The angle integration above is evaluated numerically. Using Gaussian quadrature this ensures us not to run into the logarithmic momentum space singularity of the Coulomb potential at $k = k'$. The numerical results of the above equations turn out to be stable,

4. Explicit Renormalization

when using about 250 integration points, in stark contrast to a stable integration of only about 16 points for the counter-term renormalized integral equation (4.33). There we perform the angle integration (4.34) analytically and then making use of so-called numerical counter terms as shown in (Appendix E), which unfortunately can not be applied to an integral equation like (4.37). The drastic difference in the convergence of finding a bound-state can also be understood from a more fundamental level: equation (4.33) is a pure bound-state equation, while (4.36) is a scattering equation designed to determine bound-states, thus being from beginning at a disadvantage.

Nevertheless, the numerical stability of finding bound-states within the renormalized T-matrix equation, explicitly shows that the pure Coulomb T^c -matrix (4.37) will produce no anomalies if we focus only on its bound-state part, which is embedded into equation (4.36). We can conclude, that we do not really need the exact trouble making diagonal terms $T^c(k, k)$, in order to evaluate the zeros of (4.36) properly. This certainly does not hold for the scattering region of T^c , since here the diagonal elements must be exactly available for calculating relevant scattering quantities, like a phase shift in (E.35).

4.4 Comparing renormalization schemes

Here we compare the results obtained with the counter-term renormalization, and the T-matrix renormalization. In other words, we compare the numerical results of (4.33) and (4.36) respectively.

Both renormalization methods will make use of the same physical input, namely that of the pion $M_0 = M_\pi \sim 140$ MeV as the lowest bound-state (ground state), and that of the rho $M_1 = M_\rho \sim 768$ MeV as the second lowest bound-state (first excited state). To ensure that our equations produce the pion and rho as true bound-states, we have to choose a relatively large quark mass. For no good reason other than convenience, we will fix for the rest of this section the quark mass at $m = 406$ MeV, as it was used in the calculations of [6]. The scattering threshold is thus at $M = 812$ MeV.

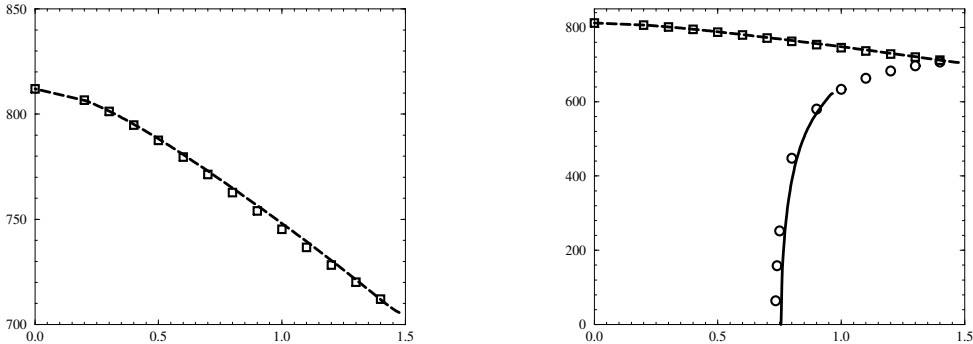
In one set of calculations, α will be varied, with fixed $\mathcal{M} = M_0 = 140$ MeV. In the other set of calculations, $\mathcal{M} = M_1 = 768$ MeV will be kept fixed. For equation (4.33) the value of Λ_0 will be fitted to that of M_0 or M_1 for a given α .

In (Fig2a), the results of M_1 as a function of α and fixed $M_0 = 140$ MeV for the two renormalization methods are shown. The agreement between these two is within few percent, which we relate to their rather drastic conceptual difference. As can be seen in (Fig1a), the values of Λ_0 for α going to zero increase towards infinity, to keep the ground state at the pion mass $M_1 = 140$ MeV, while M_1 tends to the scattering threshold at 812 MeV, as we observe in (Fig2a). For increasing α the value of Λ_0 decreases to keep $M_0 = 140$ MeV fixed, implying a Coulomb dominated M_1 , which therefore has to decrease as well.

The results for M_0 as a function of α for fixed $M_1 = 768$ MeV, are presented in (Fig2b). The threshold for zero pion mass occurs for α at a value of about 0.75. The value of M_0 increases with α , corresponding to a decreasing binding energy, which means that the intensity of the short-range interaction, that dominates the ground state, diminishes. In fact, to keep constant $M_1 = 768$ MeV as the effective Coulomb interaction increases, demands a weaker short-range interaction. The calculation of M_0 with the counter-

4. Explicit Renormalization

Figure 2:



(a) The first excited state mass M_1 (MeV) is plotted versus α for a fixed ground state mass of $M_0 = 140$ MeV. The dashed curve gives the results from the counter-term renormalized equation (4.33), the empty boxes from the T-matrix renormalized equation (4.36).

(b) The ground state mass M_0 (MeV) is plotted versus α for a fixed first excited state mass of $M_1 = 768$ MeV. The solid curve gives the results from the counter-term renormalized equation (4.33), while the empty circles give the results from the T-matrix renormalized equation (4.36). The upper curve with its empty boxes is the one of (Fig2a).

term renormalized equation (4.33) does not go beyond $\alpha = 0.97$ because Λ_0 vanishes and the mass of 768 MeV of the excited state is reproduced with the effective Coulomb interaction. The T-matrix renormalized equation (4.36) does not present the same limitation.

Conclusion: We have shown that two drastically different renormalization schemes, or even two complementary renormalization schemes, both conceptually and numerically, agree. Here we provide a simple example, that the physics of a renormalized theory does not recognize the intermediate steps one performs to mathematically define the initial undefined theory.

5 The Renormalized Singlet-Triplet (ST)-model

The explicit renormalization of the $\uparrow\downarrow$ -model (4.2) can be easily applied to the more general ST-model (3.10), which in the form of the ‘non-relativistic’ Schrödinger equation then simply reads

$$\begin{aligned} \left[E - \frac{k^2}{2m_r} \right] \phi(\vec{k}) &= -\frac{\alpha_c}{2\pi^2} \int d^3k' V(q^2) R(q^2, \lambda) \phi(\vec{k}'), \\ \text{with } V(q^2) &= \frac{1}{q^2} + \xi, \quad \text{and } \xi = \begin{cases} \frac{1}{2m_1 m_2} & \text{for singlet,} \\ 0 & \text{for triplet.} \end{cases} \end{aligned} \quad (5.1)$$

As was derived in the previous section, the renormalized regulator $R(q^2, \Lambda_0 = \lambda)$ is arbitrary in the sense that we only demand an asymptotical drop faster than $1/q^2$ and the behaviour $R \rightarrow 1$ in the opposite limit of $q^2 \rightarrow 0$. Up to now, the parameters to be determined by experiment is the renormalization scale λ , the six effective quark masses m_f and the effective color coupling constant $\alpha_c = 4/3\alpha$.

On how good the above equation simulates the mass spectrum of flavor off-diagonal pseudo-scalar and vector mesons, one has to calculate a concrete example by choosing a specific regulator function. One possible choice would be the soft cut-off

$$R(q^2, \lambda) = R_0(q^2, \lambda) = \frac{\lambda^2}{\lambda^2 + q^2}, \quad (5.2)$$

which immediately implies the usage of a more general cut-off, first introduced in [5]

$$R(q^2, \lambda) = \left[1 + \sum_{n=1}^N (-1)^n s_n \lambda^n \frac{\partial^n}{\partial \lambda^n} \right] R_0(q^2, \lambda) \equiv \mathcal{D}_\lambda^N R_0(q^2, \lambda), \quad (5.3)$$

fulfilling the requirements of a regulator as well. The arbitrary coefficients s_1, \dots, s_N are dimensionless and thus renormalization group invariants. Unsatisfactory is that they are additional parameters, which also need to be fitted to experiment. But by looking more closely at the potential in coordinate space, as well as using the fact that lower meson states show a reasonable agreement between theory and experiment if a pure harmonic oscillator potential is used [8], the number of parameters given by the coefficients s_n , can then be reduced from N down to 2. Following the line of [5], this will be shown next.

The potential in coordinate space is given by the Fourier transform

$$V(r, \lambda) = -\frac{\alpha_c}{2\pi^2} \int d^3q e^{-i\vec{q}\cdot\vec{r}} V(q^2) R(q^2, \lambda). \quad (5.4)$$

It splits up into the triplet potential

$$\begin{aligned} V_t(r, \lambda) &= -\frac{\alpha_c}{2\pi^2} \cdot \mathcal{D}_\lambda^N \int d^3q \frac{e^{-i\vec{q}\cdot\vec{r}}}{q^2} R_0(q^2, \lambda) \\ &\equiv \frac{\alpha_c}{r} \cdot \mathcal{D}_\lambda^N S(r, \lambda), \quad \text{with } S(r, \lambda) = -\frac{2}{\pi} \int_0^\infty dq \frac{\sin(qr)}{q} R_0(q^2, \lambda), \end{aligned} \quad (5.5)$$

5. The Renormalized Singlet-Triplet (ST)-model

and into its singlet potential

$$\begin{aligned}
V_s(r, \lambda) &= -\frac{\alpha_c}{2\pi^2} \cdot \mathcal{D}_\lambda^N \int d^3q e^{-i\vec{q}\cdot\vec{r}} \cdot \left(\frac{1}{q^2} + \xi\right) \cdot R_0(q^2, \lambda) \\
&= \frac{\alpha_c}{r} \cdot \mathcal{D}_\lambda^N S(r, \lambda) - \frac{\alpha_c \xi}{r} \cdot \mathcal{D}_\lambda^N \frac{\partial^2 S(r, \lambda)}{\partial r^2} \\
&= V_t(r, \lambda) - \frac{\xi}{r} \cdot \frac{\partial^2}{\partial r^2} [r \cdot V_t(r, \lambda)].
\end{aligned} \tag{5.6}$$

We clearly see that the singlet potential is fully determined by the triplet potential. In this sense we will investigate only the triplet potential in more detail, since a fixing of $V_t(r, \lambda)$ automatically determines $V_s(r, \lambda)$ according to the above relation.

5.1 Triplet potential

It is convenient to work with a dimensionless radius $R = \lambda r$ and a dimensionless triplet potential by defining

$$W(r, \lambda) := \frac{V_t(r, \lambda)}{\lambda \alpha_c}. \tag{5.7}$$

Performing the integration and the relevant derivatives one obtains

$$W_N(R) = \frac{1}{R} \left(-1 + \mathcal{D}_R^N e^{-R} \right) = \frac{1}{R} \left(-1 + e^{-R} \left[1 + \sum_{n=1}^N s_n R^n \right] \right). \tag{5.8}$$

Since the exponential decays faster than any power at large R , the asymptotic behavior is always like $W_N \sim -1/R$ independent of the numerical value of the coefficients s_n . Thus the arbitrariness of the potential only lies within small R . This behaviour is universal and applies to all possible regulators $R_0(q^2, \lambda)$ one puts into (5.1). It is fully in accord with the regularization scheme given in momentum space: the arbitrariness of regularizing a systems high momenta or energies leads to an arbitrariness in the behaviour at small distances.

Inspired by [8] we use this arbitrariness for small R of W_N , by requiring it to be an oscillator potential up to N -th order

$$W_N(R) = a + b \cdot R^2 + \mathcal{O}(R^N). \tag{5.9}$$

The coefficients s_n are determined by a series expansion of W_N around its regular origin. Thus the number of parameters given by the coefficients s_n is now reduced to only two coefficients a and b to be fixed by experiment: $s_n = s_n(a, b)$ being

$$\begin{aligned}
s_1 &= 1 + a, & s_2 &= \frac{1}{2} + a, \\
\text{and } s_n &= \frac{1}{n!} + \frac{a}{(n-1)!} + \frac{b}{(n-3)!}, & \text{for } n &\geq 3.
\end{aligned} \tag{5.10}$$

5. The Renormalized Singlet-Triplet (ST)-model

In the oscillator model of [8] there are two *universal* parameters in the triplet potential $V_{\text{h.o.}}(r) = c_t + \frac{1}{2}f_t \cdot r^2$. Comparing with the conventions above,

$$V_t(r, \lambda) = \alpha_c \lambda \cdot [a + b \cdot R^2]_{R=\lambda r}, \quad (5.11)$$

we find

$$c_t = \alpha_c \lambda a, \quad f_t = 2\alpha_c \lambda^3 b. \quad (5.12)$$

In addition to the two oscillator parameters, the quark masses have to be fixed as well. In our calculations we will exclude the top-quark, since for such mesons no reliable data is available up to now [3]. Furthermore, we put the mass of the up-quark equal the mass of the down-quark. And since the triplet potential should describe flavor off-diagonal vector mesons, we can fix these six unknowns: m_u, m_s, m_c, m_b and c_t, f_t by using the following six *experimentally inspired* (Appendix F) invariant masses in GeV

$$\begin{aligned} M_{u\bar{d}} &= 0.775, & M_{u\bar{s}} &= 0.891, & M_{u\bar{c}} &= 2.010, & M_{u\bar{b}} &= 5.325, \\ M_{u\bar{d}}^* &= 1.450, & M_{u\bar{s}}^* &= 1.569, & & & & \end{aligned} \quad (5.13)$$

where the star represents its first excited state from the ground state of the relevant flavor sector. The fixing itself is now done by using the simple binding energy formula for the harmonic oscillator, which on the light-cone has the form

$$\begin{aligned} M_n^2 &= m_s^2 + 2m_s \cdot E_n \\ &= m_s^2 + 2m_s \cdot [c_t + (2n + \frac{3}{2}) \cdot \omega] \\ &= (m_1 + m_2)^2 + 2(m_1 + m_2) \cdot \left[c_t + (2n + \frac{3}{2}) \sqrt{\frac{m_1 + m_2}{m_1 m_2}} \cdot \sqrt{f_t} \right], \end{aligned} \quad (5.14)$$

where in the last line $\omega = \sqrt{f_t/m_r}$ has been used. For the ground state the index $n = 0$, while for the first excited state $n = 1$ must be taken. As a result we have to deal with 6 non-linear equations, which can be split up into 4 coupled equations for m_u, m_s, c_t, f_t to be solved first, and then 2 uncoupled equations for m_c, m_b . For the values as in (5.13) the above equations have indeed a unique solution, which numerically can be determined as

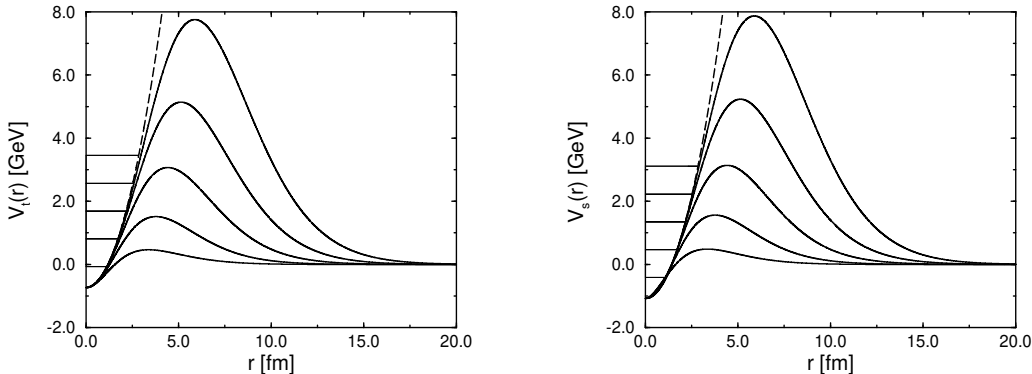
$$\begin{aligned} m_u = m_d &= 0.426, \quad m_s = 0.596, \quad m_c = 1.811, \quad m_b = 5.153 \quad [\text{GeV}] \\ c_t &= -0.735 \text{ GeV}, \quad f_t = 0.0414 \text{ GeV}^3. \end{aligned} \quad (5.15)$$

Up to the N -th order, the triplet potential (5.11) is now uniquely determined, while the asymptotical and mid-range structure of the complete potential (5.7) is still ambiguous. There are infinite many ways how to choose the parameters a, b, λ and α_c to satisfy the conditions (5.12) with the values of (5.15). A great part of this ambiguity is removed by the recent renormalization procedure found for the effective coupling constant [14]. For given effective quark masses as above, and choosing $\lambda = 0.2 \text{ GeV}$ (corresponding roughly to an experimental scale of $r = 1 \text{ fm}$), the effective coupling constant for a typical bound-state calculation (Feynman 4-momentum transfer $Q^2 \sim 0$) takes on the value

$$\alpha \equiv \bar{\alpha}_s(0) = 0.1716. \quad (5.16)$$

5. The Renormalized Singlet-Triplet (ST)-model

Figure 3:



(a) The triplet potential $V_t(r, N)$ is plotted versus r for $N = 8, 7, 6, 5, 4$ (top to bottom). All of them have the same harmonic approximation (dashed) with the first five eigenvalues for $u\bar{d}$ -mesons.

(b) The singlet potential $V_s(r, N)$ for $u\bar{d}$ -mesons is plotted versus r for the values of $N = 8, 7, 6, 5, 4$ (top to bottom) and their harmonic approximation (dashed) with the first five eigenvalues.

Together with $\alpha_c = 4/3\alpha$, the parameters a and b can now be nailed down unambiguously to the values

$$a = -16.053 \quad \text{and} \quad b = 11.298 \tag{5.17}$$

With these values (Fig3a) shows V_t for several N together with their harmonic approximation. The Figure demonstrates the harmonicity of the functions, which grows with increasing N . The functions also have a barrier which grows with increasing N , after which they tend to their asymptotic values $-1/r$. The latter can almost not be seen on the big scales of (Fig3a). The last constraint on the barrier height is fixed, by varying N until we have a satisfying agreement with experiment. As we will see later on,

$$N = 8, \tag{5.18}$$

is a reasonable choice. For $N < 8$ the harmonic approximation is so bad that the lowest states which were used to fix the parameters are too far off. And for $N > 8$ we are already nearly back to the pure oscillator model [8].

Now all parameters of the triplet potential are fixed, but before we turn to solving the bound and scattering region of the full ST-potential, we first want to illustrate the structure of the singlet potential.

5. The Renormalized Singlet-Triplet (ST)-model

5.2 Singlet potential

According to (5.6) the singlet potential is fully determined by the knowledge of the triplet potential, which again was fixed uniquely in the previous section. In other words, we absolutely have no freedom of varying the structure of the singlet potential independently from that of the triplet potential. The only pure singlet parameter $\xi = 1/2m_1m_2$ is already fixed by the mass parameters of the previous section. Looking at its expansion in r up to N -th order in the triplet potential

$$\begin{aligned}
 V_s(r) &= V_t(r) - \frac{\xi}{r} \cdot \frac{\partial^2}{\partial r^2} [r \cdot V_t(r)] \\
 &= \left[c_t + \frac{1}{2} f_t \cdot r^2 + \mathcal{O}(r^N) \right] - \frac{\xi}{r} \cdot \frac{\partial^2}{\partial r^2} \left[c_t \cdot r + \frac{1}{2} f_t \cdot r^3 + \mathcal{O}(r^{N+1}) \right] \\
 &\equiv c_s + \frac{1}{2} f_t \cdot r^2 + \mathcal{O}(r^{N-2}), \quad \text{with } c_s = c_t - 3\xi \cdot f_t,
 \end{aligned} \tag{5.19}$$

also leads to an harmonic approximation in the singlet potential, but only up to the order of $N-2$. Furthermore, it has the same frequency $\omega^2 = f_t/m_r$ as the harmonic triplet approximation, but starts with a deeper lying off-set $c_s < c_t$. (Fig3b) shows the singlet potential for $u\bar{d}$ -mesons with the same parameters as used in (Fig3a).

5.3 Numerical solution

For calculating the bound states of the complete ST-potential with the parameters given above, we see in (Fig3) that the attractive Coulomb part on these scales is so weak that its nearly of no interest for us. In this sense we can asymptotically change the Coulomb interaction by using a shielded one of a Yukawa-type. This really is a help to reduce the amount of numerical work, since it guarantees us not to run into the numerical Coulomb singularity (Appendix E). The same argument also holds for the scattering region of the potential. As we have shown in (Appendix D), the asymptotical part of an attractive Coulomb-like potential does not contribute to the pure resonant part of a cross-section. Changing the troublesome Coulomb interaction in the asymptotical region to a more well-defined interaction like a Yukawa interaction, will only have an effect on background scattering but not on the determination of resonances, as we are interested in.

The problem we face, is thus to change the potential only asymptotically and not to effect the rest, in other words only the pure Coulomb part of the potential should be changed. Since we originally work in momentum space the change is arranged as follows:

$$\begin{aligned}
 V(q^2) \cdot R(q^2, \lambda) &= \left(\frac{1}{q^2} + \xi \right) \cdot \mathcal{D}_\lambda^N R_0(q^2, \lambda) \\
 &\equiv V_t(q^2) \cdot R(q^2, \lambda) + \xi \cdot \mathcal{D}_\lambda^N R_0(q^2, \lambda).
 \end{aligned} \tag{5.20}$$

5. The Renormalized Singlet-Triplet (ST)-model

We clearly see that the entire Coulomb part of the potential can be changed within the pure triplet section

$$\begin{aligned}
 V_i(q^2) \cdot R(q^2, \lambda) &= \frac{1}{q^2} \cdot \mathcal{D}_\lambda^N R_0(q^2, \lambda) \\
 &\equiv \frac{1}{q^2} - \frac{1}{q^2} \left[1 - \mathcal{D}_\lambda^N R_0(q^2, \lambda) \right] \\
 &\simeq \frac{1}{\mu^2 + q^2} - \frac{1}{q^2} \left[1 - \tilde{\mathcal{D}}_\lambda^{N'} R_0(q^2, \lambda) \right], \text{ up to } N'\text{-th order,} \quad (5.21)
 \end{aligned}$$

where the last requirement for $N' \geq N$ in coordinate space

$$\frac{1}{R} \left(-1 + \mathcal{D}_R^N e^{-R} \right) \stackrel{!}{=} \frac{1}{R} \left(-e^{-\eta R} + \tilde{\mathcal{D}}_R^{N'} e^{-R} \right), \quad (5.22)$$

in the sense of a Taylor expansion up to N' -th order with $\eta = \mu/\lambda$, fixes the new coefficients $t_n = t_n(\eta)$

$$\begin{aligned}
 t_1 &= 1 - \eta + a, & t_2 &= \frac{1}{2}(1 - \eta)^2 + a, \\
 t_n &= \frac{1}{n!}(1 - \eta)^n + \frac{a}{(n-1)!} + \frac{b}{(n-3)!}, \text{ for } 3 \leq n \leq N, \\
 \text{and } t_n &= \frac{(-\eta)^n}{n!} + \sum_{i=1}^{n-1} (-1)^{n+i} \frac{s_i - t_i}{(n-i)!}, \text{ for } N \leq n \leq N' \text{ and } s_{i>N} = 0. \quad (5.23)
 \end{aligned}$$

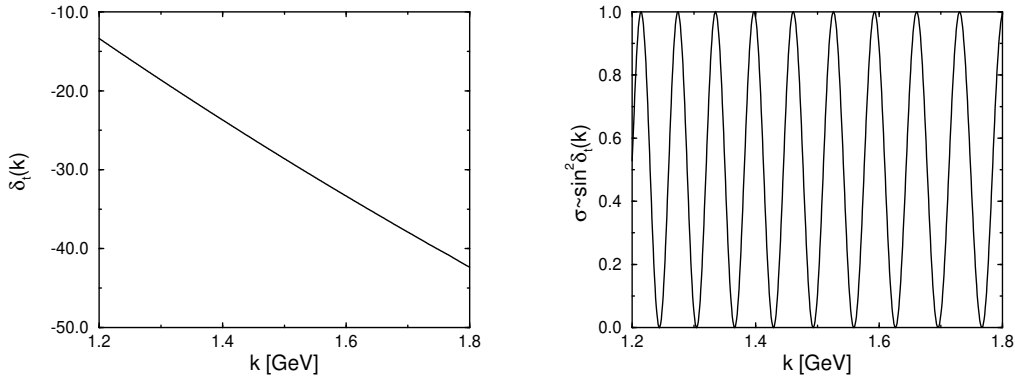
for the η -dependent differential operator $\tilde{\mathcal{D}}_R^{N'} := 1 + \sum_{n=1}^{N'} (-1)^n t_n R^n \partial_R^n$. Since the Coulomb shielding parameter η is dimensionless, it acts as a renormalization invariant. Furthermore, the smaller η is chosen the less correction terms one needs. In the following we will fix $\eta = 0.1$, in which case it is sufficient to add four more correction terms, that means $N' = 12$ if $N = 8$.

If we now start a s-wave bound-state calculation of the Coulomb-shielded ST-potential, it gives us a finite set of possible states. By construction it is not able to create the infinite number of Coulomb-like bound-states. Due to their nearly vanishing energy, as can be seen in (Fig3), we were allowed to adjust the Coulomb tail by a Yukawa shield. On the other hand, for the calculation of possible resonance states, we have prepared the theory in (Appendix D) to do a scattering experiment in momentum space, in other words by calculating the relevant scattering quantities like phase-shift and cross-section in momentum space. Unfortunately, when performing these calculations we can not resolve the resonance spectrum. Due to its very broad and high barrier, the ST-potential as in (Fig3) creates so long-lived resonances as compared to the hadronic interaction times of about 10^{-24} sec, that they nearly can be treated as bound-states. The width and the corresponding lifetime of possible resonances we can easily estimate by using the semi-classical WKB-method [32] for the tunneling probability, given as

$$T(E) \sim e^{-S}, \quad \text{with } S = 2 \int_{r_1}^{r_2} dr \sqrt{2m_r |V(r) - E|}. \quad (5.24)$$

5. The Renormalized Singlet-Triplet (ST)-model

Figure 4:



(a) The triplet phase shift for $u\bar{d}$ -mesons with the same parameter set as given in the previous section, is plotted in the momentum region of $1.2 \leq k \leq 1.8$, corresponding to the scattering energy of about $3.5 \leq E \leq 7.5$. Units are given in GeV.

(b) The triplet cross section for $u\bar{d}$ -mesons with the same parameter set as given in the previous section, is plotted in the momentum region of $1.2 \leq k \leq 1.8$, corresponding to the scattering energy of about $3.5 \leq E \leq 7.5$. Units are given in GeV.

S will be the action integral in units of $\hbar = c = 1$, while $E \geq 0$ is the energy of the scattering particle and $r_1 \geq r_2$ its classical turning points. In order to establish a connection between the tunneling probability and the lifetime of the particle, we imagine in a more classical sense that the particle bounces back and forth within the potentials barrier between r_1 and r_2 and that with every bounce the particle has the probability $T(E)$ to penetrate through the barrier. The time between two bounces is

$$t_0 = \frac{2(r_2 - r_1)}{v}, \quad (5.25)$$

with $v = \sqrt{2E/m_r}$ being the velocity of the particle. Since the particle needs in the mean $1/T$ bounces to penetrate the barrier, it makes sense to define

$$\tau \sim \frac{t_0}{T}, \quad (5.26)$$

as the lifetime of the particle, giving finally the energy width of a resonance as $\Gamma = 1/\tau$. For the width in momentum plane we use (D.84) to get $\gamma = \Gamma/2v$. A numerical evaluation of (5.24) shows that for a possible resonance located at $E = 7$ GeV in (Fig3a), the width is $\Gamma_7 = 6 \cdot 10^{-6}$ GeV ($\tau_7 \sim 3 \cdot 10^{-11}$ sec), while for $E = 6$ GeV it already shrinks down to $\Gamma_6 = 1 \cdot 10^{-12}$ GeV ($\tau_6 \sim 2 \cdot 10^{-4}$ sec). In order to resolve a resonance between these two energy values in a diagram like a cross-section one needs at least a grid size of Γ_6 . But this requires a huge amount of computational time, making here the scattering method for calculating resonances useless. (Fig4) shows the phase-shift and the cross-section for a grid size of 10^{-4} GeV, and as expected the only structure present is background scattering.

5. The Renormalized Singlet-Triplet (ST)-model

Conclusion: To find these resonances one should not use scattering techniques. More promising would be to use bound-state techniques.

Unfortunately the bound-state method described in (Appendix E) does not lead to any success. First of all, we are not able to determine the resonance via reading off the structure of a wavefunction, since we do not know what specific feature a wavefunction in *momentum space* must show in order to be a resonant wavefunction. Second, we can not read it off on the positive continuum eigenvalues, by looking at stable eigenvalues when varying the dimension of the diagonalization space, since an increase in space is directly linked to an increase in integration points and thus will show no other effect than having a better agreement on the relationship $E = k^2/2m_r$. Looking for stable eigenvalues in the continuum can only work if the space within one solves the bound-state equation can be varied independently from the the number of integration points. All in all one has to use alternative momentum space bound-state techniques. Inspired by the calculations of [17], a promising technique is the basis function method. We shall use the simplest momentum space Schrödinger equation, the s-state equation to illustrate the principles of this method. The momentum space Schrödinger equation is related to an integral equation of the form

$$\int_0^\infty dp' p'^2 K(p', p) \phi(p') = E \phi(p), \quad (5.27)$$

where the kernel $K(p', p)$ is symmetric under exchange of p and p' . The idea is now to expand the wave function in a suitable set of basis function $\{g_i\}$ which of course has to be truncated at finite \mathcal{N}

$$\phi(p) = \sum_{i=1}^{\mathcal{N}} c_i g_i(p), \quad (5.28)$$

where c_i are constant coefficients. Substituting this expansion into (5.27)

$$\sum_{i=1}^{\mathcal{N}} c_i \int_0^\infty dp' p'^2 K(p', p) g_i(p') = E \sum_{i=1}^{\mathcal{N}} c_i g_i(p), \quad (5.29)$$

and symmetrizing over i and j by multiplying with $p^2 g_j(p)$ and integrating over p

$$\sum_{i=1}^{\mathcal{N}} c_i \underbrace{\int_0^\infty \int_0^\infty dp' dp p'^2 p^2 K(p', p) g_i(p') g_j(p)}_{A_{ij}} = E \sum_{i=1}^{\mathcal{N}} c_i \underbrace{\int_0^\infty dp p^2 g_i(p) g_j(p)}_{B_{ij}}, \quad (5.30)$$

yields the matrix equation

$$\sum_{i=1}^{\mathcal{N}} A_{ij} c_i = E \sum_{i=1}^{\mathcal{N}} B_{ij} c_i, \quad (5.31)$$

which is symmetric under the exchange of i and j . Then instead of solving for the wave functions, one solves for its expansion coefficients.

5. The Renormalized Singlet-Triplet (ST)-model

According to [18] this matrix equation is a generalized eigenproblem

$$\mathbf{A} \cdot \mathbf{c} = E \mathbf{B} \cdot \mathbf{c}, \quad (5.32)$$

where \mathbf{c} is the eigenvector and E the same eigenvalue as the original equation (5.27). In addition to the symmetry condition of the matrices \mathbf{A} and \mathbf{B} , the latter must also be positive definite to ensure that the eigenvalues are all real. For more details on this and how to solve the equation via a symmetric diagonalization one can consult [18].

The matrix equation can be simplified drastically if its possible to choose such a set of basis functions that \mathbf{B} becomes the unity matrix: $B_{ij} = \delta_{ij}$. We then have an ordinary symmetrical eigenvalue equation that can be solved as usual.

Clearly, the big advantage of this basis function method is that diagonalization and integration represent two different spaces which can be varied independently in their dimension, thus as already told, making it ideal for searching at stable eigenvalues in the continuous spectrum of an system. Furthermore, the accuracy of this technique depends very much on the choice of the expansion functions $g_i(p)$. Obviously, one will be inclined to choose functions suitable to the physical problem being studied. In our case the best choice is certainly to take the radial s-wave harmonic oscillator functions $g_i(p) = R_i(p)$, which in momentum space

$$R_i(p) = Z_i \cdot e^{-\frac{1}{2}\sigma^2 p^2} \cdot L_i^{(\frac{1}{2})}(\sigma^2 p^2), \quad \text{with } 1/\sigma^2 = m_r \omega, \quad (5.33)$$

for ($i=0,1,2,\dots$) are of identical structure as in coordinate space, namely correlated to the generalized Laguerre functions

$$u_i^{(\nu)}(x) = N_i^{(\nu)} \cdot x^{\nu/2} \cdot e^{-x/2} \cdot L_i^{(\nu)}(x), \quad \text{with } N_i^{(\nu)} = \sqrt{\frac{\Gamma(1+i)}{\Gamma(1+i+\nu)}}, \quad (5.34)$$

which form an orthonormal

$$\int_0^\infty dx u_i^{(\nu)}(x) \cdot u_j^{(\nu)}(x) = \delta_{ij}, \quad (5.35)$$

and complete set

$$\sum_{i=0}^\infty u_i^{(\nu)}(x) \cdot u_i^{(\nu)}(x') = \delta(x - x'), \quad (5.36)$$

of functions. The harmonic oscillator functions in momentum space are given by the special case $\nu = \frac{1}{2}$ and $x = \sigma^2 p^2$. With these values the orthonormal condition can be written as

$$\begin{aligned} \delta_{ij} &= N_i^{(\frac{1}{2})} \cdot N_j^{(\frac{1}{2})} \cdot \int_0^\infty d(\sigma^2 p^2) \sigma p \cdot e^{-\sigma^2 p^2} \cdot L_i^{(\frac{1}{2})}(\sigma^2 p^2) \cdot L_j^{(\frac{1}{2})}(\sigma^2 p^2), \\ &= \tilde{N}_i \cdot \tilde{N}_j \cdot \int_0^\infty dp p^2 \cdot e^{-\sigma^2 p^2} L_i^{(\frac{1}{2})}(\sigma^2 p^2) \cdot L_j^{(\frac{1}{2})}(\sigma^2 p^2), \end{aligned} \quad (5.37)$$

meaning that with the normalization choice of $Z_i = \tilde{N}_i = \sigma \sqrt{2\sigma} \cdot N_i^{(\frac{1}{2})}$ in the basis functions of (5.33) will lead to the simplifying result of $B_{ij} = \delta_{ij}$ in (5.30).

5. The Renormalized Singlet-Triplet (ST)-model

When testing the Basis-Function-code, numerical stability within 5 digits of precision for the first 4 eigenvalues is already achieved by using eight basis functions $\mathcal{N} = 8$ and 128 gaussian integration points.

5.4 Comparing with experiment

At last we can represent the calculated energy eigenvalues and the corresponding invariant mass eigenvalues of the complete renormalized ST-potential (5.1).

The following tables show a typical output in GeV for every flavor combination. The second and third line of each table are the numerical calculations for the first eigenvalues, while the fourth line is an attempt to identify the relevant mesons with our ST-model. Their precise experimental values are listed in (Appendix F). The lower part of each table shows the analytical eigenvalues of the pure harmonic oscillator. The singlet data is given on the left, triplet data on the right of each sector.

Table 1: $u\bar{d}$ -mesons [GeV]

| $n^{2S+1}L_J$ | $1^1S_0 1^3S_1$ | $2^1S_0 2^3S_1$ | $3^1S_0 3^3S_1$ | $4^1S_0 4^3S_1$ |
|-------------------|------------------------|---------------------------|---------------------------|--------------------|
| E_n | -0.414 -0.074 | 0.470 0.803 | 1.351 1.671 | 2.221 2.523 |
| M_n | 0.140 0.774 | 1.236 1.447 | 1.740 1.890 | 2.124 2.242 |
| Exp. | $\pi^\pm \rho(770)$ | $\pi(1300) \rho(1450)$ | $\pi(1800) \rho(1900)$ | — — |
| M_n^{HO} | 0.134 0.775 | 1.233 1.450 | 1.738 1.898 | 2.127 2.260 |

Table 2: $u\bar{s}$ -mesons [GeV]

| $n^{2S+1}L_J$ | $1^1S_0 1^3S_1$ | $2^1S_0 2^3S_1$ | $3^1S_0 3^3S_1$ | $4^1S_0 4^3S_1$ |
|-------------------|---------------------|------------------------|--------------------|--------------------|
| E_n | -0.366 -0.123 | 0.451 0.690 | 1.264 1.495 | 2.069 2.289 |
| M_n | 0.544 0.891 | 1.402 1.567 | 1.905 2.025 | 2.296 2.392 |
| Exp. | $K^\pm K^*(892)$ | $K(1460) K^*(1680)$ | $K(1830) $ — | — — |
| M_n^{HO} | 0.543 0.891 | 1.401 1.569 | 1.905 2.032 | 2.302 2.408 |

5. The Renormalized Singlet-Triplet (ST)-model

Table 3: This is an illustrative presentation of the Tables 1&2. The dotted lines are the calculated mass values which are shown next to the experimental measured mass values. The three vector mesons $\rho(1700)$, $\rho(2150)$ and $K^*(1410)$ (labeled with an empty circle) might be D-wave mesons [3], while the scalar meson $K(1630)$ (labeled with an empty triangle) might not be a pseudo-scalar, since the value of J^P is still unknown [3].

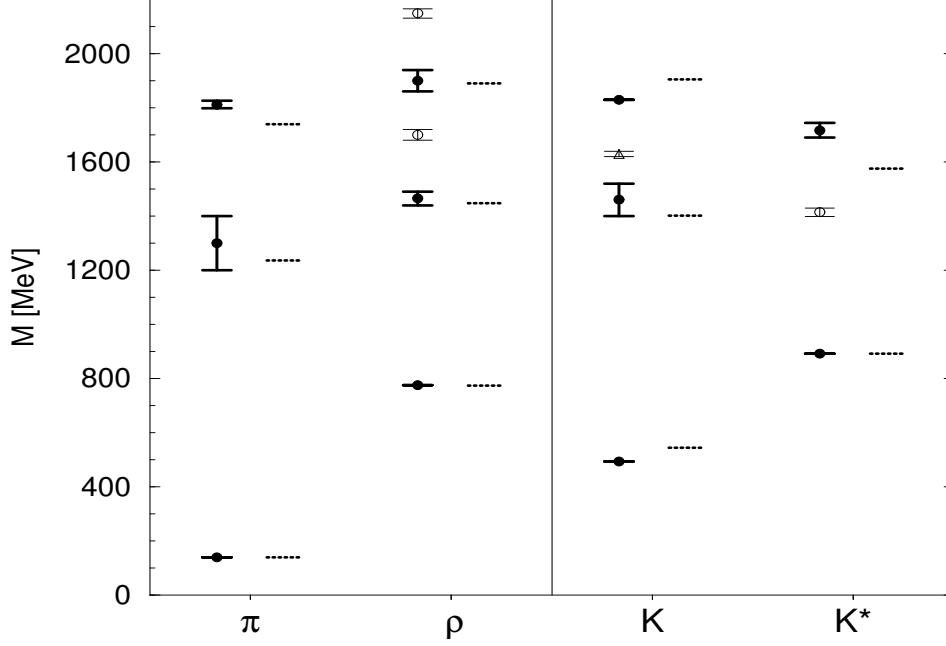


Table 4: $u\bar{c}$ -mesons [GeV]

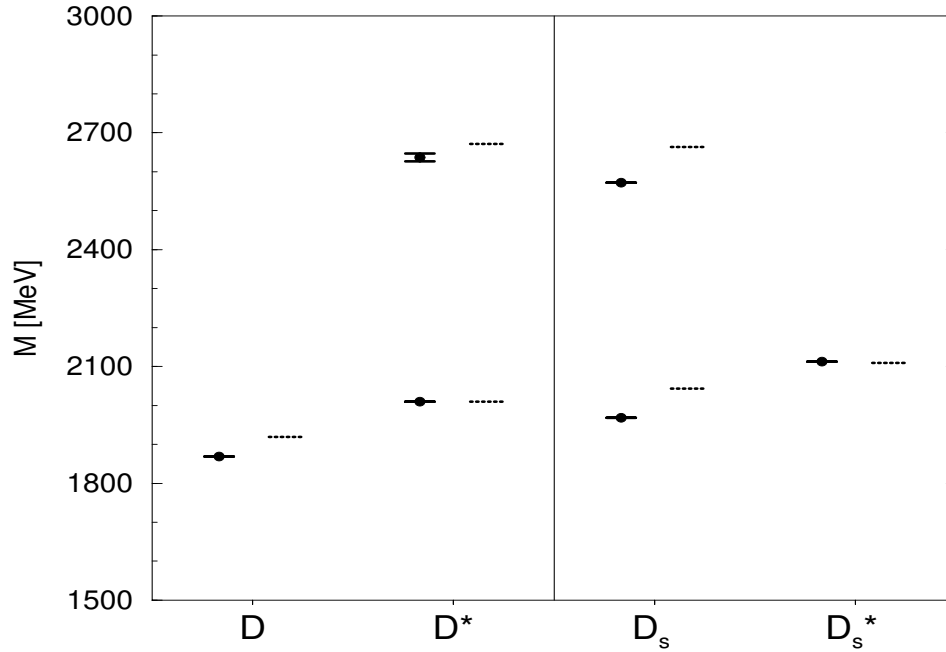
| $n^{2S+1}L_J$ | $1^1S_0 1^3S_1$ | $2^1S_0 2^3S_1$ | $3^1S_0 3^3S_1$ |
|-------------------|----------------------|--------------------|--------------------|
| E_n | -0.296 -0.215 | 0.396 0.476 | 1.085 1.163 |
| M_n | 1.919 2.010 | 2.603 2.671 | 3.140 3.195 |
| Exp. | $D^\pm D^*(2010)$ | — $D^*(2640)$ | — — |
| M_n^{HO} | 1.919 2.010 | 2.604 2.672 | 3.143 3.200 |

5. The Renormalized Singlet-Triplet (ST)-model

Table 5: $s\bar{c}$ -mesons [GeV]

| $n \ ^{2S+1}L_J$ | $1 \ ^1S_0 \parallel 1 \ ^3S_1$ | $2 \ ^1S_0 \parallel 2 \ ^3S_1$ | $3 \ ^1S_0 \parallel 3 \ ^3S_1$ |
|-------------------|---------------------------------|----------------------------------|---------------------------------|
| E_n | -0.337 -0.279 | 0.270 0.327 | 0.875 0.931 |
| M_n | 2.043 2.109 | 2.664 2.714 | 3.163 3.205 |
| Exp. | $D_s^\pm \parallel D_s^*$ | $D_s(2573) \parallel \text{---}$ | --- --- |
| M_n^{HO} | 2.043 2.110 | 2.664 2.716 | 3.166 3.209 |

Table 6: This is an illustrative presentation of the Tables 4&5. The dotted lines are the calculated mass values which are shown next to the experimental measured mass values.



5. The Renormalized Singlet-Triplet (ST)-model

Table 7: $u\bar{b}$ -mesons [GeV]

| $n^{2S+1}L_J$ | $1^1S_0 1^3S_1$ | $2^1S_0 2^3S_1$ |
|-------------------|--------------------|--------------------|
| E_n | $-0.277 -0.248$ | $0.371 0.399$ |
| M_n | $5.295 5.325$ | $5.938 5.964$ |
| Exp. | $B^\pm B^*$ | $— —$ |
| M_n^{HO} | $5.295 5.325$ | $5.939 5.966$ |

Table 8: $s\bar{b}$ -mesons [GeV]

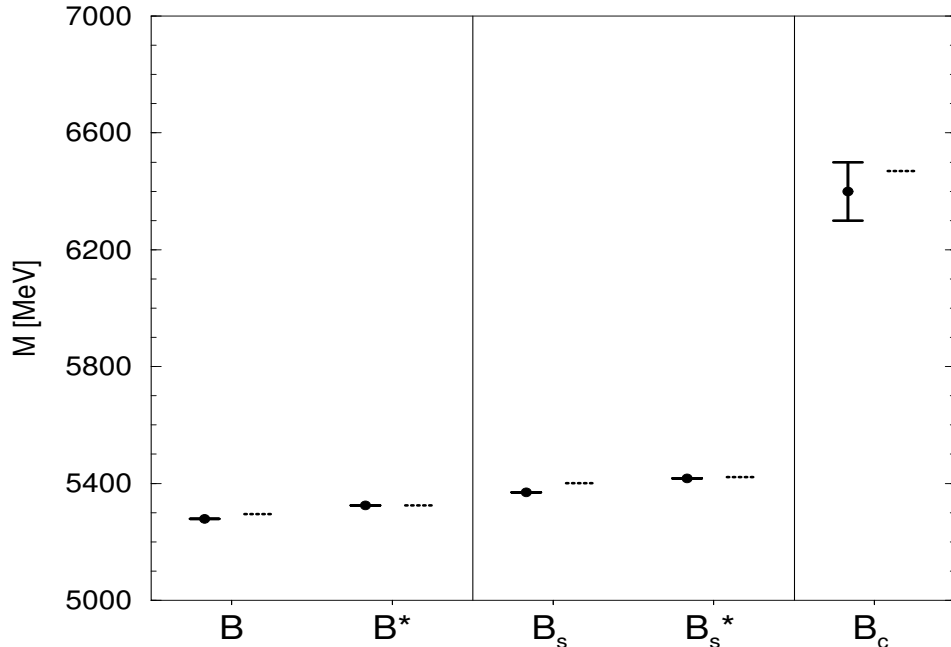
| $n^{2S+1}L_J$ | $1^1S_0 1^3S_1$ | $2^1S_0 2^3S_1$ |
|-------------------|--------------------|--------------------|
| E_n | $-0.337 -0.317$ | $0.218 0.238$ |
| M_n | $5.401 5.422$ | $5.963 5.983$ |
| Exp. | $B_s B_s^*$ | $— —$ |
| M_n^{HO} | $5.401 5.423$ | $5.964 5.983$ |

Table 9: $c\bar{b}$ -mesons [GeV]

| $n^{2S+1}L_J$ | $1^1S_0 1^3S_1$ | $2^1S_0 2^3S_1$ |
|-------------------|--------------------|--------------------|
| E_n | $-0.478 -0.471$ | $-0.125 -0.119$ |
| M_n | $6.469 6.476$ | $6.838 6.844$ |
| Exp. | $B_c —$ | $— —$ |
| M_n^{HO} | $6.469 6.476$ | $6.836 6.843$ |

5. The Renormalized Singlet-Triplet (ST)-model

Table 10: This is an illustrative presentation of the Tables 7, 8 and 9. The dotted lines are the calculated mass values which are shown next to the experimental measured mass values.



Discussion: We were able to calculate 22 mesons, which could be identified to experiment with an error less than 5%, except for some $u\bar{s}$ -mesons in (Table 2) with an error of about 10%.

For a crude model like the ST-model with its 8 parameters (if $m_u = m_d$ and if m_t is excluded) this is quite remarkable. The calculated masses are very sensitive to the initial choice of how the parameters are fixed. It might be just possible that the error can still be reduced by using a different fixing set than that given in (5.13).

The intention of this section was not to present the best fit, it rather wanted to show how the ST-model is able to quantitatively reproduce the mass-spectrum of flavor off-diagonal mesons. Furthermore, looking for a best fit one should also compare the mass-spectrum for different regulating functions $R_0(q^2, \lambda)$. There is no argument why the soft regulator (5.2) is predestinated to be the ideal regulator.

When comparing the first three analytical eigenvalues of the pure harmonic oscillator (given in the last row of the relevant tables) with the calculated ones, we see, that its almost unnecessary to go onto the computer, especially for the heavy mesons. For those, the calculated values are nearly identical with the harmonic ones. This certainly has to do with the rather large value of the parameter N , which controls the harmonicity of the ST-potential. The biggest difference of about 4% can be seen for the lightest meson, the pion.

5. The Renormalized Singlet-Triplet (ST)-model

The comparison between the ST-model and the oscillator model [8] certainly becomes more interesting when choosing $N \leq 8$, but with the parameter set (5.15) and (5.16), which can be chosen independently from N , the deviations to experiment are starting to get worse the more N is decreased.

More interesting would be to keep the harmonicity as that of $N = 8$, but to reduce the barrier width — in other words: keeping the same overall structure as shown in (Fig3), except with a smaller width. This can be achieved when choosing for example a gaussian function $R_0(q^2, \lambda) = e^{-q^2/\lambda^2}$ as a generating regulator in (5.3). The result is a width reduction of a factor 2. This statement should only emphasize that there are maybe many regulators out there, which on the level of the ST-model could improve the oscillator model of [8] in a promising way.

6 Summary and Discussion

The novel aspect of this thesis, was to show how renormalization works in a non-perturbative context within a Hamiltonian approach. It was exemplified by means of the oversimplified ST-model. Two complementary renormalization schemes were used, one more illustratively and the other in a more abstract way, to show how the renormalization program is performed and at the end leading to the same physics. Since both renormalization schemes have been implemented in momentum space, the generalization to the full relativistic case can be easily performed. Even more, these renormalization schemes are not restricted to any certain Hamiltonian model but can be applied to any Hamiltonian eigenvalue equation, for example as to our master equation given in (3.1) or to a even more general equation.

We then tested the ST-model by trying to quantitatively reproduce the mass spectrum of flavor off-diagonal mesons. Nearly all experimentally available mesons, from the light π to the heavy B , could be calculated by the simple 8-parametrical ST-model within an error less than 5%, except for some strange pseudo-scalar mesons in (Table 2) having an error of about 10%. Its not impossible that the error can still be reduced by using better fitting techniques or different regulators.

The mass spectrum was calculated in momentum space by using the bound-state technique of orthogonal basis functions. From our diploma student Harun Omer I have learned that this technique is indeed successful in finding resonances as stable eigenvalues in the continuous part of the spectrum, who calculated the mass spectrum with a different parameter set in coordinate space [17]. Unfortunately, the determination of resonances did not lead to any success when doing a scattering calculation. In any physical parameter set for mesons, the ST-potential produces resonances of such an extreme small width that they nearly can be treated as bound-states (compared to typical hadronic interaction times). A quark scattering calculation is thus condemned to fail. This justifies to see the ST-potential as a quark-confining potential. A recombination of quarks into new mesons is enormously much faster (hadronic interaction time $\sim 10^{-24}$ sec) than the process of separation (ST-resonance lifetime $\sim 10^{-6}$ sec).

For the first time, the simple ST-model let us understand how explicit renormalization works in a Hamiltonian formulation. Furthermore, it is able to show the essential mass splitting between the pseudo-scalar mesons and the vector mesons by the hyperfine interaction in the triplet part of the potential. Finally, it gives us confinement, in the sense that a forever rising potential is not necessary. But at foremost, the ST-model has the great advantage of showing a well-defined relation to QCD. Certainly, the ST-model is an oversimplified model, but there are no conceptual problems to relax the relevant simplifications in order to create a more general model. Restoring the full relativistic case and in the next step including the full spinor structure are well defined prescriptions.

First attempts were made by our postdoctorate Shan-Gui Zhou who started to calculate the relativistic ST-model. Great progress was made in the work of [19], where the authors showed how in general the singlet part can be decoupled from the triplet part

6. Summary and Discussion

within the full spinor interaction, by making use of unitary transformations. The last important step to complete the meson model would be to include the annihilation graph. This allows us to determine the mass spectrum for mesons of equal flavor in quark and anti-quark. This big project is now under the hand of our diploma student Christian Krahl.

Certainly, in order to have a serious meson model it must go beyond a simple mass spectrum fitting. It must also be able to probe the internal structure of mesons as well. For this the corresponding wave functions have to be investigated. Since we are in possession of the frame-independent light-cone wave functions, we are able to predict hadronic properties like form factors and distribution amplitudes [20]. We are lucky to compare our results with the experiments of [21]. To fit the ST-model wave function according to Asherys experimentally measured pion wave function over a large momentum range, is the present work of Harun Omer.

We see that there is still a lot of work to be done in the future. Up to now, we can say that we understand better the process of how to start from a quantum field theory like QCD, deriving an effective constituent quark model having the shape of a Schrödinger equation, performing a non-perturbative renormalization scheme and finally to compare it with the experimentally available hadron world.

A Relativistic Dynamics

According to the principle of relativity there are certain frames of reference, called inertial frames, which are equivalent. This means that coordinates x^μ in one inertial frame and x'^μ in another inertial frame must leave the scalar product invariant by satisfying the condition

$$g_{\mu\nu}dx^\mu dx^\nu = g_{\mu\nu}dx'^\mu dx'^\nu, \quad (\text{A.1})$$

where $g_{\mu\nu} = g^{\mu\nu}$ is the metric tensor. A coordinate transformation $x^\mu \rightarrow x'^\mu$ between inertial frames can only be of a linear form

$$x'^\mu = \Lambda^\mu{}_\nu x^\nu + a^\mu, \quad (\text{A.2})$$

where a^μ is a constant four-vector and $\Lambda^\mu{}_\nu$ is a constant 4×4 -matrix, which according to (A.1) must satisfy the following pseudo-orthogonality relation

$$g_{\mu\nu}\Lambda^\mu{}_\rho\Lambda^\nu{}_\sigma = g_{\rho\sigma} \quad \text{or} \quad \Lambda^T g \Lambda = g, \quad (\text{A.3})$$

which in turn implies the following structure for its inverse

$$(\Lambda^{-1})^\mu{}_\nu = g_{\nu\alpha}\Lambda^\alpha{}_\beta g^{\beta\mu} \equiv \Lambda_\nu{}^\mu. \quad (\text{A.4})$$

The linear transformations (Λ, a) form a group, known as the Poincaré group. An important subgroup is the Lorentz group with no space-time translations $a = 0$. In the following we will only consider proper ($\det\Lambda = 1$) and orthochronous ($\Lambda_0^0 \geq 1$) Lorentz transformations, that means we exclude space and time reflections. From the 16 matrix elements Λ only 6 are independent, due to the symmetric condition (A.3). So, every Poincaré transformation is specified by 10 real parameters which can be varied independently: 4 translations a_μ , 3 Euler angles θ_k , and 3 boosts or rapidity angles η_k , which define relative to the speed of light, the velocity $\vec{v} = \tanh \vec{\eta}$ between the inertial frames.

Furthermore, the transformations (Λ, a) induce unitary operators $U^{-1}(\Lambda, a) = U^\dagger(\Lambda, a)$ in a Hilbert space, where its vectors and operators transform as

$$|\Phi'\rangle = U(\Lambda, a)|\Phi\rangle \quad ; \quad \mathcal{O}' = U(\Lambda, a)\mathcal{O}U^\dagger(\Lambda, a). \quad (\text{A.5})$$

The operators U satisfy a composition rule for two successive transformations

$$U(\Lambda', a')U(\Lambda, a) = U(\Lambda'\Lambda, \Lambda'a + a'), \quad (\text{A.6})$$

which easily follows from (A.2). Using the identical transformation $U(1, 0)$ the inverse of $U(\Lambda, a)$ can be expressed as

$$U^{-1}(\Lambda, a) = U(\Lambda^{-1}, -\Lambda^{-1}a). \quad (\text{A.7})$$

A. Relativistic Dynamics

$U(\Lambda, a)$ is a local operator which transforms functions and coordinates simultaneously about a fixed point in space-time. Since a state vector Φ in the Schrödinger picture transforms in the same way as an operator \mathcal{O} in the Heisenberg picture [22],[23], we will collectively call them fields Ψ . In the coordinate representation they transform according to the following *covariant* rule

$$\begin{aligned} \Psi'(x') & \underset{\text{passive}}{=} D(\Lambda) \cdot \Psi(x) = D(\Lambda) \cdot \Psi(\Lambda^{-1}(x' - a)) \\ \Psi'(x) & \underset{\text{active}}{=} D(\Lambda^{-1}) \cdot \Psi(\Lambda x + a), \end{aligned} \tag{A.8}$$

where we have collected the fields in a column vector on which the matrix $D(\Lambda)$ can act, which again is a finite dimensional matrix representation of the Lorentz group. Translations can be excluded for pure field transformations, since all fields will behave as a scalar. There are many such representations, including the scalar $D(\Lambda) = \mathbb{1}$, the 4-vector $D(\Lambda) = \Lambda$, the Dirac-spinor $D(\Lambda) = S(\Lambda)$ or the 2-rank tensor $D(\Lambda) = \Lambda \otimes \Lambda$, just to name a few. Furthermore, this covariant transformation for fields is not restricted to coordinate space (x^μ) only. For example, doing a covariant Fourier transformation one immediately gets the corresponding rules for the conjugate energy-momentum representation (p^μ).

Under a passive transformation rule we in general understand, that *one* physical system is being described from *two* different frames which are separated by a Poincaré transformation. Thus Ψ' and Ψ represent the same field only evaluated in two different frames. While under an active transformation rule we look at *two* physical systems, which are also separated by a Poincaré transformation, but only from *one* frame. This transformation is thus ideal for investigating the property of *invariance* on fields, since here Ψ' and Ψ in general represent different fields. We can talk of an Poincaré-invariant field Ψ if its actively transformed field stays invariant $\Psi' = \Psi$.

We now return to the coordinate transformation (A.2) by looking at the transformation near the identity

$$\Lambda^\mu{}_\nu = \delta^\mu{}_\nu + \omega^\mu{}_\nu \quad ; \quad a^\mu = \epsilon^\mu \tag{A.9}$$

where $\omega^\mu{}_\nu$ and ϵ^μ are 20 sufficiently small real parameters. Plugging this transformation into (A.3) we get up to linear order in ω the antisymmetry condition $\omega^\mu{}_\nu = -\omega^\nu{}_\mu$, leaving again as already known, all together 10 transformation parameters independent. Since $U(1, 0)$ is the identity operator and since the parameters ω and ϵ can be varied independently, the unitary operator $U(1 + \omega, \epsilon)$ near its identity up to first order can be written as

$$U(1 + \omega, \epsilon) = 1 + i \cdot G(\omega, \epsilon) = 1 + \frac{1}{2} i \omega_{\mu\nu} M^{\mu\nu} + i \epsilon_\mu P^\mu, \tag{A.10}$$

This expansion defines 10 parameter independent operators $M^{\mu\nu} = -M^{\nu\mu}$ and P^μ , also known as the generators of the Poincaré group, which are of fundamental importance in any relativistic theory. They are Hermitian operators in all indices and represent observable physical quantities.

A. Relativistic Dynamics

Due to its correlation with the 4 translation parameters, P^μ can be identified as the total energy-momentum 4-vector of the field system. The pure spatial 3-vector $\vec{J} = (M^{23}, M^{31}, M^{12})$, being correlated with the 3 spatial rotation parameters, can be identified as the total angular momentum of the field, while the remaining space-time generators $\vec{K} = (M^{10}, M^{20}, M^{30})$, form what is called the Boost 3-vector.

By working out the product $U(\Lambda, a)U(1 + \omega, \epsilon)U^{-1}(\Lambda, a)$ via (A.6), (A.7) and (A.10), where (Λ, a) are the parameters of a new full transformation, will give after a comparison of the independent coefficients ω and ϵ up to first order the following result

$$\begin{aligned} U(\Lambda, a)M^{\mu\nu}U^{-1}(\Lambda, a) &= \Lambda_\rho{}^\mu\Lambda_\sigma{}^\nu(M^{\rho\sigma} + a^\rho P^\sigma - a^\sigma P^\rho) \\ U(\Lambda, a)P^\mu U^{-1}(\Lambda, a) &= \Lambda_\rho{}^\mu P^\rho. \end{aligned} \quad (\text{A.11})$$

For pure Lorentz transformations with $a^\mu = 0$, these transformation rules simply say that $M^{\mu\nu}$ is a tensor and P^μ is a vector. For pure translations with $\Lambda^\mu{}_\nu = \delta^\mu{}_\nu$, they tell us that P^μ is translation-invariant, but $M^{\mu\nu}$ not.

Next, lets apply the rules (A.11) to a transformation that is itself infinitesimal, that means $\Lambda^\mu{}_\nu = \delta^\mu{}_\nu + \omega^\mu{}_\nu$ and $a^\mu = \epsilon^\mu$, with infinitesimals $\omega^\mu{}_\nu$ and ϵ^μ unrelated to the previous ω and ϵ . Keeping only terms of first order in these independent parameters and then equating their coefficients on both sides, we find the following commutations

$$\begin{aligned} i[M^{\mu\nu}, M^{\rho\sigma}] &= g^{\nu\rho}M^{\mu\sigma} - g^{\mu\rho}M^{\nu\sigma} - g^{\sigma\mu}M^{\rho\nu} + g^{\sigma\nu}M^{\rho\mu} \\ i[P^\mu, M^{\rho\sigma}] &= g^{\mu\rho}P^\sigma - g^{\mu\sigma}P^\rho \\ [P^\mu, P^\nu] &= 0. \end{aligned} \quad (\text{A.12})$$

This is the Lie algebra of the Poincaré group, which is shortly called Poincaré algebra.

The Poincaré algebra alone does not tell us anything about covariance. For this, we look again at the transformation rules (A.8) to study in which way the generators G have to act on the fields Ψ , in order to guarantee covariance.

a): First we look at the state-vectors $|\Phi\rangle$ in the Schrödinger picture, for which according to (A.5), we can define the following total infinitesimal variation around a fixed space-time point

$$\delta|\Phi\rangle := |\Phi'\rangle - |\Phi\rangle = iG(\omega, \epsilon) \cdot |\Phi\rangle, \quad (\text{A.13})$$

where $G(\omega, \epsilon) = \frac{1}{2}\omega_{\mu\nu}M^{\mu\nu} + \epsilon_\mu P^\mu$. Since ω and ϵ can be varied independently the total variation within a passive transformation in coordinate space will read

$$\begin{aligned} \delta\Phi_r(x) &= D(1 + \omega)_{rs}\Phi_s(x + \omega^{-1}x - \epsilon) - \Phi_r(x) \\ &= (\delta_{rs} + \frac{1}{2}i\omega_{\mu\nu}[\Sigma_{rs}]^{\mu\nu}) \cdot \Phi_s(x^\mu + \omega_\nu{}^\mu x^\nu - \epsilon^\mu) - \Phi_r(x) \\ &= \frac{1}{2}i\omega_{\mu\nu}[\Sigma_{rs}]^{\mu\nu}\Phi_s(x) + \frac{1}{2}\omega_{\mu\nu}(x^\mu\partial^\nu - x^\nu\partial^\mu)\Phi_r(x) - \epsilon_\mu\partial^\mu\Phi_r(x). \end{aligned} \quad (\text{A.14})$$

Comparing (A.14) with (A.13), will give the covariant identities

$$\begin{aligned} iM^{\mu\nu}\Phi_r(x) &= i[\Sigma_{rs}]^{\mu\nu}\Phi_s(x) + (x^\mu\partial^\nu - x^\nu\partial^\mu)\Phi_r(x) \\ iP^\mu\Phi_r(x) &= -\partial^\mu\Phi_r(x). \end{aligned} \quad (\text{A.15})$$

A. Relativistic Dynamics

In coordinate space P^μ has the well known operator representation $i\partial^\mu$, while the representation of $M^{\mu\nu}$ can be split up into two parts: $M^{\mu\nu} = S^{\mu\nu} + L^{\mu\nu}$. Acting only on the coordinates of a field, the operator $L^{\mu\nu} = -i(x^\mu\partial^\nu - x^\nu\partial^\mu)$ depends explicitly on the choice of the origin of the coordinate system. Furthermore, it vanishes if $\Phi(x)$ is spherically symmetric in its space-time dependence. For these reasons, we identify this term with the orbital angular momentum. In contrast, the other term being a finite dimensional matrix representation acting only on discrete components of the field, does not depend on the origin of the coordinate frame and is determined solely by the transformation properties of the field functions. Hence, we identify it with the spin angular momentum $S^{\mu\nu} = \Sigma^{\mu\nu}$ of the field system. The explicit structure of the spin part certainly depends on the field representation one uses, for example

$$[S_{\alpha\beta}]^{\mu\nu} = -\frac{1}{4}i[\gamma^\mu, \gamma^\nu]_{\alpha\beta} \quad \text{or} \quad [S_{\rho\sigma}]^{\mu\nu} = -i[g_\rho^\mu g_\sigma^\nu - g_\sigma^\mu g_\rho^\nu], \quad (\text{A.16})$$

depending on whether $\Phi(x)$ refers to a spinor or to vector field, respectively. We observe here that a separate decomposition of angular momentum into orbital and spin part is, of course, not a covariant procedure. Also, if $M^{\mu\nu}$ represents a conserved quantity, neither of its decomposed parts are conserved separately. Furthermore, all these coordinate space representations must certainly satisfy the same commutation relations as their general operators in (A.12) do.

b): Now we look at Hilbert space operators \mathcal{O} in the Heisenberg picture. The total variation as given in (A.13) must now be adjusted accordingly to the transformation property of operators

$$\delta\mathcal{O} := \mathcal{O}' - \mathcal{O} = i[G, \mathcal{O}], \quad (\text{A.17})$$

which immediately yields the following covariant identities in coordinate space

$$\begin{aligned} i[M^{\mu\nu}, \mathcal{O}_r(x)] &= i[\Sigma_{rs}]^{\mu\nu} \mathcal{O}_s(x) + (x^\mu\partial^\nu - x^\nu\partial^\mu)\mathcal{O}_r(x) \\ i[P^\mu, \mathcal{O}_r(x)] &= -\partial^\mu\mathcal{O}_r(x). \end{aligned} \quad (\text{A.18})$$

Summary: A correct relativistic treatment of a any physical system is only given, if the corresponding Poincaré generators are not only consistent with the commutation relations (A.12), but also respect the covariant relations (A.15) and (A.18). A realization of the Poincaré algebra alone is not sufficient, as for certain systems it can happen that their Poincaré generators fulfill the commutation relations but spoil covariance. According to [2] "covariance is an additional requirement, which in contrast to the Poincaré algebra strongly restricts possible relativistic dynamics". It is not surprising that covariance imposes so severe restrictions, because on top of the general group properties (A.6), (A.10), which suffices to derive the Poincaré algebra, covariance requires an additional transformation rule (A.8) which includes a finite representation of the Lorentz group.

But we observe that nothing up to this point gives us any indication as to how these fundamental operators ($M^{\mu\nu}, P^\mu$) can be explicitly constructed. Indeed, this construction will depend entirely on the dynamical characteristics of the system we want to impose, which we have so far not even considered. Once constructed and satisfying

A. Relativistic Dynamics

all requirements discussed above, the relations (A.15) and (A.18) turn into generalized covariant Schrödinger and Heisenberg equations, respectively.

We will now address this problem of constructing the generators $(M^{\mu\nu}, P^\mu)$, by firstly considering the most simplest case, namely that of a *free* one-particle state $|\Phi_0\rangle$ in the Heisenberg picture, being totally independent of any dynamical development. If the particle is a scalar, we can identify

$$P^\mu = p^\mu \quad ; \quad M^{\mu\nu} = L^{\mu\nu} = x^\mu p^\nu - x^\nu p^\mu, \quad (\text{A.19})$$

where x^μ is the usual space-time point, with $p^\mu = d(mx^\mu)/d\tau$ as its conjugate momentum; $d\tau$ being the proper time increment and m the rest mass of the particle. Since they must satisfy the quantization condition $[x^\mu, p^\nu] = ig^{\mu\nu}$, it is easily confirmed that this identification of the generators lead to the correct requirements for a relativistic quantum mechanical system as stated above. This is certainly also true, if we include a spin operator $M^{\mu\nu} = S^{\mu\nu} + L^{\mu\nu}$, where $S^{\mu\nu}$ satisfies the Poincaré algebra and for which a finite dimensional matrix representation of the Lorentz group exists. Furthermore, the 10 independent generators P^μ , $\vec{J} = \vec{S} + \vec{L}$ and \vec{K} must be constants of motion. Since they are Hermitean operators with real eigenvalues, it is advantageous to construct representations in which the constants of motion are diagonal. This allows a labeling of the state vectors with quantum numbers. But one cannot diagonalize all ten constants of motion simultaneously because they do not commute. One has to make a choice.

Since P^0 and P^k commute, we shall use energy and momentum eigenvalues as labels, and thus select the energy-momentum representation, which in this context is a more natural one than the coordinate space representation. As momentum and angular momentum do not commute, it is convenient to introduce the Pauli-Lubanski vector, defined as

$$W^\mu = -\frac{1}{2}\epsilon^{\mu\nu\rho\sigma} P_\nu M_{\rho\sigma} = -\frac{1}{2}\epsilon^{\mu\nu\rho\sigma} P_\nu S_{\rho\sigma}, \quad (\text{A.20})$$

where $\epsilon_{\mu\nu\rho\sigma}$ is the totally antisymmetric symbol in four dimensions. W^μ is orthogonal to the generalized momenta, $W^\mu P_\mu = 0$, and obeys the algebra

$$\begin{aligned} [P^\mu, W^\nu] &= 0 \\ [W^\rho, M^{\mu\nu}] &= i(g^{\nu\rho}W^\mu - g^{\mu\sigma}W^\nu) \\ [W^\mu, W^\nu] &= i\epsilon^{\mu\nu\rho\sigma}W_\rho P_\sigma. \end{aligned} \quad (\text{A.21})$$

As a further label we can use the eigenvalue of one component of the Pauli-Lubanski vector, but only *one* component, since $[W_\mu, W_\nu] \neq 0$. The components of W have a simple interpretation; the zeroth component is proportional to helicity $W^0 = \vec{P} \cdot \vec{S}$ and the spatial components are proportional to the intrinsic spin $\vec{W} = P^0 \cdot \vec{S}$. This explains why, even in a relativistic theory, it makes sense to talk about a spin component, although it is neither conserved nor covariantly defined. Next we note that

$$P^\mu P_\mu = m^2 \quad ; \quad W^\mu W_\mu = -m^2 \vec{S}^2 \quad (\text{A.22})$$

are invariant (Casimir) operators, commuting with all 10 generators $(M^{\mu\nu}, P^\mu)$.

A. Relativistic Dynamics

If we choose a field representation where $m^2 \neq 0$, the spatial matrix \vec{S}^2 is a representation of the $SO(3)$ rotation group, with eigenvalues $s(s+1)$, where s is any positive integer or half-integer including zero. These eigenvalues can be used to characterize a massive particle by two fixed properties, its rest mass m and its spin s . If the mass is determined as the square root of the eigenvalue of P^2 , then the spin can be calculated by dividing the eigenvalue of $-W^2$ by m^2 .

For massless particles the situation is completely different. The property *spin* for massless particles is not what it is for massive ones. This can be immediately seen by putting in the above expressions $m^2 = 0$, leading to $P^2 = 0$ and $W^2 = 0$. Since W and P are orthogonal $P \cdot W = 0$, it can only mean that they must be proportional $W = \kappa P$ in all components. Thus κ can be calculated as $\kappa = W^0/P^0$, being proportional to the helicity $\lambda = W^0/|\vec{P}|$. Instead of two invariant numbers (m, s) , a massless particle is characterized by only one number κ . The values which κ can take, is beyond the scope of this section and will not be discussed here.

Finally, we can include observables into our labeling scheme that are not related to space-time symmetries, like the charge q of a particle. Its corresponding operator \mathcal{Q} canonically commutes with all generators of the Poincaré group.

Hence, the free one-particle Heisenberg state can be labeled as

$$|\Phi_0\rangle = |\vec{p}, \lambda; m, s, q\rangle, \tag{A.23}$$

where the energy eigenvalue p^0 is not included, since it can be determined from the on-shell condition $p_\mu p^\mu = m^2$.

Up to now, we considered only the simplest covariant realization of the Poincaré algebra, that of a free elementary particle, being a state of definite mass and spin. Next one may consider a collection of non-interacting particles of different masses and spins and construct covariant realizations for them. This task is almost trivial as the generators are simply the sum of the single particle generators. Much more difficult is the construction of representations in the case of a *fixed* number of *interacting* particles. This is actually the topic of relativistic dynamics proper.

In non-relativistic dynamics only one unique way is allowed: the interaction must be included in the Hamiltonian. The evolution of a non-relativistic system is governed fully by the Hamiltonian. All other generators, in this case of the Galilei group are independent of the interaction, and are said to be kinematic.

For systems that are governed by Einstein relativity, more possibilities are open as how to include interactions. One expects that certain Poincaré generators will differ from their free counterpart by some ‘potential’ term V . But how does one construct these generators in a covariant way? This problem has already been partially pointed out by Dirac [1], who stated that finding potentials which are consistent with the commutation relations of the Poincaré algebra ”provide the real difficulty in the problem of constructing a theory of a relativistic dynamical system” with a *fixed* number of particles. The difficulty is even increased if we require on top of that the covariance for wavefunctions. The physical reason for these problems is that potentials imply an instantaneous interaction which is in conflict with the existence of a limiting velocity and retardation effects. Relativistic causality is thus violated. Furthermore, a *fixed* number

A. Relativistic Dynamics

of particles is in conflict with the necessity of particle creation and annihilation and the appearance of antiparticles. Nevertheless, with considerable effort, it is possible to construct dynamical quantum systems with a *fixed* number of constituents which are consistent with the requirements of the Poincaré algebra and relativistic covariance [2], with the reason to improve or to have proper theory-based alternatives for the rather successful phenomenological constituent quark model.

A natural solution to all these problems stated above is the framework of a local covariant quantum field theory, with infinitely many degrees of freedom. These theories are usually specified by demanding a relativistically *invariant* Lagrangian.

For the construction of the Poincaré generators we naively can let us guide by classical field theory using Noethers Theorem. The Poincaré generators, all being constants of motion, are then expressed in terms of integrals of the energy-momentum tensor. The transition to quantum field theory is then imposed by the correct canonical quantization conditions onto the classical fields which will turn them into operators. Unfortunately such a construction does not allow for a simple verification of the requirements (A.12). Furthermore, for an arbitrary Lagrangian one cannot prove that its manifestly covariant Lagrangian equation of motion for a field operator will give identical results as the covariant Heisenberg equations (A.18). For every new case they have to be verified from scratch, which certainly is not straightforward. A bad way out is to simply postulate that a relativistically invariant Lagrangian fulfills all requirements of a relativistic system.

But there are better ways to see this correspondence manifestly. Probably the easiest way is provided by Schwingers variational action principle [24]. First, it is an action principle for a quantized field. It is thus the quantum-mechanical analogue of the corresponding classical variational principle. Second, it goes beyond this classical principle by including variations at the boundary which can be interpreted as the generator of field transformations. By this extension we obtain additional information regarding the dynamical characteristics of the field, which in the classical correspondence principle had to be postulated separately. This is a considerable simplification, since now the Lagrangian equations of motion, the form of the rules of quantization, the conservation laws, the Poincaré algebra with its covariant conditions, all that will follow manifestly from a relativistically invariant Lagrangian. This finally proves that a covariant quantum field theory offers a natural description for relativistic systems on a quantum-mechanical scale.

For a quantum field theory we adopt the Heisenberg picture as the framework of description. By this we mean that we specify a state vector as the simultaneous eigenket of all commuting observables at some fixed point in space-time, and express all dynamical developments of the system as the change of observables as we proceed in space and time. The natural Hilbert space of quantized fields, also called Fock space consists of subspaces, each having a basis of one-particle states $|\Phi_0\rangle = |\vec{p}, \lambda; m, s, q\rangle$ as already discussed above, where for each subspace the eigenvalues of the Casimir operators are fixed.

B Light-front QCD

* The SU(3) gauge invariant Lagrangian density for QCD is

$$\mathcal{L} = \frac{1}{2}\text{Tr}(F^{\mu\nu}F_{\mu\nu}) + \frac{1}{2} [\bar{\Psi}(i\gamma^\mu D_\mu - m)\Psi + \text{h.c.}], \quad (\text{B.1})$$

where the color-electro-magnetic fields and the covariant derivative are given as

$$\begin{aligned} F^{\mu\nu} &= \partial^\mu A^\nu - \partial^\nu A^\mu + ig[A^\mu, A^\nu], \\ D_{cc'}^\mu &= \delta_{cc'}\partial^\mu + igA_{cc'}^\mu, \quad \text{with} \quad A_{cc'}^\mu = T_{cc'}^a A_a^\mu. \end{aligned} \quad (\text{B.2})$$

$T_{cc'}^a$ are the 8 generators of the SU(3) group. Thus the gluon index a runs from 1 to 8. The physical 3×3 -matrix representation will let the color index run from 1 to 3. No distinction will be made between lower and upper gluon and color indices.

Independent variation of the gluon fields A^μ will yield the color-Maxwell equations

$$\partial_\mu F^{\mu\nu} = gJ^\nu, \quad \text{with} \quad J^\nu = \bar{\Psi}\gamma^\nu T^a \Psi T^a - i[F^{\nu\kappa}, A_\kappa], \quad (\text{B.3})$$

and the variation with respect to the quark fields give correspondingly the color-Dirac equations

$$(i\gamma^\mu D_\mu - m)\Psi = 0. \quad (\text{B.4})$$

Since the manifestly covariant QCD-Lagrangian shows no explicit space-time dependence, the Poincaré generators will be constants of motion. We are only interested in the 4-momentum operator, which can be determined as manifestly gauge invariant [12]

$$P_\nu = \int d^3x \left(F_a^{0\kappa} F_{\kappa\nu}^a + \frac{1}{4}g_\nu^0 F_a^{\kappa\lambda} F_{\kappa\lambda}^a + \frac{1}{2}[i\bar{\Psi}\gamma^0 T^a D_\nu^a \Psi + \text{h.c.}] \right). \quad (\text{B.5})$$

In the transition from instant- to front-form all 4-vectors including γ^μ are treated in the same way as the space-time coordinates x^μ . According to [12] the corresponding covariant expression in the light-front formalism reads

$$P_\nu = \int dx_+ d^2x_\perp \left(F_a^{+\kappa} F_{\kappa\nu}^a + \frac{1}{4}g_\nu^+ F_a^{\kappa\lambda} F_{\kappa\lambda}^a + \frac{1}{2}[i\bar{\Psi}\gamma^+ T^a D_\nu^a \Psi + \text{h.c.}] \right), \quad (\text{B.6})$$

which still maintains manifest gauge invariance.

The Hamiltonian $H = P_+$ as well as the other components of the energy-momentum 4-vector are highly non-trivial operators. Nevertheless, its possible to reduce them into workable expressions, since they contain time-derivatives and other constraint field components which can be eliminated by using the above equations of motion. The goal is to express P_ν in terms of *free* fields \tilde{A}^μ and $\tilde{\Psi}$ and to isolate the dependence on the coupling constant. For this, the natural light-cone gauge $A^+ = 0$ is chosen, in which the gluons only have the two physical transverse degrees of freedom. The result for the Hamiltonian can be written as a sum of five terms [12]

$$H = T + V + W_1 + W_2 + W_3. \quad (\text{B.7})$$

*This complete section is a compact summary from the work of [7],[12],[25].

B. Light-front QCD

Only the first term survives the limit $g \rightarrow 0$, and therefore is called the free part of the Hamiltonian, or its 'kinetic energy'

$$T = \frac{1}{2} \int dx_+ d^2 x_\perp \left(\tilde{\Psi} \gamma^+ \frac{m^2 + (i\nabla_\perp)^2}{i\partial^+} \tilde{\Psi} + \tilde{A}_a^\mu (i\nabla_\perp)^2 \tilde{A}_\mu^a \right). \quad (\text{B.8})$$

The vertex interaction

$$V = g \int dx_+ d^2 x_\perp \tilde{J}_a^\mu \tilde{A}_\mu^a, \quad \text{with} \quad \tilde{J}_a^\nu = \tilde{\Psi} \gamma^\nu T^a \tilde{\Psi} + f^{abc} \partial^\mu \tilde{A}_b^\nu \tilde{A}_\nu^c, \quad (\text{B.9})$$

is linear in the coupling constant and is the light-cone analogue of the conventional $J_\mu A^\mu$ -structures in the instant form. Note that the current \tilde{J}_a^μ has contributions from both quarks and gluons, with f^{abc} being the structure constants of the $SU(3)$ group. The interaction term

$$W_1 = \frac{g^2}{4} \int dx_+ d^2 x_\perp \tilde{B}_a^{\mu\nu} \tilde{B}_{\mu\nu}^a, \quad \text{with} \quad \tilde{B}_a^{\mu\nu} = f^{abc} \tilde{A}_b^\mu \tilde{A}_c^\nu, \quad (\text{B.10})$$

describes the four-point gluon-vertices which is quadratic in g . The remaining are the 'instantaneous interactions'. The instantaneous gluon interaction arises from the Coulomb equation $\partial_\mu F_a^{\mu+} = gJ_a^+$,

$$W_2 = \frac{g^2}{2} \int dx_+ d^2 x_\perp \tilde{J}_a^+ \frac{1}{(i\partial^+)^2} \tilde{J}_a^+, \quad (\text{B.11})$$

and is the light-cone analogue of the Coulomb energy. The instantaneous fermion interaction originates from the light-cone specific decomposition of Dirac's equation

$$W_3 = \frac{g^2}{2} \int dx_+ d^2 x_\perp \tilde{\Psi} \gamma^\mu T^a \tilde{A}_\mu^a \frac{\gamma^+}{i\partial^+} \left(\gamma^\nu T^b \tilde{A}_\nu^b \tilde{\Psi} \right). \quad (\text{B.12})$$

It has no analogue in the instant form.

Most remarkable is that the fully relativistic Hamiltonian is additive in the 'kinetic' and the 'potential' energy, very much like a non-relativistic Hamiltonian $H = T + U$. The symbolic notation $(i\partial^+)^{-1}$ and $(i\partial^+)^{-2}$ in the above expressions represent Green functions. Since they depend only on x^- , they are comparatively simple, much simpler than in the instant form where Δ^{-1} depends on all three space-like coordinates. Using this notation one has to be careful, there are many subtleties involved. For example looking at the Green function $G(x^-) = (\partial^+)^{-1}$ defined via

$$\partial^+ G(x^-) = \delta(x^-), \quad (\text{B.13})$$

is clearly only determined up to a homogeneous solution Z satisfying

$$\partial^+ Z = 0, \quad (\text{B.14})$$

that means up to a *zero mode* $Z = Z(x^-)$ of the operator ∂^+ . Thus, in order to uniquely specify the Green function $(\partial^+)^{-1}$, we have to provide additional information

B. Light-front QCD

in terms of *boundary conditions*. To see the physical impact of such zero modes, we briefly go to momentum space where we can replace ∂^+ by ip^+ . The equation for the Green function (B.13) becomes $ip^+G(p^+) = 1$, which has the general solution

$$G(p^+) = -i/p^+ + Z(p^+)\delta(p^+). \quad (\text{B.15})$$

Thus the zero modes will only contribute if $p^+ = 0$, that means if all particles in the system have zero longitudinal momentum. But as we know from (Section 2.2.2) these are exactly the momenta that will give rise to a complicated light-cone vacuum. No other reasons than simplicity we will put such zero modes equal to zero $Z = 0$, and therefore neglect possible boundary conditions. This will lead to a trivial light-cone QCD-vacuum being identical to the free Fock-space vacuum.

The next task is to bring the Hamiltonian (B.7) into its natural field theory representation, the momentum space representation. As usual we do a covariant Fourier transformation of the free quark and gluon fields, which in the front form are given as

$$\begin{aligned} \tilde{\Psi}_{\alpha cf}(x) &= \sum_{\lambda} \int \frac{dp^+ d^2p_{\perp}}{\sqrt{2p^+(2\pi)^3}} \left(b(q)u_{\alpha}(p, \lambda)e^{-ipx} + d^{\dagger}(q)v_{\alpha}(p, \lambda)e^{+ipx} \right), \\ \tilde{A}_{\mu}^a(x) &= \sum_{\lambda} \int \frac{dp^+ d^2p_{\perp}}{\sqrt{2p^+(2\pi)^3}} \left(a(q)\epsilon_{\mu}(p, \lambda)e^{-ipx} + a^{\dagger}(q)\epsilon_{\mu}^*(p, \lambda)e^{+ipx} \right). \end{aligned} \quad (\text{B.16})$$

The properties of the Dirac spinors u_{α} , v_{α} , and of the polarization vectors ϵ_{μ} are given in [12]. The single particle states are specified by string of quantum numbers q . A quark is characterized in general by 6 quantum numbers $q = (p^+, \vec{p}_{\perp}, \lambda, c, f)$, the three spatial momenta, the helicity λ , the color index c and the flavor index f . The knowledge of (p^+, \vec{p}_{\perp}) fixes the energy $p^- = (m^2 + \vec{p}_{\perp}^2)/p^+$. A gluon is characterized by 5 quantum numbers $q = (p^+, \vec{p}_{\perp}, \lambda, a)$ with a as the glue index. Since they are massless, their energy is $p^- = \vec{p}_{\perp}^2/p^+$. Furthermore, since a quark is a fermion and the gluon a gauge boson, their creation and destruction operators are subject to the usual relations

$$\begin{aligned} [a(q), a^{\dagger}(q')] &= \{b(q), b^{\dagger}(q')\} = \{d(q), d^{\dagger}(q')\} \\ &= (2\pi)^3 \cdot 2p^+ \cdot \delta(p^+ - p'^+) \delta^2(\vec{p}_{\perp} - \vec{p}'_{\perp}) \delta_a^{a'} \delta_{\lambda}^{\lambda'} \delta_c^{c'} \delta_f^{f'}, \end{aligned} \quad (\text{B.17})$$

which carry the operator structure and statistics of the theory.

When inserting the free fields (B.16) into the Hamiltonian (B.7) its possible to integrate over x^{μ} , producing essentially delta functions in the single particle momenta, which reflect momentum conservation. To note is that terms consisting only of creation or only of destruction operators as for example in

$$b^{\dagger}(q_1)d^{\dagger}(q_2)a^{\dagger}(q_3)\delta(p_1^+ + p_2^+ + p_3^+), \quad (\text{B.18})$$

have a vanishing contribution, since the light-cone longitudinal momenta p^+ are all positive (Section 2.2.2) and can not add to zero. As a consequence, all energy diagrams which generate the vacuum fluctuations in the usual formulation of quantum field theory are absent in the front form.

B. Light-front QCD

The final result of this evaluation will give a Hamiltonian which purely acts as a Fock-space operator $H = T + (V + F + S)$, explicitly given in [12]. The kinetic energy T is a sum of 3 diagonal operators. The interaction terms are distinguished according to the number of particles changed. The vertex interaction V is a sum of four operators, which connects Fock states whose particle number differ by 1. The four-point interactions are separated into fork F and seagull S interactions, depending on whether they have an odd or even number of creation operators. The fork interaction F is a sum of 6 operators, which change the particle number by 2. And the seagull interaction S can be written as a sum of 7 operators, which act only between Fock states with the same particle number. The remaining space-like components (P^+ , \vec{P}_\perp) of the momentum operator (B.6) are according to their kinematical behaviour diagonal operators in Fock-space.

We now aim at solving the Hamiltonian eigenvalue problem

$$H|\Psi\rangle = \frac{M^2 + \vec{P}_\perp^2}{2P^+}|\Psi\rangle, \quad (\text{B.19})$$

which is for several reasons, as discussed in (Section 2.2.3) easier to handle than its counter part equation in instant-form. If one disregards possible zero modes, the light-cone QCD-vacuum becomes trivial which has the consequence that the light-front bound states $|\Psi\rangle$ for various hadrons can be expanded in terms of the free Fock states. As usual, the Fock basis is constructed by applying products of the free field creation operators to the vacuum state $|0\rangle$:

$$\begin{aligned} n = 0 : & \quad |0\rangle, \\ n = 1 : & \quad |q\bar{q} : p_i^+, \vec{p}_{\perp i}, \lambda_i\rangle = b^\dagger(q_1)d^\dagger(q_2)|0\rangle, \\ n = 2 : & \quad |gg : p_i^+, \vec{p}_{\perp i}, \lambda_i\rangle = a^\dagger(q_1)a^\dagger(q_2)|0\rangle, \\ n = 3 : & \quad |q\bar{q}g : p_i^+, \vec{p}_{\perp i}, \lambda_i\rangle = b^\dagger(q_1)d^\dagger(q_2)a^\dagger(q_3)|0\rangle, \\ & \quad \vdots \end{aligned} \quad (\text{B.20})$$

where all discrete quantum numbers were suppressed except the helicities. We now specialize to the hadronic state of a meson (Fig5), which in a condensed notation can be described by the following expansion in Fock-space

$$\begin{aligned} |\Psi_{\text{meson}}\rangle &= \sum_i \psi_{q\bar{q}}(x_i, \vec{k}_{\perp i}, \lambda_i) |q\bar{q}\rangle \\ &+ \sum_i \psi_{gg}(x_i, \vec{k}_{\perp i}, \lambda_i) |gg\rangle \\ &+ \sum_i \psi_{q\bar{q}g}(x_i, \vec{k}_{\perp i}, \lambda_i) |q\bar{q}g\rangle \\ &+ \sum_i \psi_{q\bar{q}q\bar{q}}(x_i, \vec{k}_{\perp i}, \lambda_i) |q\bar{q}q\bar{q}\rangle \\ &+ \dots \end{aligned} \quad (\text{B.21})$$

B. Light-front QCD

Figure 5: The Hamiltonian matrix for a meson, taken from [12]. The matrix elements are represented by energy diagrams. Within each block they are all of the same type: either vertex, fork or seagull diagrams. Zero matrices are denoted by a dot (.). The singlet gluon is absent since it cannot be color neutral.

| n | Sector | 1 | 2 | 3 | 4 | 5 | 6 | 7 | 8 | 9 | 10 | 11 | 12 | 13 |
|----|---|-------------|----|---------------|-------------------------|-----|----------------|---------------------------|-------------------------------------|------|-----------------|----------------------------|---------------------------------------|---|
| | | q \bar{q} | gg | q \bar{q} g | q \bar{q} q \bar{q} | ggg | q \bar{q} gg | q \bar{q} q \bar{q} g | q \bar{q} q \bar{q} q \bar{q} | gggg | q \bar{q} ggg | q \bar{q} q \bar{q} gg | q \bar{q} q \bar{q} q \bar{q} g | q \bar{q} q \bar{q} q \bar{q} q \bar{q} |
| 1 | q \bar{q} | | | | | . | | . | . | . | . | . | . | . |
| 2 | gg | | | | . | | | . | . | | . | . | . | . |
| 3 | q \bar{q} g | | | | | | | | . | . | | . | . | . |
| 4 | q \bar{q} q \bar{q} | | . | | | . | | | | . | . | | . | . |
| 5 | ggg | . | | | . | | | . | . | | | . | . | . |
| 6 | q \bar{q} gg | | | | | | | . | . | | | | . | . |
| 7 | q \bar{q} q \bar{q} g | . | . | | | . | | | | . | | | | . |
| 8 | q \bar{q} q \bar{q} q \bar{q} | . | . | . | | . | . | | | . | . | | | |
| 9 | gggg | . | | . | . | | | . | . | | | . | . | . |
| 10 | q \bar{q} ggg | . | . | | . | | | | . | | | | . | . |
| 11 | q \bar{q} q \bar{q} gg | . | . | . | | . | | | | . | | | | . |
| 12 | q \bar{q} q \bar{q} q \bar{q} g | . | . | . | . | . | | | | . | . | | | |
| 13 | q \bar{q} q \bar{q} q \bar{q} q \bar{q} | . | . | . | . | . | . | | | . | . | . | | |

The generalized sum in (B.21) also includes the phase-space integrations of the relative frame independent coordinates x_i and $\vec{k}_{\perp i}$ respecting the constraints

$$\sum_i x_i = 1 \quad \text{and} \quad \sum_i \vec{k}_{\perp i} = 0. \quad (\text{B.22})$$

The light-cone wavefunctions ψ_n do not depend on the total momentum (P^+, \vec{P}_{\perp}) carried by the meson, since x_i is the longitudinal momentum fraction carried by the i -th constituent and $\vec{k}_{\perp i}$ is its relative transverse momentum with respect to the center-of-mass frame; both of these are frame-independent quantities. They are the probability amplitudes to find a Fock state of bare particles in the physical meson. If all wave functions are available, one can analyze any hadronic structure in terms of quarks and gluons [12].

In this Fock basis the eigenvalue equation (B.19) stands for an infinite set of coupled integral equations

$$\sum_{m=1}^{\infty} \int [d\mu'_m] \langle n: x_i, \vec{k}_{\perp i}, \lambda_i | H | m: x'_i, \vec{k}'_{\perp i}, \lambda'_i \rangle \psi_m(x'_i, \vec{k}'_{\perp i}, \lambda'_i) = \frac{M^2 + \vec{P}_{\perp}^2}{2P^+} \psi_n(x_i, \vec{k}_{\perp i}, \lambda_i).$$

B. Light-front QCD

Since P^+ and \vec{P}_\perp are diagonal operators in momentum space one can equivalently rewrite this equation as

$$\sum_{m=1}^{\infty} \int [d\mu'_m] \langle n: x_i, \vec{k}_{\perp i}, \lambda_i | P^- P^+ - \vec{P}_\perp^2 | m: x'_i, \vec{k}'_{\perp i}, \lambda'_i \rangle \psi_m(x'_i, \vec{k}'_{\perp i}, \lambda'_i) = M^2 \psi_n(x_i, \vec{k}_{\perp i}, \lambda_i). \quad (\text{B.23})$$

It is therefore possible to define a ‘light-cone Hamiltonian’ as the operator

$$H_{\text{LC}} = P^- P^+ - \vec{P}_\perp^2 = P^\mu P_\mu, \quad (\text{B.24})$$

so that its eigenvalues correspond to the invariant mass-squared spectrum M^2 . On the light-cone it is therefore possible to formulate the bound-state problem frame independently, in the sense that the operator H_{LC} is Lorentz invariant and the wavefunctions boost invariant. This reflects the fact that the boost operators on the light-cone are kinematical. To simplify things one can boost the system to an ‘intrinsic frame’ in which the transversal momentum \vec{P}_\perp vanishes, thus $H_{\text{LC}} = P^- P^+$. The transformation to an arbitrary frame with finite values of \vec{P}_\perp is then trivially performed.

In addressing to solve equation (B.23) by diagonalization one faces two major difficulties as in every field theory. First, we are dealing with a many body problem with an infinite number of constituents. There is no other choice than to construct an effective equation. The reliability of an effective interaction certainly depends on how strong the higher Fock states contribute. If a constituent picture for the meson were true, the valence state would dominate,

$$|\psi_2|^2 \gg |\psi_n|^2, \quad n > 2, \quad (\text{B.25})$$

and, in the extreme case, the meson wave function would be entirely given by the projection $\langle q\bar{q} | \Psi_{\text{meson}} \rangle$ onto the valence state. Second, we are facing all kinds of divergencies which have to be regularized and then renormalized.

B.1 Effective Hamiltonian

The eigenvalue equation (B.19) stands for an infinite set of coupled integral equations which are extremely difficult to handle. It is useful to convert it to the much more transparent case of a *finite* set of coupled matrix equations, namely by the technical trick of putting the system \mathcal{L}_{QCD} into a finite box of size L and imposing periodic boundary conditions on the vector fields A^μ and anti-periodic boundary conditions on the spinor fields Ψ_α because \mathcal{L}_{QCD} is bilinear in the latter. The boundary conditions are satisfied by discretizing the momenta in the plane wave expansion of the corresponding free fields (B.16). This formalism is also known as Discretized Light-Cone Quantization (DLCQ) [12],[25]. Why is this set finite? The longitudinal light-cone momentum p^+ is a positive number. For periodic boundary conditions the lowest possible value is $(p^+)_{\text{min}} = \pi/L$ — zero modes with $p^+ = 0$ are disregarded here, as already mentioned. Consequently, any total momentum $P^+ = K\pi/L$ ($K \in \mathbb{N}$) can be distributed over at most K bosons, or over K fermion pairs since these are subjected to anti-periodic boundary conditions.

B. Light-front QCD

Figure 6: The Hamiltonian matrix for a meson, taken from [25]. The matrix elements are represented by the letters S, V, and F, corresponding to seagull, vertex, and fork-interactions, respectively. For better orientation, the diagonal blocs are marked by D=T+S and the zero matrices by (\cdot).

| K | N_p | Sector | n | 1 | 2 | 3 | 4 | 5 | 6 | 7 | 8 | 9 | 10 | 11 | 12 | 13 |
|---|-------|---------------------------------------|----|---------|---------|---------|---------|---------|---------|---------|---------|---------|---------|---------|---------|---------|
| 1 | 2 | $q\bar{q}$ | 1 | D | S | V | F | \cdot | F | \cdot | \cdot | \cdot | \cdot | \cdot | \cdot | \cdot |
| 2 | 2 | $g g$ | 2 | S | D | V | \cdot | V | F | \cdot | \cdot | F | \cdot | \cdot | \cdot | \cdot |
| 2 | 3 | $q\bar{q} g$ | 3 | V | V | D | V | S | V | F | \cdot | \cdot | F | \cdot | \cdot | \cdot |
| 2 | 4 | $q\bar{q} q\bar{q}$ | 4 | F | \cdot | V | D | \cdot | S | V | F | \cdot | \cdot | F | \cdot | \cdot |
| 3 | 3 | $g g g$ | 5 | \cdot | V | S | \cdot | D | V | \cdot | \cdot | V | F | \cdot | \cdot | \cdot |
| 3 | 4 | $q\bar{q} g g$ | 6 | F | F | V | S | V | D | V | \cdot | S | V | F | \cdot | \cdot |
| 3 | 5 | $q\bar{q} q\bar{q} g$ | 7 | \cdot | \cdot | F | V | \cdot | V | D | V | \cdot | S | V | F | \cdot |
| 3 | 6 | $q\bar{q} q\bar{q} q\bar{q}$ | 8 | \cdot | \cdot | \cdot | F | \cdot | \cdot | V | D | \cdot | \cdot | S | V | F |
| 4 | 4 | $g g g g$ | 9 | \cdot | F | \cdot | \cdot | V | S | \cdot | \cdot | D | V | \cdot | \cdot | \cdot |
| 4 | 5 | $q\bar{q} g g g$ | 10 | \cdot | \cdot | F | \cdot | F | V | S | \cdot | V | D | V | \cdot | \cdot |
| 4 | 6 | $q\bar{q} q\bar{q} g g$ | 11 | \cdot | \cdot | \cdot | F | \cdot | F | V | S | \cdot | V | D | V | \cdot |
| 4 | 7 | $q\bar{q} q\bar{q} q\bar{q} g$ | 12 | \cdot | \cdot | \cdot | \cdot | \cdot | \cdot | F | V | \cdot | \cdot | V | D | V |
| 4 | 8 | $q\bar{q} q\bar{q} q\bar{q} q\bar{q}$ | 13 | \cdot | \cdot | \cdot | \cdot | \cdot | \cdot | \cdot | F | \cdot | \cdot | \cdot | V | D |

As illustrated in (Fig6) for the Fock space of a meson, the *harmonic resolution* K governs the number of Fock space sectors. The lowest possible value $K = 1$ allows only for one Fock-space sector with a single $q\bar{q}$ -pair — a single gluon can not be in a color singlet and thus its excluded. For $K = 2$, the Fock space contains two gluons, a $q\bar{q}$ -pair plus a gluon, and two $q\bar{q}$ -pairs. For $K = 4$ the Fock space contains at most 8 particles. One can label the Fock space sectors according to the quark-gluon content, or one can enumerate them, which is less transparent but more simple. In (Fig6) the Fock-space sectors for $K \leq 4$ are enumerated $n = 1, \dots, 13$. With increasing K more Fock-space sectors are added. Their total number grows like $N(K) = (K + 1)(K + 2)/2 - 2$. Introducing a box size L as a finite and additional length parameter, however, can be at most an intermediate step. Latest at the end of the calculations, it must be removed by a limiting procedure like $L \rightarrow \infty$, $K \rightarrow \infty$, but K/L finite, since only the continuum can be the full covariant theory. The classification scheme of the Fock space sectors as used in the continuum appears in the discrete formalism in the most natural way. In this sense we will keep on working in the continuum by dividing the Fock space into its natural subspaces

$$E_i \langle n | \Psi_i \rangle = \sum_{m=1}^{\infty} \langle n | H | m \rangle \langle m | \Psi_i \rangle = \lim_{K \rightarrow \infty} \sum_{m=1}^{N(K)} \langle n | H | m \rangle \langle m | \Psi_i \rangle. \quad (\text{B.26})$$

B. Light-front QCD

In the sense of the DLCQ prescription one can solve the above eigenvalue equation by realizing the limit $K \rightarrow \infty$ as a process which solves the eigenvalue equation in each harmonic subspace of dimension $N(K)$. One selects a particular value of the harmonic resolution K and diagonalizes the corresponding finite dimensional Hamiltonian matrix. But as one has to increase K in order to get closer to the original eigenvalue equation, the dimension of the Hamiltonian matrix grows quadratically with K , with the result that one has to diagonalize finite matrices of inconceivable large dimensions. What one needs is an effective Hamiltonian which acts in smaller matrix spaces and which has a well defined relation to the full interaction. The requirements for such an effective interaction is to preserve all Lagrangian symmetries and not to truncate the Fock space. Furthermore, it should make use of the fact that due to the nature of the Hamiltonian, more than half of the matrix elements are zero. Such a construction is given by the method of iterated resolvents [7], inspired by the well known Tamm-Dancoff [26] approach in many-body physics. For a fixed harmonic resolution K the dimension $N(K)$ of the Hamiltonian matrix is reduced step by step until it the dimension 1 is reached. This effective Hamiltonian then only acts in the lowest sector of the theory, here in the Fock space of one quark and one anti-quark. Furthermore, it has the same eigenvalue spectrum as the full problem. The whole procedure is summarized in a recursion relation, which describes all intermediate steps. Because of this recursive character any higher sector wave function $\langle n|\Psi\rangle$ with $n \leq N(K)$ can be systematically retrieved by matrix multiplication from the wave function $\langle 1|\Psi\rangle$ in the lowest sector. No additional matrix diagonalization or inversions are required.

For gaining more insight into the method of iterated resolvents we want to study it explicitly at the example of $K = 2$. The Hamiltonian matrix is then given by a 4×4 -matrix acting in the following subspace

$$\langle n|H|m\rangle = \begin{pmatrix} \langle 1|T + S|1\rangle & \langle 1|S|2\rangle & \langle 1|V|3\rangle & \langle 1|F|4\rangle \\ \langle 2|S|1\rangle & \langle 2|T + S|2\rangle & \langle 2|V|3\rangle & 0 \\ \langle 3|V|1\rangle & \langle 3|V|2\rangle & \langle 3|T + S|3\rangle & \langle 3|V|4\rangle \\ \langle 4|F|1\rangle & 0 & \langle 4|V|3\rangle & \langle 4|T + S|4\rangle \end{pmatrix}. \quad (\text{B.27})$$

As we know, the instantaneous interactions F and S arise as a consequence of working in the light-cone gauge $A^+ = 0$. They are gauge artefacts. We shall now use a trick which will simplify the construction of an effective Hamiltonian enormously. Practitioners in Light-Cone Time-Ordered Perturbation Theory know that they can omit the instantaneous interactions until they *actually compute* a particular diagram. Then, every intrinsic line in a graph must be combined with the instantaneous partner line associated with the gauge artefacts. Only then, the sum of all time ordered diagrams becomes manifestly identical with the gauge invariant Feynman scattering amplitudes. There is no exception known to this rule, thus far, in all graphs computed explicitly. In the sequel, this ‘gauge trick’ [25] will be adopted to method of iterated resolvents, since as we will see is nothing else than a compact notation for resumming all perturbative diagrams without double counting.

B. Light-front QCD

First, we will violate gauge invariance by setting all instantaneous matrix elements to zero. Then at the end of calculations we restore gauge invariance by the rule: *replace every internal line in a graph by the sum of a dynamic and an instantaneous line*. One then gets a Hamiltonian block matrix of extreme sparseness. For the above case $K = 2$ we will have the workable matrix of

$$\langle n|H|m\rangle = \begin{pmatrix} \langle 1|T|1\rangle & 0 & \langle 1|V|3\rangle & 0 \\ 0 & \langle 2|T|2\rangle & \langle 2|V|3\rangle & 0 \\ \langle 3|V|1\rangle & \langle 3|V|2\rangle & \langle 3|T|3\rangle & \langle 3|V|4\rangle \\ 0 & 0 & \langle 4|V|3\rangle & \langle 4|T|4\rangle \end{pmatrix}, \quad (\text{B.28})$$

which is subject to 4-space diagonalization

$$\sum_{m=1}^4 \langle n|H|m\rangle \langle m|\Psi_i\rangle = E_i \langle n|\Psi_i\rangle, \quad n = 1, 2, 3, 4. \quad (\text{B.29})$$

Our aim is firstly to construct an effective matrix which only acts in 3-space. For this the above eigenvalue equation is equivalently split up into two parts

$$\sum_{m=1}^3 \langle n|H|m\rangle \langle m|\Psi_i\rangle + \langle n|H|4\rangle \langle 4|\Psi_i\rangle = E_i \langle n|\Psi_i\rangle, \quad n = 1, 2, 3 \quad (\text{B.30})$$

$$\sum_{m=1}^3 \langle 4|H|m\rangle \langle m|\Psi_i\rangle + \langle 4|H|4\rangle \langle 4|\Psi_i\rangle = E_i \langle 4|\Psi_i\rangle. \quad (\text{B.31})$$

Rewriting the second equation as

$$\langle 4|E_i - H|4\rangle \langle 4|\Psi_i\rangle = \sum_{m=1}^3 \langle 4|H|m\rangle \langle m|\Psi_i\rangle, \quad (\text{B.32})$$

and observe that the quadratic matrix $E_i - H$ could be inverted to express the 4-space wavefunction $\langle 4|\Psi_i\rangle$ in terms of the 3-space wavefunctions $\langle n|\Psi_i\rangle$, with $n \leq 3$. But here is a problem: the eigenvalues E_i are unknown at this point. One therefore solves first another problem: one introduces *the starting point energy* ω as redundant parameter at disposal, and defines the 4-space resolvent as the inverse of the matrix element $\langle 4|\omega - H|4\rangle$

$$G_4(\omega) = \frac{1}{\langle 4|\omega - H|4\rangle}, \quad (\text{B.33})$$

which in the continuum limit $K \rightarrow \infty$ turn into well-defined propagators. Inserting the solution $\langle 4|\Psi_i\rangle$ into (B.30) gives an eigenvalue equation which is completely defined in 3-space

$$\sum_{m=1}^3 \langle n|H_3(\omega)|m\rangle \langle m|\Psi_i\rangle = E_i(\omega) \langle n|\Psi_i\rangle, \quad n = 1, 2, 3 \quad (\text{B.34})$$

B. Light-front QCD

with the following effective Hamiltonian acting only in 3-space

$$H_3(\omega) = H + H|4\rangle G_4(\omega)\langle 4|H \quad (\text{B.35})$$

In addition to the original Hamiltonian in 3-space, the effective Hamiltonian acquires a piece where the system is scattered virtually into the higher 4-space sector, propagating there via G_4 by impact of the true interaction, and scattered back into 3-space. Every value of ω defines a different Hamiltonian and a different spectrum. Varying ω one generates a set of energy functions $E_i(\omega)$, by solving the eigenvalue equation (B.34). Whenever one finds a solution to the fix-point equation

$$E_i(\omega) = \omega, \quad (\text{B.36})$$

one has found one of the true eigenvalues and eigenfunctions of H , by construction. It should be emphasized that one can find all eigen-solutions of the full Hamiltonian H . The effective 3-space matrix to diagonalize is given as

$$\langle n|H_3(\omega)|m\rangle = \begin{pmatrix} \langle 1|T|1\rangle & 0 & \langle 1|V|3\rangle \\ 0 & \langle 2|T|2\rangle & \langle 2|V|3\rangle \\ \langle 3|V|1\rangle & \langle 3|V|2\rangle & \langle 3|\{T+V|4\rangle G_4(\omega)\langle 4|V\}|3\rangle \end{pmatrix}, \quad (\text{B.37})$$

What do we have achieved so far? It looks as if one has mapped a more difficult problem, the diagonalization of a 4-dimensional matrix onto a more simpler problem, the diagonalization of a 3-dimensional matrix. But this is certainly only true in a restricted sense. Since one has to vary ω one has to diagonalize several 3-dimensional matrices and not only one. The numerical work is thus rather larger than smaller as compared to a direct diagonalization in 4-space. The advantage of working with an effective interaction is of analytical nature, as we will see if we keep on reducing the dimensions up to an effective matrix acting solely in 1-space.

It is easy to see that the effective Hamiltonians acting in different spaces are generated by the recursion relation

$$H_{n-1}(\omega) = H_n(\omega) + H_n(\omega)|n\rangle G_n(\omega)\langle n|H_n(\omega), \quad n \leq 4, \quad (\text{B.38})$$

where $H_4(\omega)$ is defined to be the original Hamiltonian H . The wavefunctions in each sector can be calculated as

$$\langle n|\Psi_i(\omega)\rangle = \sum_{m=1}^{n-1} G_n(\omega)\langle n|H_n(\omega)|m\rangle\langle m|\Psi_i(\omega)\rangle, \quad n \leq 4. \quad (\text{B.39})$$

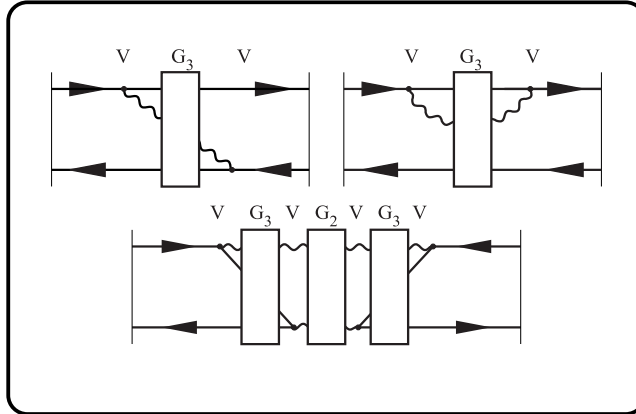
The effective Hamiltonian acting in the lowest sector can thus be calculated as

$$H_1 = T + VG_3V + VG_3VG_2VG_3V, \quad (\text{B.40})$$

where we have dropped the Dirac-bracket-notation between and the ω -notation in the propagators for more transparency.

B. Light-front QCD

Figure 7: The dressed propagators [27]



The eigenvalues of the original Hamiltonian H are now determined by computing the matrix element $\langle 1|H_1(\omega)|1\rangle = E_i(\omega)$ for different ω in order to find a solution of the fix-point equation $E_i(\omega) = \omega$. The wave functions in all sectors can be systematically retrieved from the lowest one $\langle 1|\Psi_i\rangle$ explicitly given as

$$\begin{aligned}
 \langle 2|\Psi_i\rangle &= \langle 2|VG_3V|1\rangle\langle 1|\Psi_i\rangle, \\
 \langle 3|\Psi_i\rangle &= \langle 3|G_3V + G_3VG_2VG_3V|1\rangle\langle 1|\Psi_i\rangle, \\
 \langle 4|\Psi_i\rangle &= \langle 4|G_4VG_3V + G_4VG_3VG_2VG_3V|1\rangle\langle 1|\Psi_i\rangle.
 \end{aligned}
 \tag{B.41}$$

All the above calculations refer to the case of $K = 2$. To get the effective Hamiltonians for harmonic resolutions $K = 3, 4, \dots$ is not repeated here explicitly. Important is the general feature that the effective sector Hamiltonians are separable in the kinetic energies T and the effective interactions $U(\omega)$

$$H_n(\omega) = T + U(\omega). \tag{B.42}$$

Important is also that the effective Hamiltonians in the lower sectors become independent of K — the Hamiltonian H_1 as given in (B.40) stays completely unchanged [7]. The transition to the continuum $K \rightarrow \infty$ is then rather trivial for the lower sectors and will hence forward be assumed.

The most important result of this section is that QCD has only two structurally different contributions to the effective interaction in the lowest $q\bar{q}$ -space. The first term in (B.40) is the effective one-gluon exchange

$$U_1 = VG_3V, \tag{B.43}$$

which conserves the flavor along the quark line and describes all fine and hyperfine interactions. As illustrated in the first line of (Fig7) the vertex interaction V creates a gluon and scatters the system virtually into the $q\bar{q}g$ -space. As indicated by the box G_3 , the three particles propagate there under the impact of the full Hamiltonian before

B. Light-front QCD

the gluon is absorbed. The gluon can be absorbed either by the antiquark or by the quark. If it is absorbed by the quark, it contributes to the effective quark mass \bar{m} . The second term in (B.40), the effective two-gluon-annihilation interaction

$$U_2 = VG_3VG_2VG_3V, \quad (\text{B.44})$$

shown in the second line of (Fig7), can generate an interaction between different quark flavors.

This completes the derivation for an effective Hamiltonian acting in the lowest Fock space sector $q\bar{q}$. Its effective one-body eigenvalue equation

$$H_{\text{LC}}^{\text{eff}}|\Psi_i\rangle = M_i^2|\Psi_i\rangle, \quad \text{with} \quad H_{\text{LC}}^{\text{eff}} = 2P^+H_1, \quad (\text{B.45})$$

becomes an integral equation, but a very simple one in only three continuous variables (x, \vec{k}_\perp) . The structure is rather transparent

$$\begin{aligned} M_i^2\langle x, \vec{k}_\perp, \lambda_q, \lambda_{\bar{q}}|\Psi_i\rangle &= \left[\frac{\bar{m}_q^2 + \vec{k}_\perp^2}{x} + \frac{\bar{m}_{\bar{q}}^2 + \vec{k}_\perp^2}{1-x} \right] \langle x, \vec{k}_\perp, \lambda_q, \lambda_{\bar{q}}|\Psi_i\rangle \\ &+ \sum_{\lambda'_q, \lambda'_{\bar{q}}} \int dx' d^2k'_\perp \langle x, \vec{k}_\perp, \lambda_q, \lambda_{\bar{q}}|VG_3V \\ &+ VG_3VG_2VG_3V|x', \vec{k}'_\perp, \lambda'_q, \lambda'_{\bar{q}}\rangle \langle x', \vec{k}'_\perp, \lambda'_q, \lambda'_{\bar{q}}|\Psi_i\rangle. \end{aligned} \quad (\text{B.46})$$

The eigenvalues refer to the invariant mass M_i of a physical state. The wavefunction $\langle x, \vec{k}_\perp, \lambda_q, \lambda_{\bar{q}}|\Psi_i\rangle$ gives the probability amplitude for finding in the $q\bar{q}$ -state a flavored quark with momentum fraction x , intrinsic transverse momentum \vec{k}_\perp and helicity λ_q , and correspondingly an anti-quark with $1-x$, $-\vec{k}_\perp$ and $\lambda_{\bar{q}}$. Both the mass and the wavefunctions are boost-invariant.

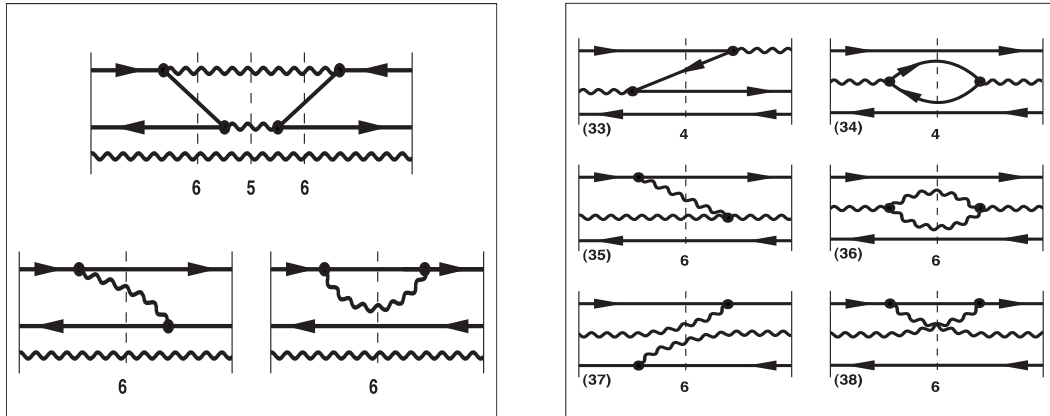
For solving the above eigenvalue equation one has to know the propagators G_3 and G_2 . For that one needs the relevant matrix elements $\langle 3|H_3|3\rangle$ and $\langle 2|H_2|2\rangle$ which are explicitly [7] given as

$$\begin{aligned} \langle 2|H_2|2\rangle &= \langle 2|T + VG_3V + VG_5V|2\rangle \\ \langle 3|H_3|3\rangle &= \langle 3|T + VG_4V + VG_6V + VG_6VG_5VG_6V|3\rangle, \end{aligned} \quad (\text{B.47})$$

which again requires the knowledge of G_4 , G_5 and G_6 , and so on. Having such dressed propagators is certainly the consequence of the iterated resolvents method used, which resums perturbative diagrams to all orders without double counting. In order to make explicit calculations one certainly has to break the propagator hierarchy somewhere. But before thinking of any approximation in the dressed propagators we first want to look at the propagator G_3 more closely, which in a certain sense turns out to be special. As already mentioned above, the relevant matrix element to be calculated is $\langle 3|H_3|3\rangle$. Its corresponding diagrams can be grouped into two topologically different classes. Some of them are displayed in (Fig8). In (Fig8a) the gluon does not change quantum

B. Light-front QCD

Figure 8: Taken from [25]



(a) Three possible graphs of the spectator interaction in the $q\bar{q}g$ -space. Note the role of the gluon as a spectator

(b) Some six graphs of the participant interaction in the $q\bar{q}g$ -space.

numbers under the impact of the interaction and acts as a spectator. Therefore, these graphs will be referred to as the ‘spectator interaction’ \bar{U}_3 . In the graphs of (Fig8b) the gluons are scattered by the interaction, and correspondingly these graphs will be referred to as the ‘participant interaction’ \tilde{U}_3 . We thus have a unique separation into spectators and participants in the quark-pair-gluon sector

$$H_3 = T + U_3 = T + \bar{U}_3 + \tilde{U}_3, \quad (\text{B.48})$$

with

$$\bar{U}_3 = VG_6V + VG_6VG_5VG_6V, \quad \text{and} \quad \tilde{U}_3 = VG_4V + VG_6V. \quad (\text{B.49})$$

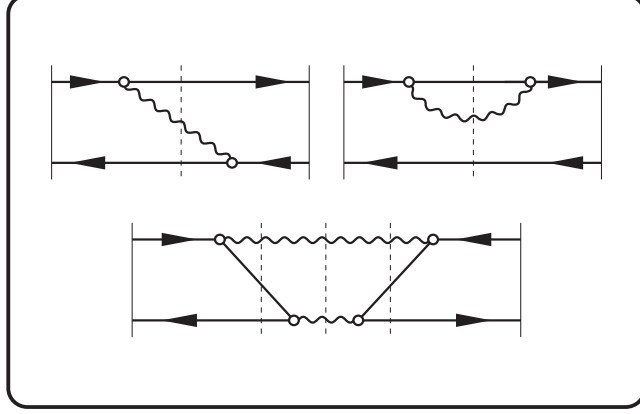
Since the Hamiltonian is additive in spectator and participant interactions, the dressed 3-space propagator can be written as

$$\begin{aligned} G_3 &= \frac{1}{\omega - H_3} = \frac{1}{\omega - T - \bar{U}_3 - \tilde{U}_3} = \frac{1}{(\omega - T - \bar{U}_3) \cdot \left(1 - \frac{\tilde{U}_3}{\omega - T - \bar{U}_3}\right)} \\ &\equiv \bar{G}_3 \cdot \frac{1}{1 - \tilde{U}_3 \cdot \bar{G}_3} = \bar{G}_3 + \bar{G}_3 \tilde{U}_3 \bar{G}_3 + \bar{G}_3 \tilde{U}_3 \bar{G}_3 \tilde{U}_3 \bar{G}_3 + \dots \end{aligned} \quad (\text{B.50})$$

The above series looks like as if one would do plain perturbation theory in the coupling constant. This is only partially true, since \bar{G}_3 is not a free propagator but which contains an interaction in the well defined form of \bar{U}_3 . The effective sector Hamiltonian $\bar{H}_3 = T + \bar{U}_3$ describes a bound state of one $q\bar{q}$ -pair which is accompanied by one free gluon. One therefore deals here with a *perturbation theory in medium* [7]. The advantage of formulating such a series, it that the system is not scattered into other

B. Light-front QCD

Figure 9: The free propagators with effective vertices [27]



sectors, it stays in sector 3. The above series can be identically rearranged to

$$\begin{aligned}
 G_3 &= \left[1 + \frac{1}{2} \bar{G}_3 \tilde{U}_3 + \frac{3}{8} \bar{G}_3 \tilde{U}_3 \bar{G}_3 \tilde{U}_3 + \dots \right] \bar{G}_3 \left[1 + \frac{1}{2} \tilde{U}_3 \bar{G}_3 + \frac{3}{8} \tilde{U}_3 \bar{G}_3 \tilde{U}_3 \bar{G}_3 + \dots \right] \\
 &\equiv R_3 \bar{G}_3 R_3^\dagger,
 \end{aligned} \tag{B.51}$$

which can be verified order by order. The operator R_3 can now be sandwiched between the quark-pair-gluon propagator \bar{G}_3 and two vertex interactions V , for which reason it is convenient to introduce \bar{V} as an abbreviation, defined by

$$V G_3 V = V G_3 V^\dagger = V R_3 \bar{G}_3 R_3^\dagger V^\dagger = \bar{V} \bar{G}_3 \bar{V}^\dagger = \bar{V} \bar{G}_3 \bar{V}. \tag{B.52}$$

One can show that R_3 is essentially diagonal and independent of the spin [7], such that each vertex element is multiplied with a number, actually with a number which depends on the momentum transfer Q across the vertex. Thus a very natural and physical interpretation is given to the operator R_3 , as being the vertex function. The transition $V \rightarrow \bar{V}$ is realized by defining an *effective coupling constant* \bar{g}

$$g \rightarrow \bar{g}(Q) = g R_3(Q). \tag{B.53}$$

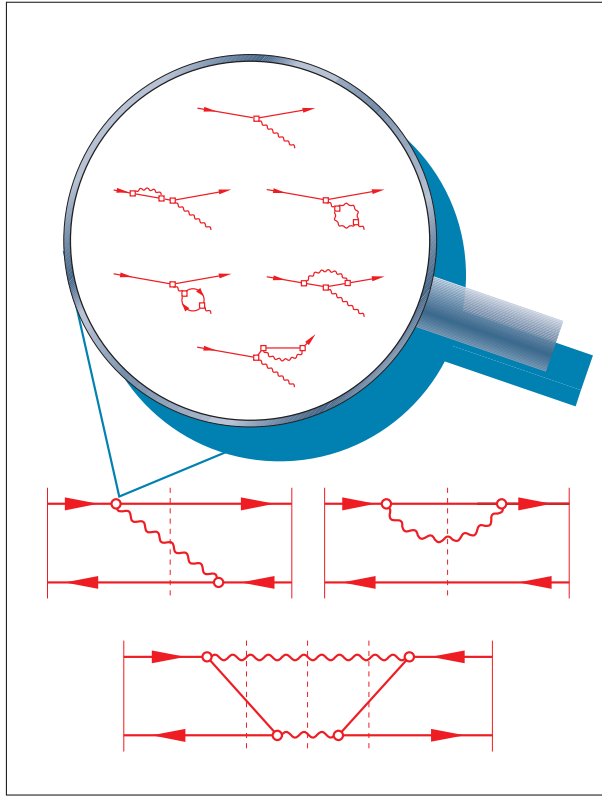
The effective one-body eigenvalue equation can now be written as

$$\begin{aligned}
 M_i^2 \langle x, \vec{k}_\perp, \lambda_q, \lambda_{\bar{q}} | \Psi_i \rangle &= \left[\frac{\bar{m}_q^2 + \vec{k}_\perp^2}{x} + \frac{\bar{m}_{\bar{q}}^2 + \vec{k}_\perp^2}{1-x} \right] \langle x, \vec{k}_\perp, \lambda_q, \lambda_{\bar{q}} | \Psi_i \rangle \\
 &+ \sum_{\lambda'_q, \lambda'_{\bar{q}}} \int dx' d^2 k'_\perp \langle x, \vec{k}_\perp, \lambda_q, \lambda_{\bar{q}} | \bar{V} \bar{G}_3 \bar{V} \\
 &+ \bar{V} \bar{G}_3 \bar{V} G_2 \bar{V} \bar{G}_3 \bar{V} | x', \vec{k}'_\perp, \lambda'_q, \lambda'_{\bar{q}} \rangle \langle x', \vec{k}'_\perp, \lambda'_q, \lambda'_{\bar{q}} | \Psi_i \rangle.
 \end{aligned} \tag{B.54}$$

Up to now all results are exact. We have seen how the method of iterated resolvents offers a compact notation of systematically resumming all perturbative diagrams without double counting. But when coming down to practical calculations one has to make

B. Light-front QCD

Figure 10: Taken from [25]. The vertical lines denote the free propagators. The coupling function at the vertices is symbolized by graphs as they would appear in a perturbative analysis.



approximations by breaking the propagator hierarchy. The reason for have written the effective equation (B.46) as (B.54) is that latter offers a better platform for doing approximations in propagators. Compared to the full dressed propagator G_3 , the propagator \bar{G}_3 is only partially dressed with the rest of its impact being shifted to the vertices. Thus approximating \bar{G}_3 by a free propagator in the $q\bar{q}g$ -space would be certainly less crude than it would be for G_3 . Unfortunately we do not have a similar construction for the full dressed propagator G_2 . To be consistent we are forced to approximate it by a free propagator in gg -space. As a net result, all what now has to be done is to update (Fig7) by replacing the dressed propagator G_2 and the partially dressed propagator \bar{G}_3 by free propagators and each point-like vertex by an effective vertex, indicated by little round circles as in (Fig9) or (Fig10).

B.2 Regularization

Before proceeding to solve the eigenvalue equation (B.54) the regularization of the theory need to be specified. As in every quantum field theory we are confronted with all kind of divergencies. In general the calculation of light-cone vertex matrix elements is seriously complicated by *ultraviolet singularities* occuring at very large values of the transverse momenta, and *infrared singularities* caused by longitudinal momenta close zero. If at each vertex a particle with four-momentum $p^\mu = (p^+, \vec{p}_\perp, p^-)$ is scattered into the momenta $p'^\mu = (zp^+, z\vec{p}_\perp + \vec{l}_\perp, p'^-)$ and $q^\mu = ((1-z)p^+, (1-z)\vec{p}_\perp - \vec{l}_\perp, q^-)$ of a second particle, the corresponding vertex matrix elements [12] are proportional to \vec{l}_\perp^2/z . They tend to diverge for $l_\perp \rightarrow \infty$ and/or $z \rightarrow 0$. Those difficulties demand the introduction of unphysical cut-off scales to regulate the theory, which in turn have to be removed by a renormalization scheme. Experience has shown [7] that a reliable method for treating the ultraviolet divergencies is to use the local *vertex regularization* scheme. Each matrix element is multiplied with a convergence enforcing form factor

$$\langle p|V|p', q\rangle \rightarrow \langle p|V|p', q\rangle R(\Lambda; p, p', q). \quad (\text{B.55})$$

There are three ways how to perform the regularization

$$R(\Lambda; p, p', q) = \begin{cases} R_Q(\Lambda; p, p'), \\ R_{M_0}(\Lambda; p', q), \\ R_Q(\Lambda; p, p') R_{M_0}(\Lambda; p', q), \end{cases} \quad (\text{B.56})$$

either by regulating the Feynman four-momentum transfer $Q^2 = -(p - p')^2$ across the vertex, or by regulating the free invariant mass $M_0^2 = (p' + q)^2$ after each vertex interaction, or if necessary both of them can be used. The regularization will be controlled by some scale parameter Λ . Since theory does not give us any hint on how to choose the regulating function R there will be an infinite number of such choices. The only requirement is that they have to drop at least quadratically for large values of Q or M_0 , while for small values the regulating function should tend to $R \rightarrow 1$, leaving the theory in this region unchanged. If not mentioned otherwise, we will focus on the following two structurally totally different functions

$$R(\Lambda) = \begin{cases} \text{sharp cut-off: } \Theta(Q^2 - \Lambda^2), \text{ or } \Theta(M_0^2 - \Lambda^2), \\ \text{soft cut-off: } \frac{\Lambda^2}{\Lambda^2 + Q^2}, \text{ or } \frac{\Lambda^2}{\Lambda^2 + M_0^2}. \end{cases} \quad (\text{B.57})$$

On the other hand the infrared singularities are taken care of by endorsing the gluon with a small regulator mass m_g . Both scale parameters Λ and m_g regulate then all divergencies on the light-cone.

Now everything is settled for calculating the relevant vertex matrix elements in equation (B.54). But before starting the calculations one first has to restore gauge invariance by resubstituting the instantaneous interactions W , which were omitted so far. As mentioned in the previous section one now makes use of the ‘gauge-trick’, where every

B. Light-front QCD

internal line has to be replaced by a dynamical and an instantaneous line. Having all this in mind and focusing only on the flavor conserving part of the interaction, the effective one-body equation takes on the form [12], [7]

$$\begin{aligned}
M_i^2 \langle x, \vec{k}_\perp, \lambda_q, \lambda_{\bar{q}} | \Psi_i \rangle &= \left[\frac{\overline{m}_q^2(\Lambda) + \vec{k}_\perp^2}{x} + \frac{\overline{m}_{\bar{q}}^2(\Lambda) + \vec{k}_\perp^2}{1-x} \right] \langle x, \vec{k}_\perp, \lambda_q, \lambda_{\bar{q}} | \Psi_i \rangle \\
&- \frac{1}{3\pi^2} \sum_{\lambda'_q, \lambda'_{\bar{q}}} \int \frac{dx' d^2 k'_\perp \langle x', \vec{k}'_\perp, \lambda'_q, \lambda'_{\bar{q}} | \Psi_i \rangle \overline{\alpha}(Q, \Lambda)}{\sqrt{x(1-x)x'(1-x')}} \frac{1}{Q^2} \\
&\times R^2(Q, \Lambda) \cdot [\overline{u}(k_q, \lambda_q) \gamma^\mu u(k'_q, \lambda'_q)] [\overline{v}(k'_{\bar{q}}, \lambda'_{\bar{q}}) \gamma_\mu v(k_{\bar{q}}, \lambda_{\bar{q}})], \quad (\text{B.58})
\end{aligned}$$

where it is convenient to see Q^2 as the mean Feynman 4-momentum transfer along the quark and the anti-quark line respectively

$$Q^2(x, \vec{k}_\perp; x', \vec{k}'_\perp) = -\frac{1}{2} [(k_q - k'_q)^2 + (k_{\bar{q}} - k'_{\bar{q}})^2]. \quad (\text{B.59})$$

The effective masses and the effective coupling constant $\overline{\alpha} = \overline{g}^2/4\pi$ have been calculated via the sharp cut-off $\Theta(M_0^2 - \Lambda^2)$:

$$\bullet \quad \overline{m}_f^2(\Lambda) = m_f^2 \left(1 + \frac{4\alpha}{3\pi} \ln \frac{\Lambda^2}{m_f^2} \right), \quad (\text{B.60})$$

$$\begin{aligned}
\bullet \quad \overline{\alpha}(Q, \Lambda) &= \frac{12\pi}{1/\alpha - (33 - 2N_f) \ln(\Lambda^2/\kappa^2) + b(Q)}, \\
\text{with } b(Q) &= 33 \ln \left((4m_g^2 + Q^2)/\kappa^2 \right) - 2 \sum_{f=1}^{N_f} \ln \left((4m_f^2 + Q^2)/\kappa^2 \right), \quad (\text{B.61})
\end{aligned}$$

$$\bullet \quad \overline{m}_g^2(\Lambda) = m_g^2 - \frac{\alpha}{4\pi} \sum_{f=1}^{N_f} m_f^2 \ln \frac{\Lambda^2}{4m_f^2}. \quad (\text{B.62})$$

As mentioned, a kinematical gluon mass m_g is introduced to control the infrared singularities. This is not in conflict with gauge theory: only the *physical gluon mass* must vanish due to gauge invariance. Thus $\overline{m}_g = 0$, which will express m_g in terms of the quark masses m_f . The arbitrary but fixed mass scale κ can be identified as the so called QCD-scale Λ_{QCD} which has to be determined by experiment.

All arguments and explicit calculations to get the above results are listed in detail in [28] and [7] and will be not repeated here.

C. Spinor Matrix

C Spinor Matrix

The Lorentz invariant spinor factor

$$S = [\bar{u}(k_1, \lambda_1) \gamma^\mu u(k'_1, \lambda'_1)] [\bar{v}(k'_2, \lambda'_2) \gamma_\mu v(k_2, \lambda_2)] \quad (\text{C.1})$$

is calculated explicitly [29]. In helicity space it can be understood as a 4×4 matrix $\langle \lambda_1, \lambda_2 | S | \lambda'_1, \lambda'_2 \rangle$ whose matrix elements are functions of x, \vec{k}_\perp and x', \vec{k}'_\perp . For convenience, S is calculated here as $S = 2T \sqrt{x(1-x)x'(1-x')}$, *i.e.*

$$\langle \lambda_q, \lambda_{\bar{q}} | T | \lambda'_q, \lambda'_{\bar{q}} \rangle = \frac{1}{2} \frac{[\bar{u}(k_1, \lambda_1) \gamma^\mu u(k'_1, \lambda'_1)] [\bar{v}(k'_2, \lambda'_2) \gamma_\mu v(k_2, \lambda_2)]}{\sqrt{xx'} \sqrt{(1-x)(1-x')}}. \quad (\text{C.2})$$

It is often useful to arrange S or T as a matrix in helicity space,

$$\langle \lambda_q, \lambda_{\bar{q}} | T | \lambda'_q, \lambda'_{\bar{q}} \rangle = \begin{matrix} & \uparrow\downarrow & \downarrow\uparrow & \uparrow\uparrow & \downarrow\downarrow \\ \begin{matrix} \uparrow\downarrow \\ \downarrow\uparrow \\ \uparrow\uparrow \\ \downarrow\downarrow \end{matrix} & \begin{pmatrix} T_{11} & T_{12} & T_{13} & T_{14} \\ T_{21} & T_{22} & T_{23} & T_{24} \\ T_{31} & T_{32} & T_{33} & T_{34} \\ T_{41} & T_{42} & T_{43} & T_{44} \end{pmatrix} & \end{matrix}. \quad (\text{C.3})$$

With $y \equiv 1 - x$ the diagonal elements are

$$\begin{aligned} T_{11} &= \frac{m_1^2}{xx'} + \frac{m_2^2}{yy'} + \frac{\vec{k}_\perp^2}{xy} + \frac{\vec{k}'_\perp^2}{x'y'} + \frac{\vec{k}_\perp \cdot \vec{k}'_\perp + i\vec{k}_\perp \wedge \vec{k}'_\perp}{xx'} + \frac{\vec{k}_\perp \cdot \vec{k}'_\perp - i\vec{k}_\perp \wedge \vec{k}'_\perp}{yy'}, \\ T_{22} &= T_{11}, \\ T_{33} &= \frac{m_1^2}{xx'} + \frac{m_2^2}{yy'} + \frac{\vec{k}_\perp \cdot \vec{k}'_\perp + i\vec{k}_\perp \wedge \vec{k}'_\perp}{xyx'y'}, \\ T_{44} &= T_{33}, \end{aligned} \quad (\text{C.4})$$

where $\vec{k}_\perp \cdot \vec{k}'_\perp = k_{\perp x} k'_{\perp x} + k_{\perp y} k'_{\perp y}$ and $\vec{k}_\perp \wedge \vec{k}'_\perp = k_{\perp x} k'_{\perp y} - k_{\perp y} k'_{\perp x}$. The off-diagonal matrix elements become

$$\begin{aligned} T_{12} &= -m_1 m_2 \frac{(x-x')^2}{xyx'y'}, & T_{21} &= -m_1 m_2 \frac{(x-x')^2}{xyx'y'}, \\ T_{13} &= \frac{m_2}{yy'} x \left[\frac{k_\perp(\uparrow)}{x} - \frac{k'_\perp(\uparrow)}{x'} \right], & T_{31} &= \frac{m_2}{yy'} x' \left[\frac{k_\perp(\downarrow)}{x} - \frac{k'_\perp(\downarrow)}{x'} \right], \\ T_{14} &= \frac{m_1}{xx'} y \left[\frac{k_\perp(\downarrow)}{y} - \frac{k'_\perp(\downarrow)}{y'} \right], & T_{41} &= \frac{m_1}{xx'} y' \left[\frac{k_\perp(\uparrow)}{y} - \frac{k'_\perp(\uparrow)}{y'} \right], \\ T_{23} &= \frac{m_1}{xx'} y \left[\frac{k_\perp(\uparrow)}{y} - \frac{k'_\perp(\uparrow)}{y'} \right], & T_{32} &= \frac{m_1}{xx'} y' \left[\frac{k_\perp(\downarrow)}{y} - \frac{k'_\perp(\downarrow)}{y'} \right], \\ T_{24} &= \frac{m_2}{yy'} x \left[\frac{k_\perp(\downarrow)}{x} - \frac{k'_\perp(\downarrow)}{x'} \right], & T_{42} &= \frac{m_2}{yy'} x' \left[\frac{k_\perp(\uparrow)}{x} - \frac{k'_\perp(\uparrow)}{x'} \right], \\ T_{34} &= 0, & T_{43} &= 0, \end{aligned} \quad (\text{C.5})$$

where $k_\perp(\uparrow) = -k_{\perp x} - ik_{\perp y}$ and $k_\perp(\downarrow) = k_{\perp x} - ik_{\perp y}$.

D Potential Scattering

The theory of stationary scattering in coordinate space, especially for potentials of finite range as well as for Coulomb potentials has been well studied and can be found in nearly any standard text book about quantum mechanics [31],[32],[33].

This is certainly not the case in momentum space. It is often advantageous to solve the scattering problem also in momentum space, because from a field-theoretical point of view momentum space represents a more natural description of physics. Unfortunately the momentum space representation suffers more on fundamental problems than its counter part representation. Especially the scattering problem for Coulomb-like potentials is far from being well understood — the scattering boundary conditions, namely to have an incoming and an outgoing scattered wave, are in momentum space far more difficult to implement than in coordinate space. But exactly these are necessary to formulate well defined quantities within Coulomb scattering. Up to now the general problem of *repulsive* Coulomb-like potentials can be regarded as solved [10]. But the scattering on *attractive* Coulomb-like potentials still seems to be terra incognita. The main problem, compared to its *repulsive* counter part lies in the fact that every *attractive* Coulomb-like potential has besides the scattering region also a bound-state region with an infinite range, which makes it nearly impossible to work with it numerically in momentum space. In our case of the ST-model we are confronted with this problem of having an *attractive* Coulomb-like potential in momentum space. At the very end of this section, a partial solution to this problem is proposed. Furthermore, our ST-potential will give rise to so called *resonances*. The word *resonance* is given many meanings in the literature, which leads to much confusion. I shall try to avoid this confusion by being as specific and illustrative as possible, and show how a resonance state can be completely described in the stationary picture, by approaching it from three different perspectives.

To attack all this, it is useful to give a brief but complete overview on stationary scattering in order to have a unique notation and to clarify still existing problems. Furthermore, it is helpful not to use a specific representation of the stationary Schrödinger equation, but rather look for a formal solution in the scattering region, which will lead us to the Lippmann-Schwinger equation.

This whole section will only deal with elastic non-relativistic one-particle scattering. Scattering of a physical particle is a dynamical process, and is treated correctly when solving the time-dependent Schrödinger equation using localized wave packets as an initial condition. A scattering experiment consists of an incident and a scattered beam, which are well separated in time. The accessible quantity for the experiment is the concept of the cross-section, which in differential form is defined as

$$d\sigma = \frac{\text{number of events in } d\Omega \text{ per time unit}}{\text{incident particle flux}} = \frac{\vec{j}_s \cdot d\vec{F}}{|\vec{j}_0|}, \quad (\text{D.1})$$

where we assumed that the detector, located in the asymptotic scattering region, opens a cone of a solid angle $d\Omega$ from the origin of the target. The quantity $\vec{j}_s \cdot d\vec{F}$ is then

D. Potential Scattering

the measured flux of the scattered particles within the area $d\vec{F} = r^2 d\Omega \cdot \hat{e}_r$ covered by the detector. Clearly, $d\sigma$ has the dimension of an area.

The big disadvantage of the time-dependent picture using wave packets is its mathematical inaccessibility. But since our main interest in scattering processes lies in the determination of (D.1), it is not necessary to work all the way in the time-dependent picture. Probability current densities as \vec{j}_s and \vec{j}_0 are also well defined expressions in the time-*independent* picture. Although this stationary picture offers a mathematically much easier approach for calculating the cross-section (D.1), general calculations and physical interpretations have to be done with great care. As we know, functions in the stationary picture are energy eigenstates, and according to the uncertainty principle the incident and the scattered state are totally unlocalized and begin to coincide in time. Furthermore, since we are focusing only on elastic scattering, the incident and the scattered state must have the same energy, thus they are both solutions of the same stationary Schrödinger equation. For this, its of utmost importance in this picture, to always have a strict separation of what is the incident and what is the scattered part of the stationary wave, in order to avoid unphysical interferences.

D.1 Potentials of finite range

This case will restrict potentials to have a limited range, or more precisely, the potentials have to fall off faster than a Coulomb potential does. Coulomb scattering is thus excluded in this section and has to be treated separately.

D.1.1 Formal stationary scattering solution

Our problem consists in finding the scattering solution of

$$H|\Psi\rangle = E|\Psi\rangle, \tag{D.2}$$

where the Hamiltonian is given by

$$H = H_0 + H_1. \tag{D.3}$$

H_0 should represent that part of H , for which the eigenvalue problem is solved

$$H_0|\varphi\rangle = E_0|\varphi\rangle, \tag{D.4}$$

and we call the auxiliary system with energy eigenvalues E_{0i} and its corresponding orthonormal state vectors $|\varphi_i\rangle$ the *reference system* — the index i represents a collection of all relevant quantum numbers characterizing this energy state.

We now must make certain assumptions as to the structure of the H - and H_0 -spectrum:

- We allow that H_0 can have, besides the continuum part of its spectrum, a discrete bound state part. The property that the eigenstates of H_0 form a complete set has the general form

$$\mathbb{1} = \sum_i |\varphi_i\rangle\langle\varphi_i| + \int dj |\varphi_j\rangle\langle\varphi_j|. \tag{D.5}$$

D. Potential Scattering

- As is always possible, we shall adjust the energy scale in H_0 in such a way that the continuum starts at $E_0 = 0$ and all states in the continuous spectrum have $E_0 \geq 0$. On the other hand if discrete bound states exist, they are supposed to lie lower than any state in the continuum.
- Furthermore we make the nontrivial assumption, namely, that the energies of the *continuum states* of H_0 are not changed by switching on H_1 . In other words, we assume that the *continuum* of both H_0 and H starts at $E = E_0 = 0$ and that to each state $|\varphi\rangle$ in the *continuous* part of the H_0 spectrum, which has an energy E_0 , there belongs a corresponding state $|\Psi\rangle$ in the *continuum* of the H -spectrum, which has *the same energy* $E = E_0$.

Thus, so long as we consider only states in the *continuum* one can write (D.4) as

$$(E - H_0)|\varphi\rangle = 0, \quad (\text{D.6})$$

and see it as a homogeneous solution of the complete equation (D.2)

$$(E - H_0)|\Psi\rangle = H_1|\Psi\rangle. \quad (\text{D.7})$$

Solving for $|\Psi\rangle$ will give the formal self-consistent solution

$$|\Psi^\pm\rangle = |\varphi\rangle + G_0^\pm \cdot H_1 \cdot |\Psi^\pm\rangle, \quad (\text{D.8})$$

where G_0^\pm stands for the Greens-function of the reference operator H_0

$$G_0^\pm = \frac{1}{E - H_0 \pm i \cdot \epsilon}, \quad (\text{D.9})$$

which according to (D.5) has the bilinear expansion

$$G_0^\pm = \sum_n \frac{|\varphi_n\rangle\langle\varphi_n|}{E - E_n} + \int_0^\infty dE' \frac{|\varphi_{E'}\rangle\langle\varphi_{E'}|}{E - E' \pm i \cdot \epsilon}. \quad (\text{D.10})$$

Equation (D.8) is a mathematically well defined equation for $|\Psi^\pm\rangle$ as long H_0 as well as H_1 only contain short-ranged potentials. It is called the Lippmann-Schwinger equation and is a complementary description of the Schrödinger equation in the scattering region. As one can regard the Schrödinger equation as a local description of the system, the Lippmann-Schwinger equation serves more as a global description, since the need for implementing boundary conditions appears automatically.

The solution $|\Psi^+\rangle$ is properly called an *outgoing* eigenstate of the full Hamiltonian, while the other linear independent solution $|\Psi^-\rangle$ has the meaning of an *incoming* eigenstate of H . Both the *out*-states and the *in*-states have a physical content — both contain incoming and outgoing wave components, which have to be matched to given boundary conditions.

D. Potential Scattering

The ultimate goal of scattering theory is the connection to experiment. A central concept is the scattering or S -matrix, which is defined as

$$|\Psi^+\rangle = S|\Psi^-\rangle. \quad (\text{D.11})$$

Normalization or probability conservation immediately yields the unitarity condition for the scattering matrix

$$S^\dagger S = \mathbb{1}. \quad (\text{D.12})$$

Other postulates on S involve invariance properties and analyticity requirements, but I will not discuss it here in further detail.

According to our previous made assumptions, the *in*- and *out*-states can be expanded in terms of eigenfunctions of the reference operator H_0

$$|\Psi^-\rangle = \sum_{\alpha} c_{\alpha} |\varphi_{\alpha}\rangle \quad , \quad |\Psi^+\rangle = \sum_f c_f |\varphi_f\rangle. \quad (\text{D.13})$$

The sum has to be seen as a generalized sum, which turns into an integral if the quantum numbers lie in a continuum. Substituting the expansion into the definition (D.11) and inserting on the right-hand side the completeness relation $\sum_f |\varphi_f\rangle\langle\varphi_f| = \mathbb{1}$, yields

$$c_f = \sum_{\alpha} c_{\alpha} S_{f\alpha} \quad , \quad \text{where} \quad S_{f\alpha} = \langle\varphi_f|S|\varphi_{\alpha}\rangle. \quad (\text{D.14})$$

Since our potential in H_1 is of finite range, it is possible to prepare the *in*-state into a definite state of the reference system $|\Psi_i^-\rangle = |\varphi_i\rangle$, that means if $c_{\alpha} = \delta_{\alpha i}$ then $c_f = S_{fi}$ and the *general out*-state $|\Psi^+\rangle$ turns into a *prepared out*-state with quantum numbers i

$$|\Psi_i^+\rangle = \sum_f S_{fi} |\varphi_f\rangle. \quad (\text{D.15})$$

The coefficient c_f of the expansion (D.13) describes the probability of finding the system in that state having the quantum numbers f . Thus the scattering matrix $c_f = S_{fi}$ is the probability amplitude for a process in which the system makes a transition from an initial state $|\varphi_i\rangle$ to a final state $|\varphi_f\rangle$ under the influence of an interaction. As follows from the unitary condition (D.12) for the scattering matrix,

$$\sum_f |S_{fi}|^2 = 1, \quad (\text{D.16})$$

the sum of all probabilities is equal to one. This makes the scattering matrix accessible for experiments. However, the squared magnitude of the amplitude S_{fi} is not a meaningful quantity in the functional sense. Since strict energy conservation is certainly guaranteed between initial and final states, we have to split off an energy-conservation factor, which is a delta function. For this we want to rewrite the scattering matrix by defining a new operator, the transition or T -matrix.

D. Potential Scattering

To get there, we first look at the adjuncated form of the definition (D.11)

$$\langle \Psi^+ | = \langle \Psi^- | S^\dagger \iff \langle \Psi^- | = \langle \Psi^+ | S. \quad (\text{D.17})$$

For the bra-kets an analog expansion (D.13) can be done, which results in

$$\langle \Psi_f^- | = \sum_i S_{fi} \langle \varphi_i |, \quad (\text{D.18})$$

where we prepared the *out*-state to a specific state of the reference system $\langle \Psi_f^+ | = \langle \varphi_f |$. The amplitude of such a prepared *in*-state with quantum numbers f with the previously prepared *out*-state with quantum numbers i , will give

$$\langle \Psi_f^- | \Psi_i^+ \rangle = \sum_{n,m} S_{fn} S_{mi} \langle \varphi_n | \varphi_m \rangle = S_{fi}. \quad (\text{D.19})$$

Thus the elements of the S -matrix between initial and final states of the *reference system* can also be expressed simply as the amplitude of the correspondingly *specified in-* and *out*-states, which are solutions of the Lippmann-Schwinger equation (D.8).

We now return to these solutions by doing one complete iteration

$$|\Psi^\pm\rangle = |\varphi\rangle + G_0^\pm H_1 |\varphi\rangle + G_0^\pm H_1 G_0^\pm H_1 |\Psi^\pm\rangle. \quad (\text{D.20})$$

Multiplying with the inverse of G_0^\pm

$$\begin{aligned} (E - H_0 \pm i\epsilon) |\Psi^\pm\rangle &= (E - H_0 \pm i\epsilon) |\varphi\rangle + H_1 |\varphi\rangle + H_1 G_0^\pm H_1 |\Psi^\pm\rangle \\ &= \pm i\epsilon |\varphi\rangle + H_1 |\Psi^\pm\rangle, \end{aligned} \quad (\text{D.21})$$

the Lippmann-Schwinger solutions can be written in an alternative way as

$$\begin{aligned} |\Psi^\pm\rangle &= \frac{\pm i\epsilon}{E - H_0 - H_1 \pm i\epsilon} |\varphi\rangle \\ &\equiv |\varphi\rangle + G^\pm H_1 |\varphi\rangle, \end{aligned} \quad (\text{D.22})$$

where G^\pm stands for the Greens-function of the full Hamiltonian H . This new form helps us to write the scattering matrix (D.19) as

$$\begin{aligned} \langle \Psi_f^- | \Psi_i^+ \rangle &= \langle \varphi_f | \Psi_i^+ \rangle + \langle \varphi_f | H_1 G_f^+ \Psi_i^+ \rangle \\ &= \langle \varphi_f | \Psi_i^+ \rangle + \langle \varphi_f | H_1 \Psi_i^+ \rangle \frac{1}{E_f - E_i + i\epsilon} \\ &= \delta_{fi} + \left[\frac{1}{E_f - E_i + i\epsilon} - \frac{1}{E_f - E_i - i\epsilon} \right] \langle \varphi_f | H_1 \Psi_i^+ \rangle \\ &= \delta_{fi} + \frac{-2i\epsilon}{\epsilon^2 + (E_f - E_i)^2} \langle \varphi_f | H_1 \Psi_i^+ \rangle \\ &\stackrel{\epsilon \rightarrow 0}{=} \delta_{fi} - 2\pi i \cdot \delta(E_f - E_i) \langle \varphi_f | H_1 \Psi_i^+ \rangle. \end{aligned} \quad (\text{D.23})$$

D. Potential Scattering

By defining the new transition or T -matrix as

$$H_1|\Psi_i^+\rangle = T|\varphi_i\rangle, \quad (\text{D.24})$$

the scattering matrix takes the form

$$S_{fi} = \delta_{fi} - 2\pi i \cdot \delta(E_f - E_i)T_{fi}, \quad (\text{D.25})$$

where $S_{fi} = \langle\varphi_f|S|\varphi_i\rangle$ and $T_{fi} = \langle\varphi_f|T|\varphi_i\rangle$. It should be clearly visualized that there is a significant difference between the roles of δ_{fi} and $\delta(E_f - E_i)$ — the symbol E_f for example represents the continuum scattering energy E which is characterized through the quantum numbers f .

With the above identity, the determination of the S -matrix is now reduced to the problem of calculating the T -matrix. By defining a more general transition operator

$$T^\pm|\varphi\rangle = H_1|\Psi^\pm\rangle, \quad (\text{D.26})$$

it is possible to write the Lippmann-Schwinger equation as a pure operator equation

$$T^\pm = H_1 + H_1 \cdot G_0^\pm \cdot T^\pm. \quad (\text{D.27})$$

A challenging task is not to find approximate solutions through iteration but to calculate the full solution

$$T^\pm = (\mathbb{1} - H_1 \cdot G_0^\pm)^{-1} \cdot H_1. \quad (\text{D.28})$$

In the case where G_0^\pm is the free-particle Greens-function this can easily be achieved numerically, as in (Appendix E).

Although the S -matrix is related to the T -matrix by means of the identity (D.25), scattering theory can be viewed from two different perspectives when working either with the T -operator or the S -operator. As the definition (D.26) reveals, the transition matrix is a connection between the full system and the reference system — in other words in (D.24) it connects an incident state with the correspondingly prepared *out*-state. In contrary to that, the scattering matrix (D.11) closes the system on itself: an *incoming* state is scattered to an *outgoing* state — it serves as a relation between the initial and final eigenstates of the full system.

If H_0 is chosen to be the free-particle Hamiltonian and H_1 to be a rotational invariant potential, the S - and T -matrix can be easily simplified into workable expressions, still without being restricted to any specific representation. The set of eigenvectors of H_0 are plane waves, or more precisely, they are momentum eigenstates characterized by the quantum number \vec{k} . In this case the S -matrix (D.25) is given as

$$\begin{aligned} S_{\vec{k}'\vec{k}} &= \langle\vec{k}'|S|\vec{k}\rangle = \delta(\vec{k}' - \vec{k}) - 2\pi i \cdot \delta(E_{k'} - E_k)T_{\vec{k}'\vec{k}} \\ &= \delta(\vec{k}' - \vec{k}) - 2\pi i \cdot \frac{m}{k} \cdot \delta(k' - k)T_{\vec{k}'\vec{k}}. \end{aligned} \quad (\text{D.29})$$

D. Potential Scattering

Since the total interaction is rotation invariant, the scattering matrix will be the same before and after a rotation U_R

$$\langle U_R \vec{k}' | S | U_R \vec{k} \rangle = \langle \vec{k}' | S | \vec{k} \rangle. \quad (\text{D.30})$$

Hence, the scattering matrix cannot depend on the absolute orientation of the vectors \vec{k} and \vec{k}' . It can be only a function of the energy and the angle between the initial and final momenta. Thus the scattering matrix can be expanded into Legendre polynomials

$$S_{\vec{k}'\vec{k}} = \langle \vec{k}' | S | \vec{k} \rangle = \frac{\delta(k' - k)}{4\pi k^2} \sum_{l=0}^{\infty} (2l + 1) S_l(k) P_l(\cos \vartheta). \quad (\text{D.31})$$

The delta function has been included as a separate factor, because we already know that the S -matrix has nonvanishing elements only on the energy shell. The unknown coefficients $S_l(k)$ can be determined by invoking the unitarity of the scattering matrix

$$\int d^3 k'' \langle \vec{k}' | S | \vec{k}'' \rangle \langle \vec{k}'' | S^\dagger | \vec{k} \rangle = \delta(\vec{k}' - \vec{k}). \quad (\text{D.32})$$

Substituting here (D.31) and carrying out the integration, we obtain

$$\frac{\delta(k' - k)}{4\pi k^2} \sum_{l=0}^{\infty} (2l + 1) |S_l(k)|^2 P_l(\cos \vartheta) = \delta(\vec{k}' - \vec{k}) \quad (\text{D.33})$$

From the completeness relation of the Legendre polynomials, the above equation will only be fulfilled if $|S_l(k)|^2 = 1$, that means if $S_l(k) = e^{2i\delta_l(k)}$, where the $\delta_l(k)$ are real functions of the momentum. An analog expansion of the T -matrix

$$T_{\vec{k}'\vec{k}} = \langle \vec{k}' | T | \vec{k} \rangle = -\frac{1}{4\pi^2 m k} \sum_{l=0}^{\infty} (2l + 1) T_l(k', k) P_l(\cos \vartheta), \quad (\text{D.34})$$

together with (D.29), will yield $T_l(k, k) = e^{i\delta_l(k)} \sin \delta_l(k)$. The interpretation and importance of the functions $\delta_l(k)$ will be discussed next.

D.1.2 Stationary scattering in the coordinate space picture

To give scattering theory a more illustrative meaning, we will now translate the previous results to coordinate space. For that, the choice of the reference system will be the free-particle Hamiltonian $H_0 = \vec{k}^2/2m$, while for the potential $H_1 = V$ we only want to demand locality. The eigenstates of H_0 are normalized to $\langle \vec{k} | \vec{k}' \rangle = \delta(\vec{k} - \vec{k}')$, while for the coordinate eigenstates we require $\langle \vec{r} | \vec{r}' \rangle = \delta(\vec{r} - \vec{r}')$.

We start off with the Lippmann-Schwinger solution (D.8)

$$\begin{aligned} \langle \vec{r} | \Psi_{\vec{k}}^\pm \rangle &= \langle \vec{r} | \varphi_{\vec{k}} \rangle + \int d^3 r' d^3 r'' \langle \vec{r} | G_0^\pm | \vec{r}' \rangle \langle \vec{r}' | V | \vec{r}'' \rangle \langle \vec{r}'' | \Psi_{\vec{k}}^\pm \rangle \\ &= \langle \vec{r} | \varphi_{\vec{k}} \rangle + \int d^3 r' \langle \vec{r} | G_0^\pm | \vec{r}' \rangle \cdot V(\vec{r}') \cdot \langle \vec{r}' | \Psi_{\vec{k}}^\pm \rangle. \end{aligned} \quad (\text{D.35})$$

D. Potential Scattering

Inserting the complete set of eigenstates of H_0

$$\begin{aligned}
 \langle \vec{r} | G_0^\pm | \vec{r}' \rangle &= \int d^3 k' d^3 k'' \langle \vec{r} | \varphi_{\vec{k}'} \rangle \langle \varphi_{\vec{k}'} | G_0^\pm | \varphi_{\vec{k}''} \rangle \langle \varphi_{\vec{k}''} | \vec{r}' \rangle \\
 &= \frac{1}{(2\pi)^3} \int d^3 k' \frac{e^{\pm i \vec{k}' \cdot (\vec{r} - \vec{r}')}}{E - \frac{k'^2}{2m} \pm i\epsilon} \quad ; \quad E = k^2/2m \\
 &= -\frac{2m \cdot e^{\pm i |\vec{k}| \cdot |\vec{r} - \vec{r}'|}}{4\pi |\vec{r} - \vec{r}'|}, \tag{D.36}
 \end{aligned}$$

equation (D.35) can be written as

$$\begin{aligned}
 \Psi_{\vec{k}}^\pm(\vec{r}) &= \frac{1}{(2\pi)^{3/2}} e^{\pm i \vec{k} \cdot \vec{r}} - \frac{m}{2\pi} \int d^3 r' \frac{e^{\pm i |\vec{k}| \cdot |\vec{r} - \vec{r}'|}}{|\vec{r} - \vec{r}'|} V(\vec{r}') \Psi_{\vec{k}}^\pm(\vec{r}') \\
 &\stackrel{r \rightarrow \infty}{=} \frac{1}{(2\pi)^{3/2}} \left[e^{\pm i \vec{k} \cdot \vec{r}} + f_{\vec{k}}(\varphi, \vartheta) \cdot \frac{e^{\pm i k r}}{r} \right], \tag{D.37}
 \end{aligned}$$

where $f_{\vec{k}}(\varphi, \vartheta)$ is called the scattering amplitude, depending only on the momentum parameter \vec{k} and the direction of \vec{r}

$$f_{\vec{k}}(\varphi, \vartheta) = -\frac{m}{2\pi} (2\pi)^{3/2} \int d^3 r' e^{\mp i |\vec{k}| \cdot \hat{r} \cdot \vec{r}'} V(\vec{r}') \Psi_{\vec{k}}^\pm(\vec{r}') \quad ; \quad |\hat{r}| = |\vec{r}'/r| = 1. \tag{D.38}$$

The last step in equation (D.37) is allowed for all potentials V falling off faster than a Coulomb potential. So the scattering amplitude as given in (D.38) is a well defined expression only for short-ranged potentials.

The asymptotic solution in (D.37) is a superposition of a plane wave and a spherical wave. To adjust this solution to the boundary conditions of a scattering problem, namely having an *incident* beam and an *outgoing* scattered beam, the only reasonable solution is $\Psi_{\vec{k}}^+(\vec{r})$. This solution is called the physical solution and will simply be denoted by $\Psi_{\vec{k}}(\vec{r})$. Its asymptotic structure makes it possible to strictly separate the incident flux from the scattered flux, necessary for calculating the cross-section (D.1). For this calculation, the precise value of the overall asymptotic normalization constant, here $N = (2\pi)^{-3/2}$ is unimportant. The wave function $\Psi_{\vec{k}}(\vec{r})$ can also be normalized to unit incident flux by choosing $N = (|\vec{k}|/m)^{-1/2}$, or by requiring $\int d^3 r \Psi_{\vec{k}'}^* \Psi_{\vec{k}} = \delta(\vec{k}' - \vec{k})$. But certainly the simplest normalization is that where the incident amplitude is of unity. Performing the calculation (D.1), the differential cross-section per unit angle is

$$\frac{d\sigma}{d\Omega} = |f_{\vec{k}}(\varphi, \vartheta)|^2. \tag{D.39}$$

For knowing the cross-section one has to know the scattering amplitude, which again is determined from the asymptotic behaviour of the full wavefunction.

D. Potential Scattering

From (D.38) and the definition of the T -matrix (D.24), the scattering amplitude can also be written as

$$\begin{aligned} f_{\vec{k}}(\varphi, \vartheta) &= -4m\pi^2 \langle \varphi_{\hat{k}} | V | \Psi_{\vec{k}} \rangle \quad ; \quad \hat{k} = |\vec{k}| \cdot \hat{r} \\ &\equiv -4m\pi^2 \langle \varphi_{\vec{k}'} | T | \varphi_{\vec{k}} \rangle \quad ; \quad k'^2 = k^2. \end{aligned} \quad (\text{D.40})$$

Due to its representation independence the above relationship between the scattering amplitude and the T -matrix is of great importance, since it opens the possibility to calculate scattering amplitudes and with it cross-sections in a representation different than that of coordinate space, as for example in momentum space.

The asymptotic wavefunction in (D.37) can be simplified tremendously, if we restrict ourselves on incident beams that propagate in the z -direction with momentum k and potentials that are spherically symmetric $V(\vec{r}) = V(|\vec{r}|)$. The whole scattering problem becomes symmetric around the z -axis and thus independent of the polar angle φ . Choosing the overall normalization for the amplitude of the incident beam as unity, the physical axial-symmetric solution reads

$$\begin{aligned} \Psi_k(r, \vartheta) &\underset{r \rightarrow \infty}{=} e^{ikz} + f_k(\vartheta) \cdot \frac{e^{ikr}}{r}, \\ \text{with } f_k(\vartheta) &= -\frac{m}{2\pi} \int d^3r' e^{-ikr' \cos \alpha} V(r') \Psi_k(r', \vartheta'), \end{aligned} \quad (\text{D.41})$$

where α is the angle between \vec{r} and \vec{r}' . The underlying symmetry now allows for a partial wave analysis in coordinate space

$$\Psi_k(r, \vartheta) = \sum_{l=0}^{\infty} a_{l,k} \frac{u_{l,k}(r)}{r} P_l(\cos \vartheta), \quad (\text{D.42})$$

where the wavefunction $u_{l,k}(r)$ can be related to the solutions of the radial Schrödinger equation

$$\frac{d^2}{dr^2} u_{l,k}(r) + \left(k^2 - 2mV(r) - \frac{l(l+1)}{r^2} \right) u_{l,k}(r) = 0. \quad (\text{D.43})$$

For large r , terms of the order smaller than $1/r$ can be neglected and the general asymptotic solution for finite range potentials is

$$\begin{aligned} u_{l,k}(r) &\underset{r \rightarrow \infty}{=} B_{l,k} \sin(kr) + C_{l,k} \cos(kr) \\ &\equiv A_{l,k} \sin\left(kr - \frac{l\pi}{2} + \delta_{l,k}\right). \end{aligned} \quad (\text{D.44})$$

When fixing the normalization constant of $u_{l,k}$ in the asymptotic region as $A_{l,k} = e^{i\delta_{l,k}}$, it is possible to make an identical comparison between the wavefunctions (D.41) and (D.42).

D. Potential Scattering

This can be seen when using the following identity

$$e^{i\delta_{l,k}} \sin(kr - \frac{l\pi}{2} + \delta_{l,k}) \equiv \sin(kr - \frac{l\pi}{2}) + e^{i\delta_{l,k}} \sin \delta_{l,k} \cdot e^{i(kr - \frac{l\pi}{2})}. \quad (\text{D.45})$$

For large r this will force the expansion (D.42) to have the structure

$$\begin{aligned} \Psi_k(r, \vartheta) \underset{r \rightarrow \infty}{=} & \sum_{l=0}^{\infty} a_{l,k} \frac{\sin(kr - \frac{l\pi}{2})}{r} P_l(\cos \vartheta) \\ & + \left[\sum_{l=0}^{\infty} (-i)^l a_{l,k} e^{i\delta_{l,k}} \sin \delta_{l,k} P_l(\cos \vartheta) \right] \frac{e^{ikr}}{r}. \end{aligned} \quad (\text{D.46})$$

The above expression has to be equal to the right hand side of (D.41), and together with the next identity

$$\begin{aligned} e^{ikz} = e^{ikr \cos \vartheta} &= \sum_{l=0}^{\infty} i^l (2l+1) j_l(kr) P_l(\cos \vartheta) \\ &\underset{r \rightarrow \infty}{=} \sum_{l=0}^{\infty} i^l (2l+1) \frac{\sin(kr - \frac{l\pi}{2})}{kr} P_l(\cos \vartheta), \end{aligned} \quad (\text{D.47})$$

where j_l stand for the at the origin regular spherical Bessel-functions, will fix the coefficients $a_{l,k} = i^l (2l+1)/k$ and the scattering amplitude can be identified as

$$f_k(\vartheta) = \frac{1}{k} \sum_{l=0}^{\infty} (2l+1) e^{i\delta_{l,k}} \sin \delta_{l,k} P_l(\cos \vartheta). \quad (\text{D.48})$$

As we clearly can see, all the information of the scattering process within spherical symmetric potentials is hidden in the asymptotic parameter $\delta_{l,k}$, which is called the phase-shift. This is the well known result $f_k(\vartheta) = -4m\pi^2 \langle \vec{k}' | T | \vec{k} \rangle \big|_{k'=k}$ of (D.34), and was to be expected. The total cross-section of (D.39) can be calculated as

$$\sigma_k = \int d\Omega \frac{d\sigma_k}{d\Omega} = \int d\Omega |f_k(\vartheta)|^2 = \frac{4\pi}{k^2} \sum_{l=0}^{\infty} (2l+1) \sin^2 \delta_{l,k} \equiv \frac{4\pi}{k^2} \sum_{l=0}^{\infty} \sigma_{l,k}. \quad (\text{D.49})$$

The more important point is, the way how we manipulated the radial Schrödinger solution, by using the freedom of the normalization constant to get the asymptotic form

$$u_{l,k}(r) \underset{r \rightarrow \infty}{=} \sin(kr - \frac{l\pi}{2}) + T_l(k) \cdot e^{i(kr - \frac{l\pi}{2})}, \quad (\text{D.50})$$

with $T_{l,k} = e^{i\delta_{l,k}} \sin \delta_{l,k}$. As stated before in the abstract formalism, we clearly see here how the T -matrix, or more precise the diagonal elements of the T -matrix connects two different wave-types. The first term represents the incident beam, having here the properties of a standing wave, while the second term is the scattered outgoing wave. The scattering process adds to the free-particle plane wave function an outgoing spherical wave whose amplitude is T_l . This representation is thus also called the T -matrix solution of the radial Schrödinger equation.

D. Potential Scattering

On the other hand, the identity (D.45) may also be written as

$$e^{i\delta_{l,k}} \sin(kr - \frac{l\pi}{2} + \delta_{l,k}) \equiv \frac{i}{2} \left[e^{-i(kr - \frac{l\pi}{2})} - e^{2i\delta_{l,k}} \cdot e^{i(kr - \frac{l\pi}{2})} \right]. \quad (\text{D.51})$$

The same is true for the incident beam in (D.47), which can be split up into incoming and outgoing wave components. Since the choice of our boundary condition only allows for incoming waves for the incident beam, the scattering amplitude can again be identified as in (D.48), as expected. But now the asymptotic radial Schrödinger solution has the structure

$$u_{l,k}(r) \underset{r \rightarrow \infty}{=} \frac{i}{2} \left[e^{-i(kr - \frac{l\pi}{2})} - S_l(k) \cdot e^{i(kr - \frac{l\pi}{2})} \right], \quad (\text{D.52})$$

with the S -matrix $S_{l,k} = e^{2i\delta_{l,k}}$, or more precise the diagonal elements of the S -matrix which connects two similar wave-types. Here we can see that the incoming spherical wave is unaffected by the scattering process, while the outgoing wave is multiplied by the quantity S_l . Only the phase, and not the amplitude of the outgoing spherical wave is affected by the presence of the potential. This solution is called the S -matrix solution of the radial Schrödinger equation, and from now on we simply call $S_l(k)$ the scattering function.

The S -matrix representation in general is very convenient for investigating certain structures, like minima, maxima or sharp peaks in the cross-section.

The reason of a vanishing cross-section for a particular energy can immediately be understood, if one looks at (D.52). For all momenta k where the scattering function $S_l(k) = 1$, the outgoing wave $e^{i(kr - \frac{l\pi}{2})}$ and the incoming wave $e^{-i(kr - \frac{l\pi}{2})}$ can be combined to give the standing wave $\sin(kr - \frac{l\pi}{2})$, which looks like a component of an incident plane wave with no scattered portion. *Classically* speaking, there is zero scattering when the final trajectory is in the same direction as the initial one.

The effects which cause sharp peaks in the scattering cross-section, are called resonances, and are not so easy to understand. They are linked to particular properties of the scattering function $S_l(k)$. For this we rewrite (D.52) as follows

$$u_{l,k}(r) \underset{r \rightarrow \infty}{=} \frac{i}{2} S_l(k) \left[\frac{1}{S_l(k)} e^{-i(kr - \frac{l\pi}{2})} - e^{i(kr - \frac{l\pi}{2})} \right]. \quad (\text{D.53})$$

According to Gamow [34] we obtain a resonance, if we postulate that the above asymptotic solution consists of outgoing waves only. This is equivalent to the condition $1/S_l(k) = 0$. But the resulting equation $e^{-2i\delta_l(k)} = 0$ has no solution for real k . Thus our only choice is to go into the complex momentum plane $k \rightarrow q = k + i\eta$, with $k \geq 0$, and study the effects of the complex zeros of $1/S_l(q)$ upon its behaviour on the real k -axis — because all the above results on a scattering wave function strictly apply only for real momenta. It can be shown that the closer the complex zero q lies toward the real k -axis, the more it becomes to a physically observed effect in the cross-section. Before going into the complex momentum plane q , it is helpful to rewrite the scattering function $S_l(k)$ as

$$S_l(k) = e^{2i\delta_l(k)} \equiv \frac{F_l(k)}{F_l^*(k)}, \quad \text{with} \quad \delta_l(k) = \arg[F_l(k)] \quad \text{and} \quad k \in \mathbb{R}, \quad (\text{D.54})$$

D. Potential Scattering

where $F_l(k)$ is a complex function of a real argument, which is called the Jost-function. Now for finding the zeros of $1/S_l(k)$, or equivalently the poles of the scattering function $S_l(k)$, we have to do an analytical continuation into the complex momentum plane for the Jost-function $F(k) \rightarrow F(q)$. For the analytic properties of the Jost-function one can refer to [33] — just important to note is that its analytical continuation in the complex momentum plane is different from that being done in the complex energy plane, due of having the problem of double mapping $E \sim k^2$.

The reason why this postulate of having only outgoing waves causes sharp peaks or rapid changes in the cross-section and what the physical interpretations and implications of complex momenta and energies are, will be discussed in detail in the next section under the more simplified condition of s-wave scattering on potentials with a strict range R . Before ending this first discussion on resonances, it is interesting to see how bound states and resonances are embedded in the stationary formalism. Bound states are obtained when requiring in the energy region $E < 0$ the boundary condition of having a vanishing wave in the asymptotic region. Since this boundary condition is real, it will only allow for certain discrete real and negative energy eigenvalues, which are characterized by one parameter, namely the energy value itself. On the other hand, resonances are obtained when requiring in the scattering region $E > 0$ the boundary condition of having a pure outgoing wave in the asymptotic region. As in the case of the bound state condition, this resonance condition will also only allow for certain discrete values, but since the boundary condition is complex, these discrete energy eigenvalues are also expected to be complex, and thus must be characterized by two parameters, their energy and width (E_R, Γ) — in the scattering region it is justified to talk of an energy width, since the relevant energy spectrum is lying in a continuum.

An interesting application of the analytical continued Jost-function $F_l(q)$ is the so called Levinson Theorem. It connects the real scattering phase-shift to existing bound states in that system. I state it here without proof [33]

$$\delta_l(0) - \delta_l(\infty) = \begin{cases} (N_l^B + \frac{1}{2})\pi & \text{for } l = 0 \text{ if } F_0(0) = 0, \\ N_l^B \pi & \text{for all } l \text{ if } F_0(0) \neq 0, \end{cases} \quad (\text{D.55})$$

where N_l^B stands for the number of bound states in the relevant l -wave sector. An important requirement for the above relation, is that the real phase-shift $\delta_l(k)$ has to be a continuous function. This can always be achieved, since the phase-shift is no physical quantity and therefore not unique. It can be changed into any desired form, as long as the cross-section via $\sigma_{l,k} \sim \sin^2 \delta_{l,k}$ stays unchanged — it is invariant under the substitution $\delta_l(k) \rightarrow \tilde{\delta}_l(k) = \delta_l(k) + \pi \cdot n(k)$, $n(k) \in \mathbb{Z}$.

Only for those potentials which create a phase shift $\delta(k)$ that is changing monotonic over the whole range of k , the Levinson Theorem helps to understand the last important structure in a cross section, the maxima. Every time when an additional bound state appears, the phase goes through $\pi/2$ and increases by π . At $\pi/2$ the cross-section $\sigma_{l,k} \sim \sin^2 \delta_{l,k}$ takes on a maximum value. So under the assumption of a monotonous phase shift, the number of maxima in a l -wave cross-section is directly linked to the number of bound states in that system. We will see that this is realized by potentials which cannot create resonances.

D. Potential Scattering

D.1.3 S-wave scattering on potentials with a strict range R

Before starting, we first want to focus on the probability interpretation of a wave function which lies in a continuous energy spectrum. The reason is, if we have a proper probability interpretation in the continuum part of the spectrum, it is possible to fully understand and interpret resonances in the stationary picture — there is no need to go into the time-dependent picture. For this we have to take a closer look at the procedure of normalization in the continuum.

The full energy eigensolutions $\Psi_E(\vec{r})$ of the stationary Schrödinger equation, as we well know, form an orthonormal set

$$\int d^3r \Psi_{E'}^*(\vec{r}) \Psi_E(\vec{r}) = \begin{cases} \delta_{EE'} & \text{if } E \text{ discrete,} \\ \delta(E - E') & \text{if } E \text{ continuous.} \end{cases} \quad (\text{D.56})$$

Thus it is always possible to normalize a wavefunction in the bound state region to $\int d^3r |\Psi_E(\vec{r})|^2 = 1$, implying that the probability of finding a particle somewhere in space must be unity. The quantity $|\Psi_E(\vec{r})|^2 d^3r$ is then the probability of finding the particle with a discrete energy E in its volume element d^3r . The squared wave function itself $|\Psi_E(\vec{r})|^2$ has therefore the meaning of a position probability density.

Looking at the continuous part of the spectrum, a wavefunction in the scattering region can always be normalized to $\int dE \int d^3r |\Psi_E(\vec{r})|^2 = 1$. Since a probability interpretation must be also valid within a scattering region, the quantity $|\Psi_E(\vec{r})|^2 d^3r dE$ must be the probability of finding the particle in its volume element d^3r within the continuous energy interval dE . Due to the smeared energy distribution, the squared scattering wave function $|\Psi_E(\vec{r})|^2$ can not represent an *absolute* position probability density, as in the case of the bound-state wave function. But the ratio of $|\Psi_E(\vec{r})|^2$ in two different points of space determines a unique *relative* position probability density. In the scattering region it is not possible to have an absolute position probability interpretation, one rather has to work with relative probabilities, since a scattering particle is not bound to a certain region in space.

For spherically symmetric potentials $V(r)$ and axial symmetric boundary conditions, the general scattering wave function $\Psi_E(\vec{r})$ is given by (D.42). Focusing only on s-wave scattering, the radial wave function $u_k(r)$ satisfies the radial Schrödinger equation

$$u_k''(r) + [k^2 - 2mV(r)] = 0, \text{ with } k^2 = 2mE \geq 0. \quad (\text{D.57})$$

Since this is a real equation, the general solution can be given in a real form. For a potential of a strict range R , the general radial s-wave solution is given by

$$u_k(r) = \begin{cases} u_k^<(r) & \text{for } 0 \leq r \leq R \text{ with } u_k^<(0) = 0, \\ A(k) \sin[kr + \delta(k)] & \text{for } r \geq R. \end{cases} \quad (\text{D.58})$$

First we want to normalize this s-wave function to unity, in the sense

$$\begin{aligned} \delta(E - E') &= \int d^3r \Psi_{E'}^*(\vec{r}) \Psi_E(\vec{r}) \\ &\stackrel{\text{axialsym}}{=} \int d^3r \Psi_{k'}^*(r, \varphi) \Psi_k(r, \varphi) \stackrel{\text{s-wave}}{=} 4\pi \int_0^\infty dr u_{k'}^*(r) u_k(r). \end{aligned} \quad (\text{D.59})$$

D. Potential Scattering

The unity normalization for the *real* radial wave function (D.58) is thus given by

$$\int_0^\infty dr u_k(r)u_{k'}(r) = \frac{1}{4\pi} \frac{m}{k} \delta(k - k'). \quad (\text{D.60})$$

Without having any specific knowledge on $u_k^<(r)$ the above condition can be used to fix the asymptotic normalization constant $A(k)$ in (D.58). The procedure goes as follows: multiplying the radial s-wave Schrödinger equation for u_k with $u_{k'}$ and vice versa, subtracting these two equations and then integrating over the range $[0; L]$ with $L \geq R$, will result in the equation

$$\begin{aligned} \int_0^L dr u_k(r)u_{k'}(r) &= \frac{1}{k'^2 - k^2} \left[u_k'(r)u_{k'}(r) - u_k(r)u_{k'}'(r) \right]_0^L \\ &= \frac{A(k)A(k')}{2} \left[\frac{\sin[(k - k')L + (\delta_k - \delta_{k'})]}{k - k'} + \frac{\sin[(k + k')L + (\delta_k + \delta_{k'})]}{k + k'} \right]. \end{aligned} \quad (\text{D.61})$$

For the limit $L \rightarrow \infty$, we make use of the following functional identities

$$\lim_{a \rightarrow \infty} \frac{\sin(ax)}{x} = \pi \delta(x) \quad ; \quad \lim_{a \rightarrow \infty} \frac{\cos(ax)}{x} = 0. \quad (\text{D.62})$$

With these we have

$$\begin{aligned} &\lim_{L \rightarrow \infty} \int_0^L dr u_k(r)u_{k'}(r) \\ &= \frac{A(k)A(k')}{2} \left[\cos(\delta_k - \delta_{k'}) \lim_{L \rightarrow \infty} \frac{\sin[(k - k')L]}{k - k'} + \cos(\delta_k + \delta_{k'}) \lim_{L \rightarrow \infty} \frac{\sin[(k + k')L]}{k + k'} \right] \\ &= \pi \frac{A(k)A(k')}{2} [\cos(\delta_k - \delta_{k'}) \cdot \delta(k - k') + \cos(\delta_k + \delta_{k'}) \cdot \delta(k + k')] \\ &= \pi \frac{A^2(k)}{2} \delta(k - k'), \text{ because } k, k' > 0. \end{aligned} \quad (\text{D.63})$$

When identifying the above equation with (D.60) the normalization constant must take on the value

$$A^2(k) = \frac{1}{2\pi^2} \frac{m}{k}. \quad (\text{D.64})$$

Since the normalization constant $A(k)$ can be fixed as being positive or negative for any value k , the phase shift function $\delta(k)$ in (D.58) can therefore be chosen as a function which is only unique within modulo π , without changing the wave function. As we already know, this ambiguity in the phase shift within modulo π can also be seen when looking at the cross-section (D.49) — the cross-section as given in (D.49) is also valid for the normalization given here, since every general cross-section (D.39), being determined from the asymptotical behaviour of the wave function, is independent of an overall asymptotic normalization constant. The differential and total s-wave cross-section, which are isotropic in their angular distribution are given as

$$\frac{d\sigma_{s,k}}{d\Omega} = \frac{1}{k^2} \sin^2 \delta(k) \quad ; \quad \sigma_{s,k} = \frac{4\pi}{k^2} \sin^2 \delta(k). \quad (\text{D.65})$$

D. Potential Scattering

Now our aim is to determine the phase shift $\delta(k)$ in (D.58) from the continuity requirements of $u_k(r)$ and its first derivative at $r = R$. For this we define the dimensionless logarithmic derivative of the inner region $r < R$

$$\beta(k) = \left[r \frac{d}{dr} \ln u_k^<(r) \right]_{r=R} = \frac{R \cdot u_k^<'(R)}{u_k^<(R)}, \quad (\text{D.66})$$

which must be equal to the logarithmic derivative of the outer region $r > R$

$$\beta(k) = kR \cdot \cot[kR + \delta(k)] \iff \delta(k) = -kR + \arctan\left(\frac{kR}{\beta(k)}\right) + \pi \cdot n(k), \quad (\text{D.67})$$

where the integer values $n(k) \in \mathbb{Z}$ for every k , are chosen such that the phase shift $\delta(k)$ is a continuous function. Before calculating the cross-section we first want to look at will happen to the phase shift $\delta(k)$ if the potential $V(r)$ turns into the following two extremes:

- if the potential goes to zero, or equivalently if the incident energy of the particle is far more larger compared to the energy range of the potential, the particle will behave as a free particle, that means $u_k^<(r) \rightarrow \sin(kr)$ or $\delta(k) \rightarrow 0 \pmod{\pi}$.
- if the potential turns into an infinitely hard-sphere potential at $r = R$, there will be no penetration of the particle into the inside region $r < R$, that means $u_k^<(r) = 0$ for all $0 \leq r \leq R$. Furthermore the outside wave function must take on the form $u_k^>(r) = A(k) \sin(kr - kR)$ in order to satisfy the continuity requirement $u_k^<(R) = u_k^>(R)$. This gives the hard-sphere phase shift denoted by $\eta(k) = -kR$. So for having pure full range hard-sphere scattering, the corresponding potential must imply the behaviour $|\beta(k)| \rightarrow \infty$ for all k .

The phase shift function $\delta(k)$ in (D.67) can thus be written as

$$\delta(k) = \eta(k) + \arctan\left(-\frac{\eta(k)}{\beta(k)}\right) + \pi \cdot n(k), \quad (\text{D.68})$$

where the hard-sphere phase shift $\eta(k)$ can be seen as a background scattering term, while $\beta(k)$ carrying all the information of the potential acts as the actual potential scattering term. As already mentioned, if $\beta(k)$ changes constantly over a wide range where $|\beta(k)| \gg 1$, the overall scattering behaviour will be that of a hard-sphere. On the other hand, if it tends to the opposite extreme by going rapidly through a region where $\beta(k) \sim 0$, the overall scattering behaviour must be certainly different than that of a hard-sphere. This will be studied next.

Let the function $\beta(k)$ change rapidly $|\beta'(k)| \gg 1$ within a sufficiently small region $|\Delta k| = |k - k_0| \ll 1$ around k_0 , where $\beta(k_0) = 0$. Making a Taylor-expansion up to first order in Δk

$$\beta(k) = (k - k_0) \cdot \beta'(k_0), \quad (\text{D.69})$$

D. Potential Scattering

and assuming furthermore that the change of $\beta(k)$ over this region Δk is so drastic, that when compared to the linear change of the pure background phase shift $\eta(k)$ it would be justified to approximate it by the constant $\eta(k) \rightarrow \eta_0 = -k_0 R$, the corresponding continuous phase shift function has the approximation

$$\delta(k) = \eta_0 + \arctan \left(-\frac{\eta_0}{\beta'(k_0) \cdot (k - k_0)} \right) + \pi \cdot n(k). \quad (\text{D.70})$$

That the approximation of $\delta(k)$ by the approximation of $\beta(k)$ is reasonable, one has to be sure that the arctan-function is a slow varying function, so that $\delta(k)$ is more or less insensitive in a variation of $\beta(k)$. In the above approximation this is certainly guaranteed, since the approximation region is where $\beta(k) \sim 0$, that means in the asymptotic region of the arctan-function where it shows a very slow or nearly no variation at all. Defining the parameter $\gamma_0 = \eta_0/\beta'(k_0)$ the phase shift and the corresponding cross-section have the following 3-parameter structure in the region Δk around k_0

$$\begin{aligned} \delta(k) &= \eta_0 + \arctan \left(-\frac{\gamma_0}{k - k_0} \right) + \pi \cdot n(k), \\ \sigma_s(k) \sim \sin^2 \delta(k) &= \frac{\gamma_0^2}{(k - k_0)^2 + \gamma_0^2} + \sin^2 \eta_0 \\ &\quad - \frac{\gamma_0^2}{(k - k_0)^2 + \gamma_0^2} \left[2 \sin^2 \eta_0 + \frac{k - k_0}{\gamma_0} \sin 2\eta_0 \right]. \end{aligned} \quad (\text{D.71})$$

The first term in the above cross-section is the pure potential term, also called the Breit-Wigner resonance term. The second term is the pure hard-sphere or background term, being totally independent of the scattering potential, while the last term is the complicated interference term.

(Fig11) on the next page shows two characteristic plots of the phase shift and the cross-section for a fixed parameter set (k_0, γ_0) but with a different background parameter η_0 . The plots show that when the scattering particle has a momentum close to k_0 , its wave function phase shift changes rapidly, in the ideal case even by the amount of π and implies a sharp peak in the corresponding cross-section. In every case a sharp change of the phase shift $\delta(k)$ by π causes a sharp structure in the cross-section $\sigma_s(k)$. Experimentally, resonances are usually associated with a sharp variation of the cross-section as a function of energy. We therefore want to take as the preliminary definition of a resonance at the energy $E_0 \sim k_0^2$ that $\delta(E)$ *changes rapidly by approximately π when E passes through E_0 causing manifestly a sharp structure change in the cross-section relative to a slow varying background.* A resonance is characterized by the two parameters (k_0, γ_0) , where γ_0 can be seen as the width of the resonance.

To summarize, there are two striking behaviours in a scattering process, which can be well separated, if the following conditions on the inner logarithmic derivative $\beta(k)$ are fulfilled: $\beta'(k) \sim 0$ and $|\beta(k)| \gg 1$ over a wide momentum range leads to hard-sphere or background scattering, while $|\beta'(k_0)| \gg 1$ where $\beta(k_0) \sim 0$ leads to the contrary resonant scattering around k_0 . If these conditions are not met, there will be subtle interplay between hard-sphere and resonance scattering, which then is no longer so easy to disentangle as before.

D. Potential Scattering

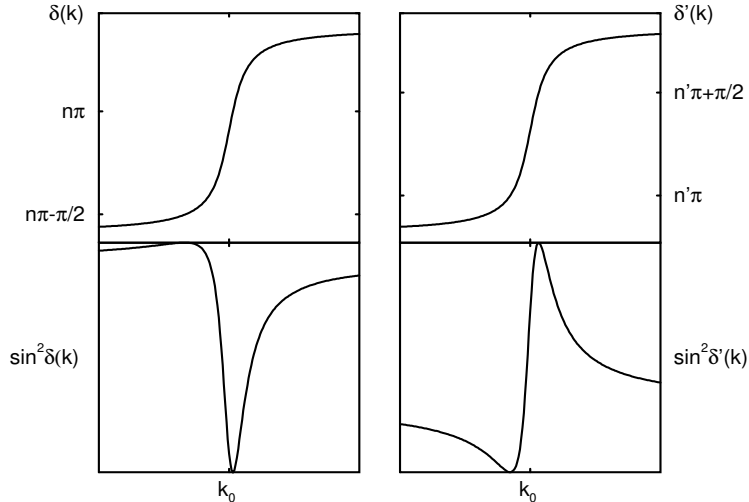


Figure 11: Resonance profiles for the phase shift and cross-section

To study the feature resonance more thoroughly, we now want to go beyond the cross-section and look at the next physical quantity, the relative position probability density of the radial scattering wave function (D.58) in the inside and outside region of a potential with strict range R

$$P_k(r_1, r_2) = \frac{|u_k(r_1)|^2}{|u_k(r_2)|^2}, \text{ with } 0 \leq r_1 \leq R \text{ and } r_2 \geq R. \quad (\text{D.72})$$

We will gain more insight if we only focus on average values of the wave function squared in the inside and outside region respectively

$$\overline{P}(k) = \frac{|\overline{u}_k^<|^2}{|\overline{u}_k^>|^2} = \frac{\frac{1}{R} \int_0^R dr |u_k^<(r)|^2}{\frac{1}{2} A^2(k)}. \quad (\text{D.73})$$

According to (D.61) the above integral can be determined as

$$\begin{aligned} \frac{1}{R} \int_0^R dr |u_k^<(r)|^2 &= \frac{1}{R} \lim_{k' \rightarrow k} \frac{u_k'(R) u_{k'}(R) - u_k(R) u_{k'}'(R)}{k'^2 - k^2} \\ &= \frac{A^2(k)}{2R} \left[\frac{d\delta(k)}{dk} + R - \frac{\sin[2(kR + \delta_k)]}{2k} \right], \end{aligned} \quad (\text{D.74})$$

without knowing the precise wave function in the inner region. Since the left-hand side of the above relation is a positive quantity, we get as an intermediate result the following striking inequality

$$\frac{d\delta(k)}{dk} \geq -R + \frac{\sin[2(kR + \delta_k)]}{2k} \geq -R - \frac{1}{2k}. \quad (\text{D.75})$$

D. Potential Scattering

It states that the phase shift cannot decrease faster than at a certain rate. Thus if the phase changes rapidly, then it must be increasing. This relation was first calculated by Wigner [35] in the more complicated time-dependent picture and is called Wigner's causality principle. The principle of causality states, that a scattered wave cannot leave the scatterer before the incident wave has reached it. Wigner connects the above energy derivative of the scattering phase shift with the time delay, that an incident wave experiences inside the range of the potential before it is being scattered. Furthermore Wigner gives the following simple physical interpretation: when $d\delta/dk$ assumes large positive values, the incident particle is in fact captured and retained for some time by the scattering center and is therefore in a state of resonance; on the other hand if $d\delta/dk$ will be close to $(-R)$ or its minimum $(-R - 1/2k)$ the incident particle hardly enters the scatterer.

For the moment we acknowledge Wigner's time-dependent result and keep on working in the stationary picture, by inserting the phase shift function (D.67) into (D.74). After some calculations we get

$$\frac{1}{R} \int_0^R dr |u_k^<(r)|^2 = \frac{1}{2} A^2(k) \cdot k \cdot \frac{-\beta'(k)}{(kR)^2 + \beta^2(k)}. \quad (\text{D.76})$$

Since again the left-hand side is a positive quantity, $\beta'(k) \leq 0$ for all values k , that means the inner logarithmic derivative $\beta(k)$ is a monotonic decreasing function. Inserting the above relation into (D.73) we finally have the average relative position probability for the inside and outside region

$$\bar{P}(k) = k \cdot \frac{-\beta'(k)}{\eta^2(k) + \beta^2(k)} \equiv \frac{k^>}{\bar{k}^<} \equiv \frac{\bar{\tau}}{\tau}, \quad (\text{D.77})$$

where $k^> = k$ is the incident momentum given in the outside region, while $\bar{k}^<$ can be seen as an average momentum in the inside region. If we define $\tau = 2Rm/k$ as the time a particle stays within the region of $2R$ without any potential, then $\bar{\tau} = 2Rm/\bar{k}^<$ can be seen as the average time the particle would spend in this region in the presence of a potential of strict range R . Thus the average relative position probability \bar{P} not only gives a spacial particle profile but also represents a profile in time.

When now applying the well defined conditions for hard-sphere and resonance scattering we come to the same physical conclusions in the stationary picture as Wigner [35] does in the time-dependent picture, due of having a proper probability interpretation in the scattering region. The hard-sphere condition $\beta' \sim 0$ and $|\beta| \gg 1$ over a wide momentum range implies $d\delta/dk \sim -R$ and $\bar{P} \sim 0$, meaning that the probability of finding the particle inside the potential region relative to the outside region is zero. This is consistent with the fact, that during hard-sphere scattering there is no penetration into the inside region. For the resonance condition $|\beta'| \gg 1$ where $\beta \sim 0$ around some k_0 , we have $d\delta/dk \sim -\beta' \gg 1$. If now a very narrow energy region $|\Delta k| = |k - k_0| \ll 1$ around such a special value k_0 is taken, we can perform the same Taylor expansion for the logarithmic derivative as in (D.69), and obtain the following 3-parametric approximation for \bar{P} around k_0 :

D. Potential Scattering

$$\overline{P}(k) = k_0 \cdot \frac{-\beta'(k_0)}{\eta_0^2 + [\beta'(k_0)(k - k_0)]^2} \equiv \frac{1}{\gamma_0 R} \cdot \frac{\gamma_0^2}{\gamma_0^2 + (k - k_0)^2}, \quad (\text{D.78})$$

where the amplitude of \overline{P} scales with $1/R$. The parameter $\gamma_0 = \eta_0/\beta'(k_0) > 0$ is the very same as defined in (D.71). For a particle with momentum $k \sim k_0$ we will have $\overline{P}(k_0) \gg 1$. Physically this implies that the particle at this certain energy accumulates in the inside region of the potential, or equivalently when the particle enters this region, it remains there for some time before being allowed to escape again to the outside — the particle is thus in a resonance state and is characterized by the very same two independent parameters (k_0, γ_0) which imply a rapid structure change in the cross-section. This certainly only holds if the resonance condition is fulfilled. If not, a subtle interplay between background and resonance scattering will emerge again, resulting in a complicated structure of maxima and minima in \overline{P} , which no longer can be correlated so easily to significant structures in a cross-section.

The last perspective to understand the feature resonance, is to look at it from the scattering function $S(k)$, being the diagonal elements of the S -matrix as discussed in the previous sections.

Besides the solution (D.58), the general solution of the radial s-wave Schrödinger equation (D.57) can also be given in the form

$$u_k(r) = \begin{cases} u_k^<(r) & \text{for } 0 \leq r \leq R \text{ with } u_k^<(0) = 0, \\ B(k)e^{-ikr} + C(k)e^{ikr} & \text{for } r \geq R. \end{cases} \quad (\text{D.79})$$

If we choose $u_k^<(r)$ to be a real function, the complex amplitudes $A(k)$ and $B(k)$ with $k \in \mathbb{R}$, can be determined by the continuity requirements of $u_k(r)$ and its first derivative at $r = R$ as

$$B(k) = C^*(k) = \frac{1}{2}e^{ikR} \left[u_k^<(R) + \frac{i}{k} \cdot u_k^<'(R) \right]. \quad (\text{D.80})$$

When comparing (D.79) with (D.52) irrespective of some overall asymptotic normalization constant, the scattering function is given by

$$S(k) = -\frac{C(k)}{B(k)} = \frac{e^{-ikR} [\beta(k) + ikR]}{e^{ikR} [\beta(k) - ikR]} \equiv \frac{F(k)}{F^*(k)} = e^{2i\delta(k)}, \quad (\text{D.81})$$

with the same notations as used in (D.54). Within this special condition of s-wave scattering in a potential with strict range R , it is easy to verify and understand Gamow's more general statement [34], that a resonance structure in a cross-section is directly linked to the pole structure of the S -matrix. For finding the poles of $S(k)$ one has to do an analytical continuation into the complex momentum q -plane. It can be shown that $S(q)$ is a meromorphic function and that its poles are either located on the positive imaginary axis (bound state region) or in the lower half-plane (scattering region) [33]. In the following we are only interested in finding the scattering poles of $S(k)$, and for that one has to determine the complex zeros of the equation $\beta(k) - ikR = 0$. Lets say the complex momentum $q_0 = k_0 - i\gamma_0$ ($\gamma_0 > 0$) is such a solution.

D. Potential Scattering

Next, we will focus only on a special class of complex zeros, namely on those for which the real part of q_0 satisfies the real condition $\beta(k_0) = 0$. If we now assume that the complex zero q_0 is lying very close to the real axis, that means $\gamma_0 \ll 1$, then $\beta(q_0)$ can be expressed by the first order Taylor expansion around the real point k_0

$$\beta(q_0) = (q_0 - k_0)\beta'(k_0), \text{ with } |q_0 - k_0| = \gamma_0 \ll 1. \quad (\text{D.82})$$

In the region $k \sim k_0$ where $|q_0 - k_0| \ll 1$ one can thus approximate the scattering function (D.81) by

$$S(k) = e^{2i\delta(k)} = e^{-2ik_0R} \cdot \frac{(k - k_0)\beta'(k_0) + ik_0R}{(k - k_0)\beta'(k_0) - ik_0R} = e^{2i\eta_0} \cdot \frac{k - [k_0 + i \cdot \eta_0/\beta'(k_0)]}{k - [k_0 - i \cdot \eta_0/\beta'(k_0)]}, \quad (\text{D.83})$$

and the imaginary part of the scattering pole $q_0 = k_0 - i\gamma_0$ can be identified as the positive quantity $\gamma_0 = \eta_0/\beta'(k_0)$ with the condition $\gamma_0 \ll 1$. When solving for $\delta(k)$ we get the very same resonance phase shift function as in (D.71) with the same conditions and parameters, meaning that only if a scattering pole is sufficiently close to the real k -axis, the pole turns into a physically observed resonance-effect in the cross-section. A scattering pole at the point $q = k - i\gamma$ ($\gamma > 0$) is associated with the complex energy

$$\begin{aligned} \mathcal{E} &= q^2/2m = (1/2m)(k^2 - \gamma^2 - 2ik\gamma) \\ &\equiv E - i(\Gamma/2), \text{ with } \Gamma > 0. \end{aligned} \quad (\text{D.84})$$

Manifest physically meaningless scattering poles are those which are located in the region of the complex q -plane where the real part E of the complex energy \mathcal{E} is negative, that means in the region where $k < \gamma$.

We now may well ask what is the physical meaning of a complex energy. Doing an analytic continuation of the Schrödinger equation to complex energies \mathcal{E} , the time dependence of the scattering solution will be

$$\Psi_{\mathcal{E}}(t) = \Psi_{\mathcal{E}}(0)e^{-i\mathcal{E}t}, \quad (\text{D.85})$$

which gives a time dependence for the probability density of

$$|\Psi_{\mathcal{E}}(t)|^2 = |\Psi_{\mathcal{E}}(0)|^2 e^{-\Gamma t}. \quad (\text{D.86})$$

This steady decrease of probability means that the state is continually decaying away with a lifetime $1/\Gamma$. This exponential decrease of probability with time is a direct consequence of our assumption in the previous section of having outgoing waves only. A pole in the S -function is equivalent to the condition $B = 0$ in (D.79). When looking more closely at the outside wavefunction ($r > R$)

$$u_q(r) = C(q) \cdot e^{ikr} e^{\gamma r}, \quad (\text{D.87})$$

it certainly represents a pure outgoing wave but with an exponentially growing amplitude. This increase is an expression of the fact that the parts of the wave function farther away from the potential well correspond to emissions at a time when the intensity inside the well was stronger.

D. Potential Scattering

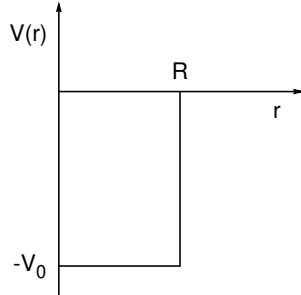
The problem with such waves are, that they cannot be normalized at all. This difficulty is usually circumvented by saying that the requirement of only outgoing waves does not correspond precisely to any physically realizable situation [36]. Before the state can decay by emitting outgoing waves, it must first be formed. During the period of formation of the state, incoming waves must be present, whereas our requirement $B = 0$ excludes incoming waves altogether at all times. However, we can obtain an *approximate physical realization of a decaying state*, $B = 0$, by considering a system formed a very long time T before we start observation. The wave function $u_k(r)$ for $r > R$ is then a purely outgoing wave for values of $r \leq vT$ and is zero for $r > vT$, where $v = k/m$ is the speed of the particle in the outside region. This new wave function differs from the wave function of a pure decaying state only for very large values of $r > vT$, where it is zero and thus normalizable.

Summary: If a potential with a strict range R allows for a resonance, we have seen that there are three ways to determine the resonance parameters (k_0, γ_0) within a stationary scattering picture. All three methods are comparable and give the same results, if and only if the resonance condition $|\beta'(k_0)| \gg 1$ with $\beta(k_0) \sim 0$ is fulfilled. But for a scattering problem which can not be approached in an analytical sense, the verification of the resonance condition will be very difficult or sometimes even not possible. The problem then of establishing the best method to determine the resonance parameters by fitting is a rather academic one. In practice, at a sharp peak in a cross-section all three methods give an energy inside the width of the peak. Only for very broad peaks the methods can give different energies. When this occurs, it is a warning that the interpretation in terms of a resonance is then not a suitable one. It still is very difficult to give a precise and general formulation of the scattering problem in the case of short-lived decaying states.

The remaining part of this section will be devoted to the scattering problem on specific examples. These are selected in such a way, that they can be treated not only numerically but also analytically. This is necessary for checking the stability of numerics, as well as having a reliable interpretation of possible resonances. Furthermore, these examples can be seen as little building blocks for constructing at the end a simplified finite range potential, having the same basic structures as our model-potential in (Fig3). The main task is to calculate phase-shifts. For the numerical calculation the T -matrix relationship (D.40) in *momentum space* is used (Appendix E), while for the analytical calculation the corresponding radial Schrödinger equation in *coordinate space* is solved.

D. Potential Scattering

D.1.3.1 Square-well potential



$$V(r) = \begin{cases} -V_0 & \text{for } 0 \leq r \leq R, V_0 \geq 0, \\ 0 & \text{for } r > R. \end{cases} \quad (\text{D.88})$$

According to (D.58) the radial s-wave scattering solution for the above potential is

$$\begin{aligned} 0 \leq r \leq R : & \quad u_k(r) = N \sin(Kr) \quad ; \quad K = \sqrt{k^2 + 2mV_0} \\ r > R : & \quad u_k(r) = A \sin(kr + \delta), \end{aligned} \quad (\text{D.89})$$

where A is given by (D.64). By requiring the continuity of $u_k(r)$ and its first derivative at $r = R$ will fix the remaining two parameters

$$\begin{aligned} N(k) &= A(k) \frac{\sin[kR + \delta(k)]}{\sin(KR)} \\ \delta(k) &= -kR + \arctan\left(\frac{kR}{\beta(k)}\right) + \pi \cdot n(k), \quad \text{with } \beta(k) = KR \cot(KR). \end{aligned} \quad (\text{D.90})$$

When trying to plot the phase shift function $\delta(k)$ for different depths and widths of the potential $V(r)$, it is reasonable to combine these parameters and introduce the following dimensionless scale $\zeta = R\sqrt{2mV_0}$. The phase shift then takes on the following one parametrical form

$$\delta(x) = -x + \arctan\left[\frac{x}{\beta(x)}\right] + \pi \cdot n(x), \quad \beta(x) = \sqrt{x^2 + \zeta^2} \cot \sqrt{x^2 + \zeta^2}, \quad (\text{D.91})$$

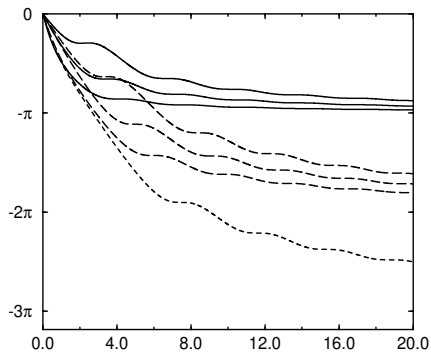
where $x = kR$. Then other relevant functions as the scattering function and the relative probability, which here can be well approximated as the ratio N/A due to a constant amplitude in the inner region, are also dimensionless one parametrical functions

$$\bar{P}(x) = -\frac{x \cdot \beta'(x)}{x^2 + \beta^2} \sim \frac{N^2(x)}{A^2(x)} \quad ; \quad S(k) = e^{-2ix} \cdot \frac{\beta(x) + ix}{\beta(x) - ix}. \quad (\text{D.92})$$

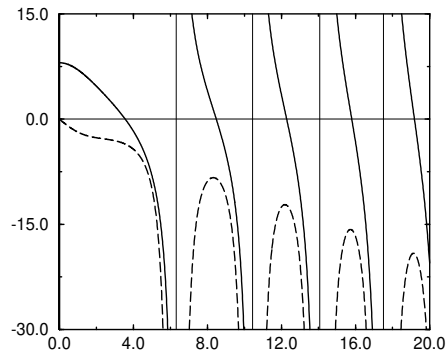
(Fig12a) shows the phase-shift function for various values of ζ . All functions are monotonic decreasing and show no rapid structure change over a wide energy range. One striking effect although is that all functions converge towards a multiple of π and for certain ζ they even jump asymptotically about π . This effect is a pure realization of the Levinson Theorem (D.55). For example if $\zeta = 7$ the phase-shift converges towards 2π , meaning that the system must have two bound states. If the scale ζ is then increased to $\zeta = 8$ the phase-shift jumps by π , which now can only mean that the scale has a sufficient size to allow for another bound state. Since the phase-shifts are monotonic, the number of maxima in the corresponding cross-sections are directly linked to the number of bound states in that system, which can be seen in (Fig12c).

D. Potential Scattering

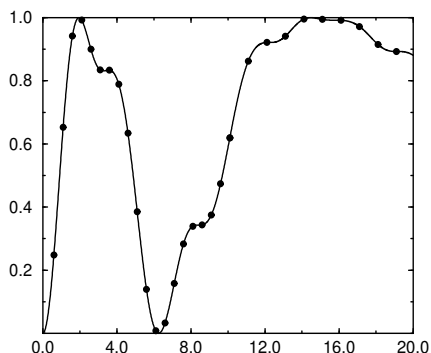
Figure 12: Square-well potential



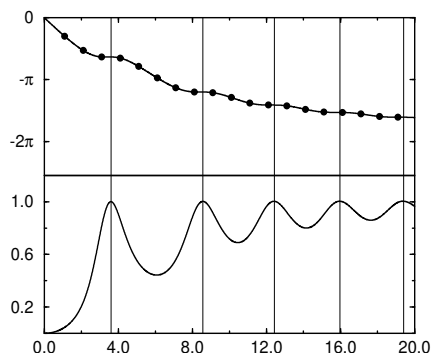
(a) The phase-shift function δ is plotted versus $x = kR$ for different ζ . From bottom to top the solid lines are showing $\zeta = 2, 3, 4$, the long-dashed lines $\zeta = 5, 6, 7$ and the dashed line displays $\zeta = 8$. All lines are converging towards mod π .



(b) This figure shows in solid the inner logarithmic derivative $\beta(x)$ and in long-dashed its first derivative $\beta'(x)$ for $\zeta = 7$. The thin vertical lines go through the poles of $\beta(x)$.



(c) The cross-section $\sigma_s(x) \sim \sin^2(x)$ is plotted for $\zeta = 7$. The solid line represents the analytical calculation, while the single points were calculated numerically via the T-matrix in momentum space. For $x > 20$ the cross-section is steadily decreasing, going to zero for $x \rightarrow \infty$.



(d) The top part of the figure shows the phase-shift function $\delta(x)$ for $\zeta = 7$. The solid line represents the analytical calculation, while the single points were calculated numerically via the T-matrix in momentum space. The bottom part of the figure shows the average relative position probability $\overline{P}(x)$ for $\zeta = 7$. The thin vertical lines go through the maxima of $\overline{P}(x)$.

D. Potential Scattering

When looking more closely at one representative phase-shift in (Fig12d), we see that for small x the phase-shift starts off as that of a hard-sphere, since its slope is more or less a constant. Then as x increases up to $x \sim 4$, we see how the phase-shift changes its behaviour in the sense that it turns away from the hard-sphere behaviour by gaining a less steeper slope. And as x grows beyond $x \sim 4$ it reacts contrary to its previous behaviour by turning again towards a hard-sphere slope. But as x increases more and more there is no chance for the phase-shift to restore its structure as to that of a hard sphere. The phase-shift deviates more and more from a hard-sphere as x grows.

This behaviour can be compared in the bottom part of (Fig12d), where the maxima $\bar{P} \sim 1$, representing a transparent potential, coincide with the region of scattering which is different than that of a hard-sphere. For large x the square well potential becomes more and more transparent, since $\bar{P} \rightarrow 1$. This is consistent with the fact, that for very large incident energy values, where the energy range of the potential is negligible, the particle behaves as a free particle.

In summary we see in (Fig12d) and even in the cross-section (Fig12c) the subtle interplay between background scattering and resonance scattering. We clearly see the attempt of forming a resonance out of the background scattering. But the attractive square-well potential is too weak to produce proper resonances, it can not fulfill the condition $|\beta'(x_0)| \gg 1$ with $\beta(x_0) \sim 0$ in order to produce rapid structure changes in the scattering functions δ , σ_s and \bar{P} .

This can also be seen if we calculate the poles of scattering function (D.81), for which we have to solve the complex equation

$$\sqrt{z^2 + \zeta^2} \cot \sqrt{z^2 + \zeta^2} - iz = 0. \quad (\text{D.93})$$

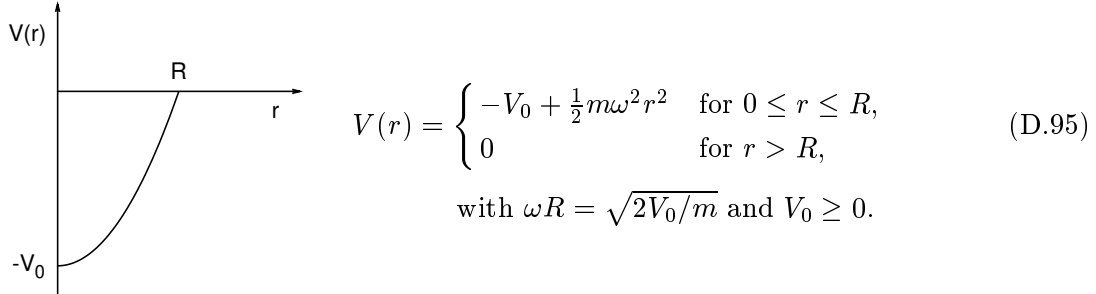
A very nice and thorough treatment on the general behaviour of the above solutions $z = x_0 - iy_0$, $x_0, y_0 \geq 0$ can be found in the paper [37]. The result is that for all scales ζ the imaginary part y_0 of the solution is always larger than 1. The condition for observing a proper resonance is that a scattering pole must be sufficiently close to the real x -axis, but for a square-well scattering pole this is not possible. Up to two significant digits the first three scattering poles for $\zeta = 7$ are

$$(x_0, y_0) = (3.38, -1.07); (8.36, -1.32); (12.18, -1.52). \quad (\text{D.94})$$

The next examples will not be investigated in such detail, since all the above discussed properties are very similar to those of the square well potential. Important results will still be the plots of the functions $\beta(x)$, $\delta(x)$ and $\bar{P}(x)$.

D. Potential Scattering

D.1.3.2 Oscillator-well potential



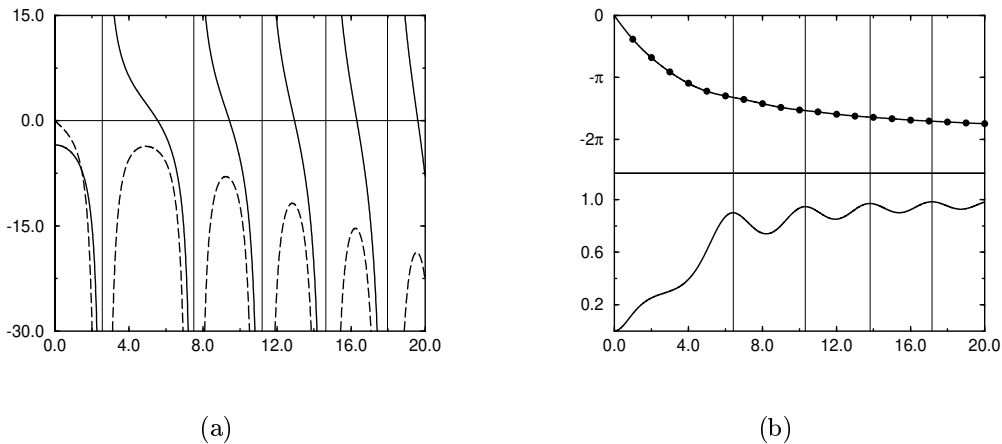
The general real scattering solution of the oscillator well is

$$\begin{aligned} 0 \leq r \leq R: & \quad u_k(r) = N \cdot Kr \cdot e^{-\frac{m\omega}{2}r^2} {}_1F_1\left[\frac{3}{4} - \frac{K^2}{4m\omega}; \frac{3}{2}; m\omega r^2\right] \\ r > R: & \quad u_k(r) = A \sin(kr + \delta), \end{aligned} \quad (\text{D.96})$$

where A is given by (D.64), $K = \sqrt{k^2 + 2m\alpha}$ and ${}_1F_1$ is the Kummer-function or the confluent hypergeometric function which is regular at the origin [30].

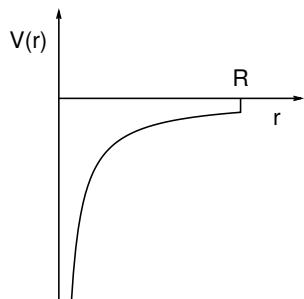
Continuity requirements of $u_k(r)$ and its first derivative at $r = R$, will fix the two parameters δ and N . When doing plots, it is also possible to reduce the above functions down to one parametrical ones with the same dimensionless scale $\zeta = R\sqrt{2mV_0}$ as used in the case of the square-well potential. (Fig13) shows a plot of $\beta(x)$ and the corresponding functions $\delta(x)$ and $\bar{P}(x)$ versus $x = kR$ for the same scale $\zeta = 7$ as in (Fig12). One clearly sees that the structures in (Fig13b) for the oscillator-well are much weaker than in the square-well potential. Otherwise (Fig12b,d) and (Fig13) are nearly of similar structure. This also holds for the cross-section which is not plotted here.

Figure 13: $\zeta = 7$



D. Potential Scattering

D.1.3.3 Coulomb-well potential



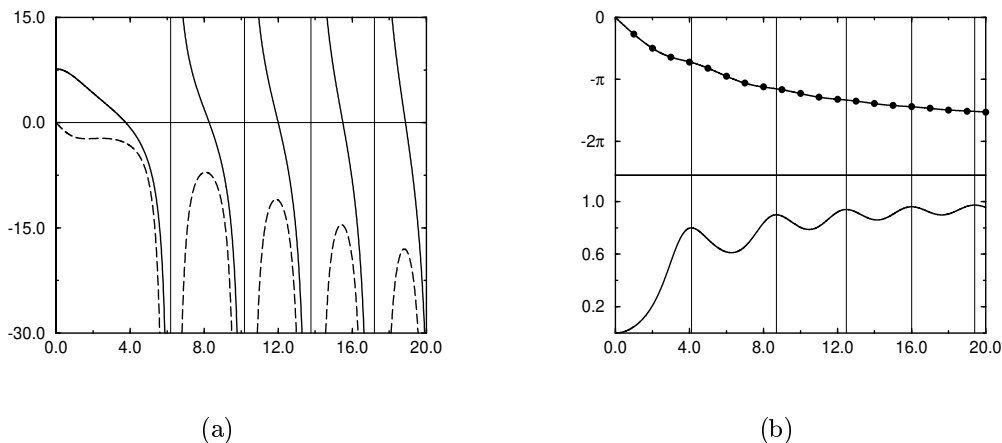
$$V(r) = \begin{cases} -\alpha/r & \text{for } 0 \leq r \leq R, \alpha \geq 0, \\ 0 & \text{for } r > R. \end{cases} \quad (\text{D.97})$$

The general real scattering solution of the Coulomb-well is

$$\begin{aligned} 0 \leq r \leq R : & \quad u_k(r) = N \cdot F(-m\alpha/k; kr) \\ r > R : & \quad u_k(r) = A \sin(kr + \delta), \end{aligned} \quad (\text{D.98})$$

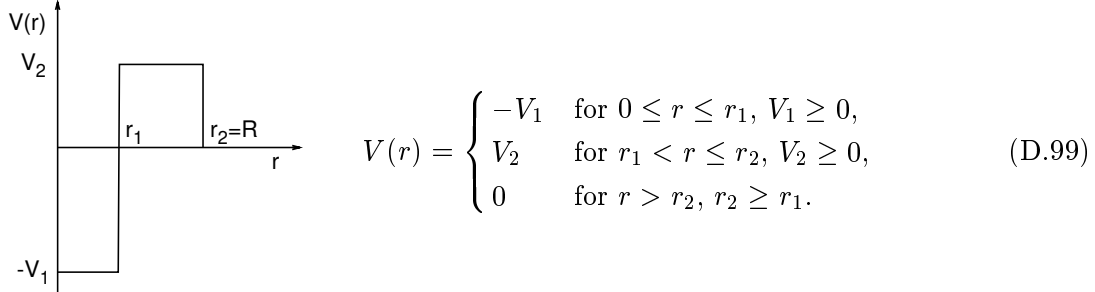
where A is given by (D.64) and F the dimensionless at the origin regular s-wave Coulomb function [30]. After requiring continuity at $r = R$, and introducing the dimensionless scale $\zeta_c = R \cdot m\alpha$ the resulting one parametrical functions $\beta(x)$, $\delta(x)$ and $\overline{P}(x)$ can be plotted versus $x = kR$, and are shown in (Fig14) for the scale $\zeta_c = 7$. What surprises is that the Coulomb singularity at $r \sim 0$ apparently does not effect the scattering behaviour to much, since $\beta(x)$ which carries all information of the scattering potential, is nearly alike with that of the square-well potential.

Figure 14: $\zeta_c = 7$



D. Potential Scattering

D.1.3.4 Step-well potential



The general real scattering solution of the step well is divided into two separate energy regions. The first region is $0 \leq E \leq V_2$ with its corresponding solution

$$\begin{aligned} 0 \leq r \leq r_1 : & \quad u_k(r) = N \sin(K_1 r) \quad ; \quad K_1 = \sqrt{k^2 + 2mV_1} \\ r_1 < r \leq r_2 : & \quad u_k(r) = B e^{K_2 r} + C e^{-K_2 r} \quad ; \quad K_2 = \sqrt{-(k^2 - 2mV_2)} \in \mathbb{R} \\ r > r_2 : & \quad u_k(r) = A \sin(kr + \delta), \end{aligned} \quad (\text{D.100})$$

while the solution of the second region $E \geq V_2$ is given by

$$\begin{aligned} 0 \leq r \leq r_1 : & \quad u_k(r) = N \sin(K_1 r) \quad ; \quad K_1 = \sqrt{k^2 + 2mV_1} \\ r_1 < r \leq r_2 : & \quad u_k(r) = B \sin(K_2 r) + C \cos(K_2 r) \quad ; \quad K_2 = \sqrt{k^2 - 2mV_2} \in \mathbb{R} \\ r > r_2 : & \quad u_k(r) = A \sin(kr + \delta). \end{aligned} \quad (\text{D.101})$$

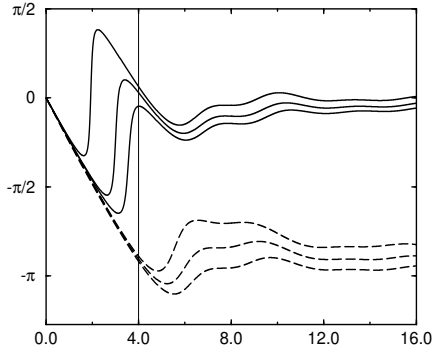
The step-well scattering problem can be characterized by three dimensionless scales: the depth scale $\zeta_1 = R\sqrt{2mV_1}$, the height scale $\zeta_2 = R\sqrt{2mV_2}$ and the relative width scale $a = R/r_1 \geq 1$. All relevant functions for this problem are plotted in (Fig15) versus $x = kR$. First of all, we see that in all figures the step-well potential, under certain scale configurations is capable of producing resonances, as expected, due to rapid structure changes over a small region.

Starting with (Fig15a), it shows a representable phase-shift with fixed height and width scales but for different depth scales. The thin vertical line displays the energy threshold of the step-well potential. As the depth of the potential increases the more the resonance moves towards lower energies. At a certain depth the resonance disappears and the phase-shift jumps asymptotically about π , which according to the Levinson Theorem can only imply that the resonance switched into a bound-state.

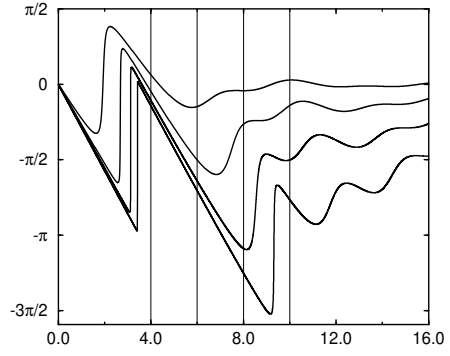
(Fig15b) shows the phase-shift at fixed depth and width but for different heights. The thin vertical lines show the corresponding energy thresholds. As the height increases the structure of the resonance becomes sharper until it makes the ideal jump of π . Furthermore, the higher the barrier of the potential the more resonances can prevail. We see how a second resonance is created as the height scale tends to the value $\zeta_2 = 10$.

D. Potential Scattering

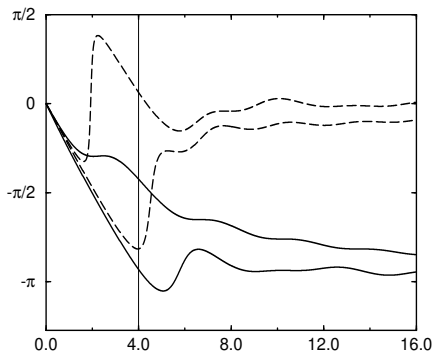
Figure 15: Step-well potential



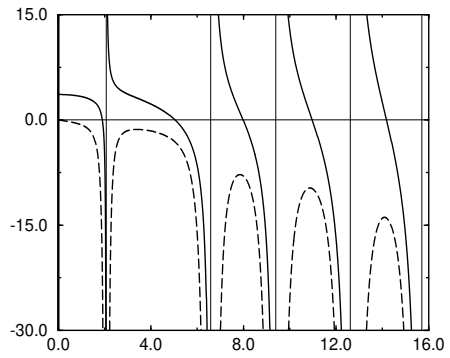
(a) $\zeta_1 = 2, \dots, 7; \zeta_2 = 4; a = 2$



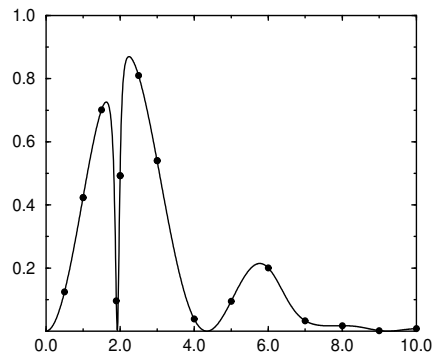
(b) $\zeta_1 = 4; \zeta_2 = 4, 6, 8, 10; a = 2$



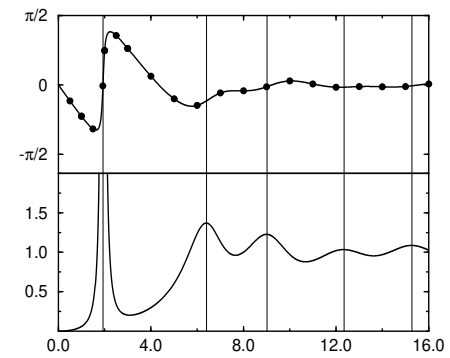
(c) $\zeta_1 = 4; \zeta_2 = 4; a = 1, 3/2, 2, 4$



(d) $\zeta_1 = 4; \zeta_2 = 4; a = 2$



(e) $\zeta_1 = 4; \zeta_2 = 4; a = 2$



(f) $\zeta_1 = 4; \zeta_2 = 4; a = 2$

D. Potential Scattering

(Fig15c) shows the phase-shift at fixed depth and height but for different widths. We start with the top solid line $a = 1$ which represents the phase-shift for the pure square-well potential with no barrier. As the width increases from the bottom solid line to the top dashed line, we clearly see how a resonance is formed from the region above the energy threshold given by the thin vertical line. During this process the phase-shift made an asymptotical jump about π to zero, implying that the system loses its last bound-state. As the width increases even more, it will become impossible for the system to prevail or create a resonance. That the system loses its bound- and resonance-states for $a = R/r_1 \gg 1$ is reasonable, since the barrier width relative to the attractive square-well width is so large, that the total potential acts effectively as a pure repulsive square-well of strength ζ_2 with no bound- and resonance-states.

(Fig15d) shows in solid the inner logarithmic derivative $\beta(x)$ and in dashed its first derivative $\beta'(x)$ for a fixed parameter set. This set is also used for the cross-section $\sigma_s(x) \sim \sin^2 \delta(x)$ in (Fig15e) and for the relative probability function $\bar{P}(x)$ in the bottom part of (Fig15f).

Finally we want to determine the dimensionless resonance parameters (x_0, y_0) , where $x_0 = Rk_0$ and $y_0 = R\gamma_0$ with the set $(\zeta_1, \zeta_2, a) = (4, 4, 2)$ as used in (Fig15d,e,f). Compared to the previous examples we see in (Fig15d) that the resonance condition $|\beta'(x_0)| \gg 1$ with $\beta(x_0) \sim 0$ is more or less fulfilled at $x \sim 2$. Thus y_0 can be calculated as $y_0 = -x_0/\beta'(x_0)$. Up to two significant digits the resonant parameters are $(x_0, y_0) = (1.90, 0.08)$.

Although everything is settled we still want to compare these resonance parameters by those when calculating the exact scattering poles of the scattering function $S(x)$ and doing a fit in a small region around $x \sim 2$ to the exact functions given in (Fig15f). The fits of the phase-shift (D.71) as well as the relative probability function (D.78), are in the dimensionless formalism 2-parametric functions

$$\begin{aligned} \delta(x) &= -x_0 + \arctan\left(-\frac{y_0}{x-x_0}\right) + \pi \cdot n(x) \\ \bar{P}(x) &= \frac{1}{y_0} \cdot \frac{y_0^2}{y_0^2 + (x-x_0)^2}. \end{aligned} \quad (\text{D.102})$$

The resulting resonance parameters up to two significant digits are

$$(x_0, y_0) = S\text{-pole: } (1.93, 0.07) ; \delta\text{-fit: } (1.90, 0.08) ; \bar{P}\text{-fit: } (1.93, 0.07). \quad (\text{D.103})$$

These results convince us, that for the parameter set $(\zeta_1, \zeta_2, a) = (4, 4, 2)$ we really have a resonance-state at $x \sim 2$ with a width $y \sim 0.1$.

D. Potential Scattering

D.1.3.5 Step+Coulomb-well potential

$$V(r) = \begin{cases} -V_1 & \text{for } 0 \leq r \leq r_1, V_1 \geq 0, \\ V_2 & \text{for } r_1 < r \leq r_2, V_2 \geq 0, \\ -\alpha/r & \text{for } r_2 < r \leq R, \alpha \geq 0, \\ 0 & \text{for } r > R, R \geq r_2 \geq r_1. \end{cases} \quad (\text{D.104})$$

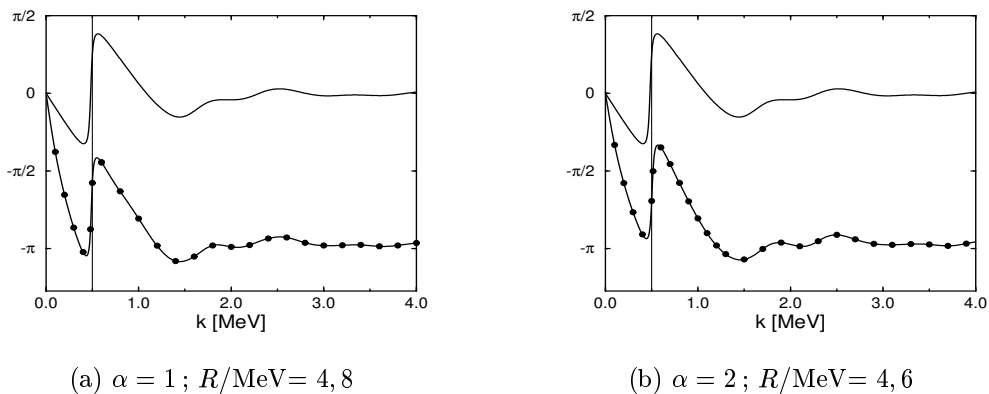
The scattering solution of this potential is the same as in the previous case, except in

$$r_2 < r \leq R : \quad u_k(r) = D_1 \cdot F(\kappa, \rho) + D_2 \cdot G(\kappa, \rho) ; \quad \kappa = -m\alpha/k, \rho = kr, \quad (\text{D.105})$$

where F is the regular and G the linear independent irregular s-wave Coulomb wavefunction [32],[30]. In this problem we want to fix the step parameters (V_1, V_2, r_1, r_2) and tune the Coulomb parameters (α, R) , in order to study the pure influence of a Coulomb interaction on possible resonance-states in the step-well. For this we turn away from the dimensionless formalism of the previous examples and transform the step parameters $(\zeta_1, \zeta_2, a) = (4, 4, 2)$ as used in (Fig15d,e,f) into the following physical example: $m = 0.5\text{MeV}$, $V_1 = V_2 = 1\text{MeV}$ and $r_1 = 2/\text{MeV}$, $r_2 = 4/\text{MeV}$.

(Fig16) then shows the phase-shift versus the incident scattering momentum k , for fixed α and different Coulomb ranges R . The range $R = 4/\text{MeV}$, which represents the pure step-well part, serves as a reference and is displayed at the top of each subfigure. For the corresponding resonance parameters, we get up to two significant digits $(k_0, \gamma_0) = (0.48, 0.02)\text{MeV}$ for $R = 4/\text{MeV}$ as already known from the previous example. If the Coulomb interaction is now switched on, we get $(0.49, 0.02)\text{MeV}$ for (Fig16a) and $(0.52, 0.03)\text{MeV}$ for (Fig16b). All these results I will leave without comments until we deal with the problem of full range Coulomb interaction.

Figure 16:



D. Potential Scattering

D.1.4 S-wave scattering on potentials with an effective range R_{eff}

In order to have an illustrative picture of stationary scattering theory and to keep mathematics as simple as possible, we focused in the previous section on potentials with a strict range R . Unfortunately such potentials do not exist in nature. In the worst case, if they can not be used even for modeling, they are rather artificial constructs. More physical potentials are those of a Yukawa-type

$$V(r) = -\alpha \cdot \frac{e^{-\mu r}}{r}, \quad (\text{D.106})$$

where α is the strength and where $R_{\text{eff}} \sim 1/\mu$ can be seen as the effective range of the potential. The special case $\mu = 0$ gives the Coulomb potential, and is still excluded in this section, since no effective range can be defined. Otherwise all previous definitions and results of scattering on potentials with a strict range R can be transferred to Yukawa-like potentials by working with the approximation $R \sim R_{\text{eff}}$. A more precise treatment on this is given in [38]. There it is also shown how R_{eff} can be determined from the low-energy scattering phase-shift, even for potentials different than Yukawa. For the rest of this section we focus on the following Step+Yukawa-potential:

$$V(r) = \begin{cases} -V_1 & \text{for } 0 \leq r \leq r_1, V_1 \geq 0, \\ V_2 & \text{for } r_1 < r \leq r_2, V_2 \geq 0, \\ -\alpha \cdot e^{-\mu r} / r & \text{for } r > r_2, r_2 \geq r_1, \alpha \geq 0. \end{cases} \quad (\text{D.107})$$

Up to now there exists no analytical scattering solution for any kind of potential which contains a Yukawa-potential. So the above scattering problem is accessible only by numerical means. Since our numerical methods (Appendix E) are constructed for calculating phase-shifts and not the full scattering wavefunctions, the only way to calculate possible resonance parameters is to fit the numerical phase-shift function by

$$\delta(k) = \eta_0 + \arctan \left(-\frac{\gamma_0}{k - k_0} \right) + \pi \cdot n(k), \quad (\text{D.108})$$

as given in (D.71), but where now η_0 has to be seen as an effective background parameter which can be well approximated by $\eta_0 \sim -k_0 R_{\text{eff}}$. The corresponding cross-section is given as usual $\sigma_s(k) \sim \sin^2 \delta(k)$.

For the same reason as in the case of the Step+Coulomb-well (D.1.3.5) we again want to fix the step parameters (V_1, V_2, r_1, r_2) and only tune the Yukawa parameters (α, μ). To have comparable results we take the same step parameters as before: $m = 0.5\text{MeV}$ and $V_1 = V_2 = 1\text{MeV}$, $r_1 = 2/\text{MeV}$, $r_2 = 4/\text{MeV}$.

D. Potential Scattering

Figure 17: Step+Yukawa potential

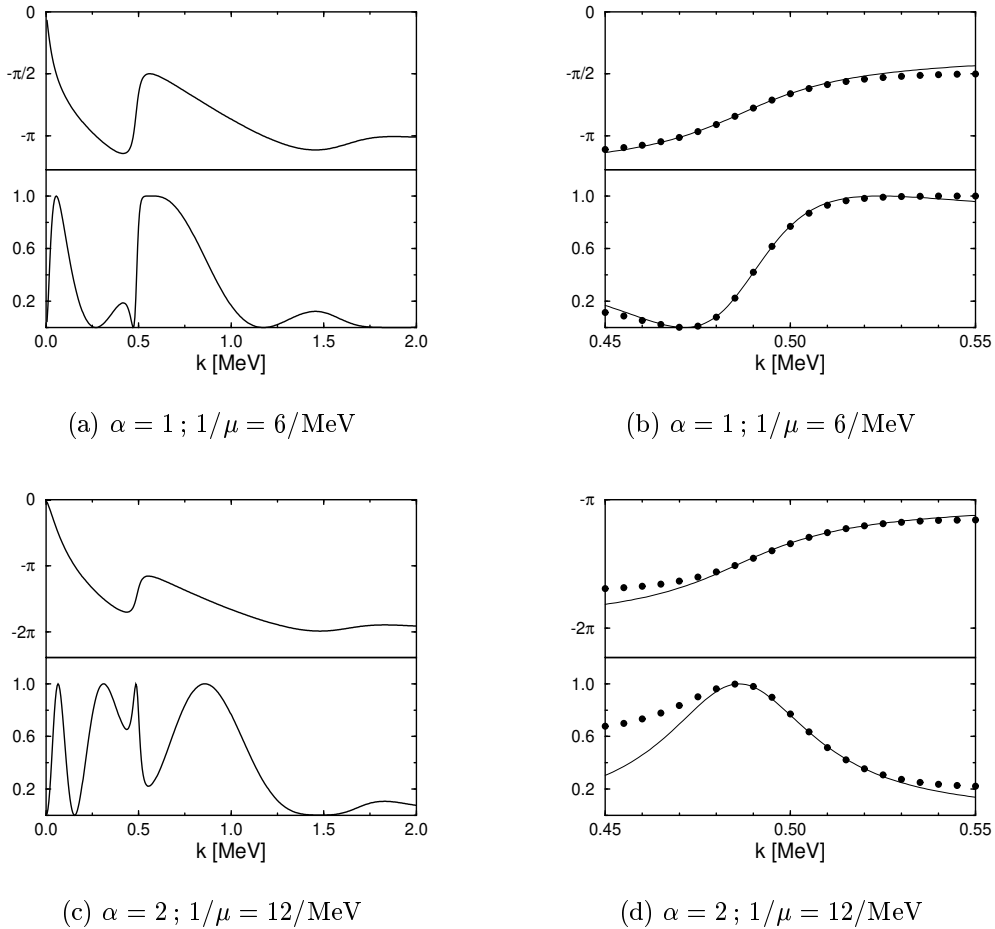


(Fig17a,c) show in the top part of each subfigure the phase-shift and in the bottom part the cross-section versus the incident scattering momentum k for different Yukawa parameters (α, μ) . (Fig17b,d) are the corresponding zoomed figures where the thin lines show the best fit around the resonance region. The resulting resonance parameters up to two significant digits are $(k_0, \gamma_0) = (0.49, 0.02)\text{MeV}$ for (Fig17b) and $(0.50, 0.03)\text{MeV}$ for (Fig17d). The interpretation of these results I also want to postpone until we treat the problem of full range scattering via a Coulomb potential.

We clearly see that the fit for $R_{\text{eff}} \sim 12/\text{MeV}$ is rather poor compared to the one of $R_{\text{eff}} \sim 6/\text{MeV}$. This is more or less a fundamental problem and has to do with the background approximation in (D.71). Its approximation by a constant is only justified if the background change is sufficiently weak within a resonance region — an important condition in approximating the phase-shift (D.68) to the 3-parametric function (D.71), otherwise the parameters η_0 and γ_0 must be treated as k -dependent functions. So, the larger R_{eff} gets, the less is (D.108) suited to fit the phase-shift near a resonance. The problem of finding a better fitting function is beyond the scope of this section.

D. Potential Scattering

D.2 Coulomb scattering

The problem of having potentials which behave asymptotically as a Coulomb potential, i.e. which are of infinite range, is that general abstract scattering equations and definitions, like (D.8) and (D.24), are not well defined expressions anymore [11]. Coulomb scattering can not be treated in an abstract way. Every representation has its own problems and must be interpreted differently. For example in coordinate space the problem of scattering by Coulomb-like potentials is theoretically well understood [32], while the same problem in momentum space still seems to be inaccessible. It may appear strange that a problem which has a well defined solution in coordinate space should occasion difficulty in momentum space. The fact is twofold [10], as we will see in more detail later on. Firstly, the logarithmic singularity in the scattering phase, which can be treated easily in coordinate space, is far more intractable in momentum space. Secondly, Coulomb-like wavefunctions in momentum space are ill-defined. Both prevent a numerical calculation in momentum space.

For the moment we look at the pure Coulomb potential in coordinate space, where the scattering solution can be calculated analytically [32]. From this we will see that the asymptotical behaviour of the Coulomb wavefunction is a totally different one than (D.41) for potentials of finite range. But it is still possible to define a r -independent phase shift parameter, at the expense that the incident waves can no longer be represented by pure plane waves, one rather has to work with distorted waves. Since the Coulomb potential is of infinite range, the particles will always feel scattering even if they are infinitely far away from the core of the potential — in a Coulomb potential there is no region where free particles can exist.

D.2.1 Pure Coulomb potential

The pure scattering Coulomb Schrödinger equation with the Hamiltonian $H = H_0 + V$, $H_0 = k^2/2m$ and $V = -\alpha/r$, in coordinate space

$$(\Delta + \vec{k}^2)\Psi_{\vec{k}}(\vec{r}) = U(r)\Psi_{\vec{k}}(\vec{r}) \quad ; \quad U(r) = 2mV(r), \quad (\text{D.109})$$

can be solved analytically in two different ways, either by solving it in spherical coordinates, as usual, or by using parabolic coordinates [32]. The latter one being a representation which is independent of angular momenta.

Treating the above Schrödinger equation in parabolic coordinates is very useful, since these coordinates prefer a certain direction in space and thus suits the scattering problem perfectly. We know that a unique scattering solution only exists if certain boundary conditions have been implemented before. The most simplest boundary condition is to put the basis of H_0 , that means plane waves, along the infinite negative z -axis, which then move along the positive direction with momentum k .

When using parabolic coordinates, the general physical axial-symmetric solution is given by

$$\Psi_k(r, z) = C(\kappa) \cdot e^{ikz} {}_1F_1[-i\kappa; 1; ik(r-z)] \quad ; \quad \kappa = -m\alpha/k, \quad (\text{D.110})$$

where ${}_1F_1$ is the at the origin regular confluent hypergeometric function [30]. In the above solution the sign of α is not fixed. If $\alpha \geq 0$ it is the general physical solution for

D. Potential Scattering

an attractive Coulomb potential, otherwise for a repulsive Coulomb potential. When calculating cross sections, only the asymptotic behaviour of the wavefunction (D.110) is relevant. Following the asymptotic behaviour of the hypergeometric function [30]

$${}_1F_1(a; b; z) \underset{|z| \rightarrow \infty}{=} \frac{\Gamma(b)}{\Gamma(b-a)} (-z)^{-a} + \frac{\Gamma(b)}{\Gamma(a)} e^z z^{a-b}, \quad (\text{D.111})$$

will give

$$\Psi_k(r, z) \underset{|r-z| \rightarrow \infty}{=} C(\kappa) \cdot \frac{e^{\kappa\pi/2}}{\Gamma(1+i\kappa)} \left\{ e^{i[kz + \kappa \ln[k(r-z)]]} + f_k^c(\vartheta) \cdot \frac{e^{i[kr - \kappa \ln(2kr)]}}{r} \right\}$$

with $f_k^c(\vartheta) = -\frac{\Gamma(1+i\kappa)}{\Gamma(1-i\kappa)} \cdot \frac{\kappa e^{-i\kappa \ln[(1-\cos\vartheta)/2]}}{k(1-\cos\vartheta)}$; $z = r \cos \vartheta$. (D.112)

We see that both the incident and outgoing scattered waves are modified from their usual form (D.41) by logarithmic phase distortion factors. The overall normalization constant C can be fixed such that the incident beam has an amplitude of one. It can now be shown that when calculating the ratio of the outgoing flux and the flux of the incident beam, which will give the differential cross section, these r -dependent phase factors do not contribute. This allows us to identify the coefficient f_k^c of the outgoing wave as the scattering amplitude with the same relation as given in (D.39).

This gives us the Rutherford formula for the differential elastic scattering cross section in a Coulomb field

$$\frac{d\sigma^c}{d\Omega} = |f_k^c(\vartheta)|^2 = \frac{\kappa^2}{4k^2 \sin^4(\vartheta/2)}. \quad (\text{D.113})$$

As is well known, the total Coulomb cross section diverges.

Now we try to solve the pure Coulomb problem in spherical coordinates, or equivalently we try to make a partial wave analysis. Using the same boundary condition as before, our scattering problem is axial-symmetric and therefore allows the following expansion in Legendre polynomials

$$\Psi_k(r, \vartheta) = \sum_{l=0}^{\infty} a_{l,k} \frac{u_{l,k}}{r} P_l(\cos \vartheta), \quad (\text{D.114})$$

where the wave function $u_{l,k}$ satisfies the radial Schrödinger equation with the general solution [32]

$$u_{l,k}(r) = A_{l,k} \rho^{l+1} e^{i\rho} {}_1F_1[l+1+i\kappa; 2l+2; -2i\rho] \equiv B_{l,k} F(\kappa, \rho), \quad (\text{D.115})$$

where $F(\kappa, \rho)$ is the regular Coulomb wave function [32],[30] and $\kappa = -m\alpha/k$, $\rho = kr$.

D. Potential Scattering

Using again (D.111), the asymptotic radial wave function reads

$$\begin{aligned} u_{l,k}(r) &\underset{r \rightarrow \infty}{=} A_{l,k} \cdot \frac{\Gamma(2l+2)e^{\kappa\pi/2}}{2^l |\Gamma(l+1+i\kappa)|} \cdot \sin(\rho - l\pi/2 + \sigma_{l,k} - \kappa \ln 2\rho) \\ &\equiv \tilde{A}_{l,k} \cdot \sin(\rho - l\pi/2 + \sigma_{l,k} - \kappa \ln 2\rho), \end{aligned} \quad (\text{D.116})$$

where $\sigma_{l,k} = \arg\Gamma(l+1+i\kappa)$ is the pure Coulomb phase-shift. Fixing the normalization constant as $\tilde{A}_{l,k} = e^{i\sigma_{l,k}}$ and using the identity (D.45), the full wave function will have the following asymptotic structure

$$\begin{aligned} \Psi_k(r, \vartheta) &\underset{r \rightarrow \infty}{=} \sum_{l=0}^{\infty} a_{l,k} \frac{\sin(kr - l\pi/2 - \kappa \ln 2kr)}{r} P_l(\cos \vartheta) \\ &\quad + \left[\sum_{l=0}^{\infty} (-i)^l a_{l,k} \sin \sigma_{l,k} P_l(\cos \vartheta) \right] \frac{e^{i[kr - \kappa \ln 2kr]}}{r}. \end{aligned} \quad (\text{D.117})$$

The above expression must be equal to (D.112). Furthermore, they must also coincide when the Coulomb potential is absent, that means if $\alpha = \kappa = 0$. When fixing the normalization constant C such that the incident wave has an amplitude of one, the coefficients $a_{l,k}$ can be identified as $a_{l,k} = i^l (2l+1)/k$, which are independent of α . Thus the identification is also valid for $\alpha \neq 0$ and makes it possible to identify the Coulomb scattering amplitude as follows

$$f_k^{\mathcal{C}}(\vartheta) = \frac{1}{k} \sum_{l=0}^{\infty} (2l+1) e^{i\sigma_{l,k}} \sin \sigma_{l,k} P_l(\cos \vartheta). \quad (\text{D.118})$$

All the information of a Coulomb scattering process is also hidden here in an asymptotic phase-shift parameter $\sigma_{l,k}$. Although we can now calculate cross sections in the same manner as before by adjusting the scattering boundary condition in the above way from plane waves to distorted waves, it is, as already stated in the beginning of this section, not possible to construct an abstract relationship between the scattering amplitude and the T -matrix as in (D.40). Rakishly speaking it is not clear how to adjust the boundary condition in an abstract space, in order to have well-defined scattering objects. In the next section it will be shown how at least under certain conditions, the abstract formalism in Coulomb scattering can be maintained.

But before going there, we quickly want to look again at the s-wave Coulomb-well solution (D.98) in the limit $R \rightarrow \infty$. Since the asymptotical regular s-wave Coulomb function is given by [32],[30]

$$F(\kappa, \rho) \underset{\rho \rightarrow \infty}{=} \sin(\rho + \sigma - \kappa \ln 2\rho), \quad (\text{D.119})$$

the correct asymptotical behaviour of (D.98) in the limit $R \rightarrow \infty$ can only be achieved if (D.98) coincides with (D.116), i.e. if the continuity requirements at $r = R$ are organized such that it fixes the parameters as follows: $N = A = e^{i\sigma}$ and $\delta = \sigma - \kappa \ln 2kR$, where $\sigma = \arg\Gamma(1+i\kappa)$ is the partial s-wave Coulomb phase shift. We clearly see that its numerically impossible to calculate the Coulomb-well phase-shift δ in the limit $R \rightarrow \infty$ within the scattering boundary condition of incident plane waves.

D. Potential Scattering

D.2.2 Coulomb-like potentials

This section wants to show a possible way, how the problem of Coulomb scattering in momentum space can be attacked, at least in a numerical sense. At the end, only a solution for *repulsive* Coulomb-like potentials is given. The basic ideas of this section are taken from [10].

Lets say our Hamiltonian is given as follows: $H = K + V$, where K is the kinetic part, or free Hamiltonian and V is an arbitrary spherical symmetric Coulomb-like potential. When adding and subtracting the pure Coulomb potential, our Hamiltonian can be written as

$$H = K + V = K + V^c + V - V^c \equiv H_0^c + V^s, \quad (\text{D.120})$$

where V^s is now a short ranged potential and H_0^c is the Coulomb reference system, for which the eigenvalue problem $H_0^c|\chi^c\rangle = E_0^c|\chi^c\rangle$ is already known.

The first guess how to solve the corresponding scattering problem would be to write down the Lippmann-Schwinger equation as in (D.8). Although the potential V^s is of finite range, one has to be careful when working with this abstract equation, since the Coulomb Greens-function G_0^c of the reference system is not a well defined operator in this abstract notation. For example if one chooses momentum representation, the eigenfunctions $\langle \vec{k}|\chi^c\rangle$ of G_0^c , which must be Fourier transforms of the coordinate space Coulomb functions $\langle \vec{r}|\chi^c\rangle$, do not exist in a functional sense [10].

Since our numerical calculations are done in momentum space and since we have some analytical information in coordinate space, it is essential to work out a way, such that Coulomb scattering can be treated in a formal manner. The easiest possible way would be to construct a reference Hamiltonian of finite range, either by introducing a Coulomb shielding parameter, or by cutting the Coulomb potential at some distance. By introducing these cut-off parameters, everything is of finite range and therefore well-defined. Thus the scattering problem can be solved as usual. But when restoring the original problem by letting the cut-offs go into their corresponding limits, we run again into problems. On the one hand, this restoring is numerically very inefficient, in the worst case even numerically unstable. On the other hand, if it is possible to work analytically, this limiting process can sometimes not be accomplished, or leads to the same ill-defined expressions as before. So this procedure alone is not necessarily successful, but *together* with the following 2-potential formula we are in a better situation [10].

As a regularized reference Hamiltonian $\hat{H}_0^c = K + \hat{V}^c$ we will choose \hat{V}^c to be the Coulomb-well potential, with the finite range of $0 \leq r \leq R$. The full Hamiltonian $\hat{H} = K + \hat{V}^c + V^s$ is then also of finite range and we can write down the well defined formal outgoing Lippmann-Schwinger equation in two equivalent ways

$$|\Psi_{\vec{k}}\rangle = \begin{cases} |\varphi_{\vec{k}}\rangle + G_0 \cdot (\hat{V}^c + V^s) \cdot |\Psi_{\vec{k}}\rangle & \text{with } G_0 = \frac{1}{E - K + i\epsilon}, \\ |\hat{\chi}_{\vec{k}}^c\rangle + \hat{G}_0^c \cdot V^s \cdot |\Psi_{\vec{k}}\rangle & \text{with } \hat{G}_0^c = \frac{1}{E - \hat{H}_0^c + i\epsilon}, \end{cases} \quad (\text{D.121})$$

where $|\varphi_{\vec{k}}\rangle$ are the eigenfunctions of $K = \vec{k}^2/2m$ and $|\hat{\chi}_{\vec{k}}^c\rangle$ the eigenfunctions of the Coulomb-well Hamiltonian \hat{H}_0^c .

D. Potential Scattering

The 2-potential formula can be derived very easily, if one changes to the equivalent T-operator equation

$$T = (\widehat{V}^c + V^s) + (\widehat{V}^c + V^s) \cdot G_0 \cdot T. \quad (\text{D.122})$$

This equation can be rewritten as

$$T = (\mathbb{1} - \widehat{V}^c \cdot G_0)^{-1} (\widehat{V}^c + V^s + V^s \cdot G_0 \cdot T). \quad (\text{D.123})$$

When writing down the T-operator equation for the single potential \widehat{V}^c

$$\widehat{T}^c = \widehat{V}^c + \widehat{V}^c \cdot G_0 \cdot \widehat{T}^c, \quad (\text{D.124})$$

and studying the expression

$$(\mathbb{1} - \widehat{V}^c \cdot G_0)(\mathbb{1} + \widehat{T}^c \cdot G_0) = \mathbb{1} + (\widehat{T}^c - \widehat{V}^c - \widehat{V}^c \cdot G_0 \cdot \widehat{T}^c) \cdot G_0 \equiv \mathbb{1}, \quad (\text{D.125})$$

then (D.123) is equivalent to

$$\begin{aligned} T &= (\mathbb{1} + \widehat{T}^c \cdot G_0)(\widehat{V}^c + V^s + V^s \cdot G_0 \cdot T) \\ &\equiv \widehat{T}^c + (\mathbb{1} + \widehat{T}^c \cdot G_0) \cdot V^s \cdot (\mathbb{1} + G_0 \cdot T). \end{aligned} \quad (\text{D.126})$$

If two operators are multiplied to give unity, then the order of multiplication is irrelevant. Thus (D.125) gives the identity $\widehat{V}^c \cdot G_0 \cdot \widehat{T}^c = \widehat{T}^c \cdot G_0 \cdot \widehat{V}^c$, and (D.126) can be written as

$$T = \widehat{T}^c + \widehat{T}^c \cdot [(\widehat{V}^c)^{-1} \cdot V^s \cdot (\widehat{V}^c + V^s)^{-1}] \cdot T. \quad (\text{D.127})$$

Using the definition (D.24), the above equation takes the final form

$$\langle \varphi_{\vec{k}'} | T | \varphi_{\vec{k}} \rangle = \langle \varphi_{\vec{k}'} | \widehat{T}^c | \varphi_{\vec{k}} \rangle + \langle \widehat{\chi}_{\vec{k}'}^c | V^s | \Psi_{\vec{k}} \rangle \quad ; \quad k' = k. \quad (\text{D.128})$$

or equivalently in the form of (D.40)

$$f_{\vec{k}}(\varphi, \vartheta) = \widehat{f}_{\vec{k}}^c(\varphi, \vartheta) - 4m\pi^2 \langle \widehat{\chi}_{\vec{k}}^c | V^s | \Psi_{\vec{k}} \rangle \quad ; \quad k' = k \quad (\text{D.129})$$

where $f_{\vec{k}}$ is the scattering amplitude of the full problem, while $\widehat{f}_{\vec{k}}^c$ is the scattering amplitude of the Coulomb-well.

The above formula is the celebrated 2-potential formula. Although the full Hamiltonian is additive in \widehat{V}^c and V^s , the full scattering amplitude $f_{\vec{k}}$ is not simply the sum of the scattering amplitude due to \widehat{V}^c in the absence of V^s and the scattering amplitude due to V^s in the absence of \widehat{V}^c but, instead, involves the scattering amplitude due to V^s in the presence of \widehat{V}^c .

The problem of calculating the full scattering amplitude is reduced to the determination of the matrix element $\langle \widehat{\chi}^c | V^s | \Psi \rangle$. We know that the eigenfunctions of the Coulomb-well Hamiltonian \widehat{H}_0^c form a complete set. For numerical calculations it is now essential if the pure Coulomb-well potential \widehat{V}^c is attractive or repulsive. The completeness relation of an attractive Coulomb potential is nasty due to its additional bound state part and therefore makes it impossible to work with it numerically.

$$\mathbb{1} = \begin{cases} \sum_{E \leq 0} |\widehat{\chi}_{\vec{k}}^c\rangle \langle \widehat{\chi}_{\vec{k}}^c| + \int d^3k |\widehat{\chi}_{\vec{k}}^c\rangle \langle \widehat{\chi}_{\vec{k}}^c| & \text{if } \widehat{V}^c \text{ is attractive,} \\ \int d^3k |\widehat{\chi}_{\vec{k}}^c\rangle \langle \widehat{\chi}_{\vec{k}}^c| & \text{if } \widehat{V}^c \text{ is repulsive.} \end{cases} \quad (\text{D.130})$$

D. Potential Scattering

For a repulsive Coulomb potential it is easy to evaluate the above matrix element. Inserting the second form of the Lippmann-Schwinger equation (D.121) and sandwiching the relevant completeness relation between \widehat{G}_0^c will give

$$\begin{aligned} \langle \widehat{\chi}_{k'}^c | V^s | \Psi_{\vec{k}} \rangle &= \langle \widehat{\chi}_{k'}^c | V^s | \widehat{\chi}_k^c \rangle \\ &+ \int d^3 k'' \langle \widehat{\chi}_{k'}^c | V^s | \widehat{\chi}_{k''}^c \rangle \frac{1}{E - \widehat{E}_0^c + i\epsilon} \langle \widehat{\chi}_{k''}^c | V^s | \Psi_{\vec{k}} \rangle \quad ; \quad k' = k. \end{aligned} \quad (\text{D.131})$$

The structures of (D.129) and (D.131) allow us now to take the limit $R \rightarrow \infty$ from the pure Coulomb-well to full Coulomb potential in an analytical way. If the limit is taken in coordinate space as in (D.119), it is a well defined procedure, since we know how the wavefunction and the scattering amplitude for a pure Coulomb potential are defined in coordinate space. For the axial symmetric boundary condition, they are

$$\begin{aligned} \langle \vec{r} | \widehat{\chi}_k^c \rangle &\underset{R \rightarrow \infty}{=} \langle r, \vartheta | \chi_k^c \rangle = \sum_{l=0}^{\infty} i^l (2l+1) e^{i\sigma_{l,k}} \frac{F(\kappa, kr)}{kr} P_l(\cos \vartheta), \\ \widehat{f}_k^c(\vartheta) &\underset{R \rightarrow \infty}{=} f_k^c(\vartheta) = \frac{1}{k} \sum_{l=0}^{\infty} (2l+1) e^{i\sigma_{l,k}} \sin \sigma_{l,k} P_l(\cos \vartheta), \end{aligned} \quad (\text{D.132})$$

where $\sigma_{l,k} = \arg \Gamma(l+1+i\kappa)$ is the Coulomb phase shift and $\kappa = -m\alpha/k$ the charge parameter. Consequently in the coordinate space limit the hat-symbol in (D.129) and (D.131) may be removed, and the final solution for the full scattering amplitude of a Coulomb-like potential V with the short range part $V^s = V - V^c$ is

$$f_{\vec{k}}^c(\varphi, \vartheta) = f_k^c(\varphi, \vartheta) + \langle \chi_{\vec{k}'}^c | V^s | \Psi_{\vec{k}} \rangle \quad ; \quad k' = k. \quad (\text{D.133})$$

If V^s is local and if the pure Coulomb potential V^c is *repulsive*, then the matrix element

$$\begin{aligned} \langle \chi_{\vec{k}'}^c | V^s | \Psi_{\vec{k}} \rangle &= \int d^3 r \chi_{\vec{k}'}^c(\vec{r}) V^s(r) \chi_{\vec{k}}^c(\vec{r}) \\ &+ \int d^3 k'' \int d^3 r \chi_{\vec{k}'}^c(\vec{r}) \frac{V^s(r)}{E - E_0^c + i\epsilon} \chi_{\vec{k}''}^c(\vec{r}) \cdot \langle \chi_{\vec{k}''}^c | V^s | \Psi_{\vec{k}} \rangle, \end{aligned} \quad (\text{D.134})$$

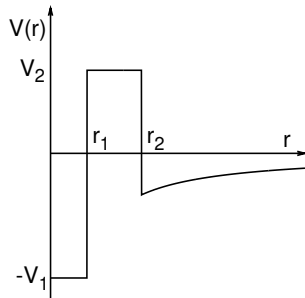
is of an form that is numerically easy accessible. Even if V^s is non-local, the numerical evaluation of this self consistent equation works as usual (Appendix E), except that now Coulomb basis functions has to be used instead of plane waves as in former calculations. This integration is numerically stable because the coordinate space Coulomb wavefunctions are well defined and the relevant potential V^s is short ranged. If V^s is known initially in momentum space, the above prescription for calculating the matrix element involves another step, that is we must first find V^s in coordinate space by Fourier-transforming V^s from momentum space into coordinate space. Those Fourier transforms do exist because of the finite range of V^s .

This completes the proof. It shows that a considerable amount of numerical effort is necessary in order to treat Coulomb scattering in momentum space properly. To note again, this overall procedure only holds for repulsive Coulomb-like potentials, which do not have a discrete spectrum.

D. Potential Scattering

D.2.3 Step-well plus attractive Coulomb potential

In the previous section we have seen that *attractive* Coulomb-like potentials are still numerically inaccessible. But since we are confronted with this problem in our ST-model and no numerical techniques are at hand, we have to work analytically. For this, the ST-potential as in (Fig3) is broken down to the following over-simplified potential:



$$V(r) = \begin{cases} -V_1 & \text{for } 0 \leq r \leq r_1, V_1 \geq 0, \\ V_2 & \text{for } r_1 < r \leq r_2, V_2 \geq 0, \\ -\alpha/r & \text{for } r > r_2, r_2 \geq r_1, \alpha \geq 0, \end{cases} \quad (\text{D.135})$$

The general real s-wave scattering solution of the above potential is the same as given in (D.100) and (D.101), except in the region $r > r_2$ where now the free solution has to be exchanged by the general Coulomb wavefunctions

$$r > r_2 : \quad u_k(r) = D_1 \cdot F(\kappa, \rho) + D_2 \cdot G(\kappa, \rho) \quad ; \quad \kappa = -m\alpha/k, \rho = kr, \quad (\text{D.136})$$

with their asymptotic behaviour [32]

$$\begin{aligned} F(\kappa, \rho) &\underset{\rho \rightarrow \infty}{=} \sin(\rho + \sigma - \kappa \ln 2\rho) \\ G(\kappa, \rho) &\underset{\rho \rightarrow \infty}{=} \cos(\rho + \sigma - \kappa \ln 2\rho), \end{aligned} \quad (\text{D.137})$$

where $\sigma = \arg\Gamma(1 + i\kappa)$ is the s-wave Coulomb phase shift. To calculate the phase shift δ of the full problem, we will rewrite the asymptotic wavefunction (D.136) as follows

$$\begin{aligned} u_k(r) &\underset{r \rightarrow \infty}{=} \sin(\rho - \kappa \ln 2\rho) \cdot [D_1 \cos \sigma - D_2 \sin \sigma] \\ &\quad + \cos(\rho - \kappa \ln 2\rho) \cdot [D_1 \sin \sigma + D_2 \cos \sigma]. \end{aligned} \quad (\text{D.138})$$

If we now put $X := D_1 \cos \sigma - D_2 \sin \sigma$ and $Y := D_1 \sin \sigma + D_2 \cos \sigma$, then because of $X^2 + Y^2 = D_1^2 + D_2^2$, the parameters X and Y can be represented as

$$\begin{aligned} X &= \sqrt{D_1^2 + D_2^2} \cos \delta \equiv \sqrt{D_1^2 + D_2^2} \cos(\sigma + \gamma) \\ Y &= \sqrt{D_1^2 + D_2^2} \sin \delta \equiv \sqrt{D_1^2 + D_2^2} \sin(\sigma + \gamma), \end{aligned} \quad (\text{D.139})$$

with $\tan \gamma = D_2/D_1$. Then (D.138) takes the form

$$u_k(r) \underset{r \rightarrow \infty}{=} \sqrt{D_1^2 + D_2^2} \cdot \sin(\rho + \delta - \kappa \ln 2\rho). \quad (\text{D.140})$$

D. Potential Scattering

This confirms, according to (D.116) that δ is the full phase shift function that completely characterizes this s-wave scattering problem. Consequently the scattering amplitude and the cross-section for the s-wave component are given by

$$f(k) = \frac{1}{k} e^{i\delta(k)} \sin \delta(k) \quad ; \quad |f(k)|^2 \sim \sin^2 \delta(k)$$

with $\delta(k) = \sigma(k) + \arctan(D_2/D_1) + \pi \cdot n(k)$. (D.141)

This phase-shift reminds us strongly at the one given in (D.68). We can draw the following analog, and see $\sigma(k)$, since it carries only the information of the *pure* Coulomb potential as the background phase-shift, while the last term carrying all the information of the complete potential can be seen as the actual potential scattering term which give rise to possible resonances. The decisive difference between the background $\sigma(k)$ and the background $\eta(k)$ in (D.68) is that the latter is changing constantly over the whole momentum range k , while the behaviour of $\sigma(k)$ can be divided into two separate regions: strong oscillations for sufficiently small momenta while relatively slow changes and a convergence towards zero for sufficiently large momenta. So, only if a resonance (k_0, ν_0) is embedded into region of a slow varying background $\sigma(k)$, it is justified to approximate the complete phase-shift $\delta(k)$ similar as in (D.71), by

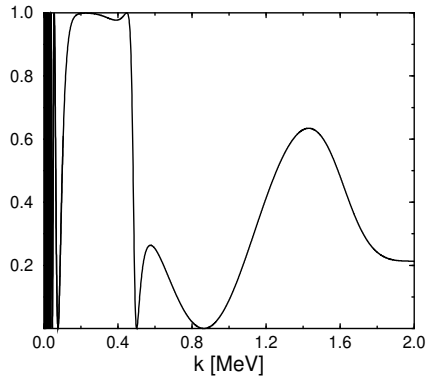
$$\delta(k) = \sigma_0 + \arctan\left(-\frac{\nu_0}{k - k_0}\right) + \pi \cdot n(k). \quad (D.142)$$

Otherwise the parameters σ_0 and ν_0 must be treated as k -dependent functions within a small region around the resonance point k_0 .

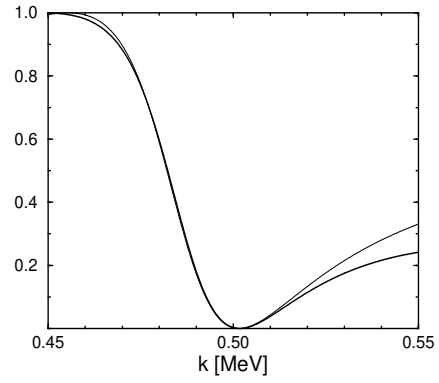
To study this problem, we will take up the same physical step-parameters as in sections (D.1.3.4/5) and (D.1.4), where the results still need to be interpreted. Then (Fig18a,c) show the cross-section versus the incident scattering momentum k for different Coulomb strengths α . For this parameter set we see that up to $\alpha \leq 1$ the resonance at $k \sim 0.5$ lies well outside the rapid changing background region, for $\alpha = 0.5$ even better than for $\alpha = 1$. This allows us to fit the resonance by the 3-parametric function (D.142). (Fig 18b,d) are the corresponding zoomed graphs where the thin lines show again the best fit around the resonance region. As expected, the fit for $\alpha = 0.5$ is better than that for the stronger $\alpha = 1$. The resulting resonance parameters up to two significant digits are the same $(k_0, \nu_0) = (0.49, 0.02)$ MeV for both (Fig18b,d). These values are identical with those for a pure step-potential, where $\alpha = 0$ as in section (D.1.3.4). This is a surprising effect, since it tells us that for a fixed step potential the Coulomb potential can be switched on or off, in both cases we get the same resonance — the global structure of the cross-section is certainly a complete different one in each case. Now, one has to be very careful to conclude such a behaviour for all Coulomb strengths α , since we have only shown it for $\alpha \leq 1$. For stronger α the background scattering gets predominant and our technique for calculating the resonance width ν_0 via (D.142) fails. On the other hand the parameter k_0 is certainly independent of background scattering, which explicitly can be seen in (Fig18e), where only the pure resonant term in the cross-section $\sim \sin^2 \gamma(k)$ with $\gamma(k) = \arctan(D_2/D_1)$ is plotted for various strengths α , all giving the same result $k_0 \sim 0.5$ over a wide range. The solid line displays $\alpha = 1$, the long-dashed $\alpha = 5$ while the dashed line shows $\alpha = 25$.

D. Potential Scattering

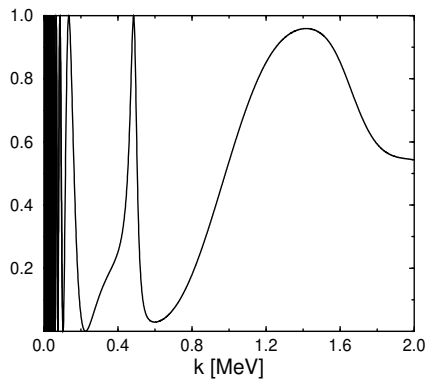
Figure 18: Step+(attractive)Coulomb potential



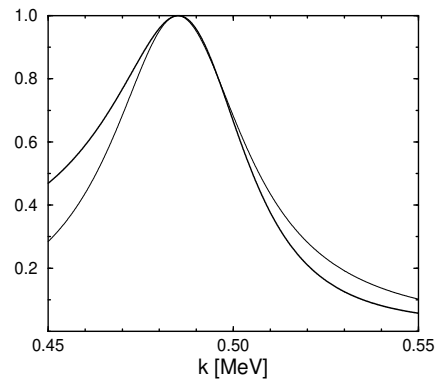
(a) $\alpha = 0.5$



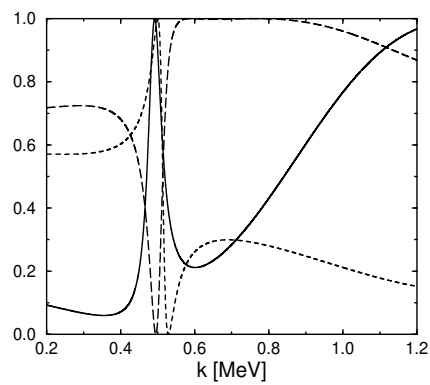
(b) $\alpha = 0.5$



(c) $\alpha = 1$



(d) $\alpha = 1$



(e) $\alpha = 1, 5, 25$

D. Potential Scattering

Is it maybe true that background scattering behaves in such a complicated way that it leaves the width ν_0 , and therefore the complete resonance state (k_0, ν_0) invariant, but can not be detected by the methods we use up to now? For moderate backgrounds this is true as I have shown in a numerical sense not only for the pure full range Coulomb potential but also when using instead of it a Coulomb-well (D.1.3.5) or a Yukawa potential (D.1.4). All of them yield the same resonance whether the potential is rescaled or even turned on or off.

If its possible to prove this effect in general, there would be immediately a reasonable explanation at hand: *since all potentials which have no overshoot into the positive energy region show no resonance structure, they will also show no influence on possible resonance states.* This statement would be extremely helpful, when we have to deal with more general *attractive* Coulomb-like potentials. If we only look at the resonant part in a s-wave cross-section, its irrelevant whether we work in the *asymptotic region* with the full attractive Coulomb potential or with any other short-range potential, having only contributions in the negative energy region. All of them give the same resonance values (k_0, ν_0) .

Certainly a clear-cut proof of this general statement still needs to be worked out. But anyhow, for moderate Coulomb strenghts α , I have shown that this statement can be verified. After all this implies an important result for this section, namely that this technique offers an easy implementation in momentum space, since asymptotical Coulomb shielding in coordinate space can be easily transferred to momentum space and vice versa. This technique is certainly only to be seen as a first step towards solving the full problem of Coulomb scattering in momentum space.

E Numerics in Momentum Space

The theory and equations of quantum mechanics are represented equally well in coordinate and momentum space. Bound state problems, which by definition deal with normalizable wavefunctions, can actually be solved without any conceptual problems in either space, while scattering problems, which deal with non-normalizable states, are more of a challenge in momentum space. This challenge arises, as we have seen in (Appendix D), in part, because boundary conditions are more naturally imposed in coordinate space, and in part, because non-normalizable states in general cannot be Fourier transformed.

In spite of these difficulties, there is a considerable interest in momentum space methods. First of all momentum space offers a more natural description of many-body and field theories. Dealing with nonlocal potentials or the extension to relativistic equations can be handled more easily in momentum space than in coordinate space.

In coordinate space the equations of motion are mostly differential equations, while in momentum space they are mostly integral equations. These integral equations can be represented as matrix equations, where the problem of solving the equation is either reduced to a diagonalization (bound state problem) or to the determination of an inverse matrix (scattering problem). In both cases one has to be careful of the so called fundamental singularities in momentum space. In the bound state region for example, the Coulomb potential is showing a q^2 (single-pole) and the linear potential even a q^4 (double-pole) singularity. We will show that the Coulomb singularity can be completely controlled by using the numerical technique of counter terms, while the linear singularity can only be reduced to a single-pole singularity. The scattering region will not suffer from these singularities if the potentials are restricted to have a finite range, but rather shows its fundamental singularity only once in the free-particle Greens function, which also can be controlled by a numerical counter term.

For showing the basic structures of a numerical code in momentum space, it is sufficient to restrict ourselves to the simplest case, namely working non-relativistic and with local spherical symmetric potentials.

E.1 Bound state domain

To treat as a many potentials simultaneously, we will study the following compact potential focusing on three parameter sets

$$V(r) = -\alpha_n \cdot r^n \cdot e^{-\mu r} = \begin{cases} \text{Yukawa potential} & \text{if } n = -1, \mu > 0, \\ \text{Coulomb potential} & \text{if } n = -1, \mu = 0, \\ \text{Linear potential} & \text{if } n = 1, \mu = 0. \end{cases} \quad (\text{E.1})$$

The advantage of introducing an exponential function or screening function for the Coulomb and Linear potential is twofold. First of all it serves as a converging factor in the relevant Fourier transformations and secondly it makes it possible to treat the fundamental singularities of the Coulomb and Linear potential in the very same way.

E. Numerics in Momentum Space

The Schrödinger equation in coordinate space is given as

$$-\frac{\Delta}{2m}\psi(\vec{r}) + V(r)\psi(\vec{r}) = E\psi(\vec{r}). \quad (\text{E.2})$$

By Fourier transforming the coordinate wavefunctions, we get the Schrödinger equation in momentum space

$$\frac{p^2}{2m}\phi(\vec{p}) + \int d^3p' V(\vec{q})\phi(\vec{p}') = E\phi(\vec{p}), \quad (\text{E.3})$$

with the same eigenvalues E as in coordinate space and $\vec{q} = \vec{p} - \vec{p}'$. The momentum space potential $V(\vec{q})$ is the Fourier transform of the coordinate space potential (E.1)

$$\begin{aligned} V(\vec{q}) &= \frac{1}{(2\pi)^3} \int d^3r e^{i\vec{q}\cdot\vec{r}} \cdot V(r) \\ &= (-1)^n \cdot \frac{\alpha_n}{2\pi^2} \cdot \frac{\partial^{n+1}}{\partial \mu^{n+1}} \left[\frac{1}{\mu^2 + q^2} \right] \equiv \frac{1}{2\pi} \cdot \mathcal{D}_\mu^{n+1} \left[\frac{1}{\mu^2 + q^2} \right]. \end{aligned} \quad (\text{E.4})$$

This representation gives well defined momentum space potentials for the three parameter sets given in (E.1). If I rakishly speak of putting $\mu = 0$, we have to understand the following process: first the derivatives after which the limit $\mu \rightarrow 0$ has to be taken. We see that $V(\vec{q}) \equiv V(|\vec{q}|)$, and because $|\vec{q}| = p^2 + p'^2 - 2pp' \cos \theta$, the momentum space potential can therefore only depend on the magnitudes p , p' and the relative angle θ between the momentum vectors \vec{p} and \vec{p}' . This allows us to expand the potential into the complete set of Legendre polynomials

$$V(q) = V(p, p', \theta) = \sum_{l=0}^{\infty} \frac{2l+1}{4\pi} V_l(p, p') P_l(\cos \theta). \quad (\text{E.5})$$

The expansion coefficients can be determined by integrating over the above equation by weighting the integral with a Legendre polynomial in the range of $\cos \theta \in [-1, 1]$. Using then the orthogonality relation of Legendre polynomials will give

$$V_l(p, p') = 2\pi \int_{-1}^1 V(q) P_l(\cos \theta) d \cos \theta. \quad (\text{E.6})$$

With the potential (E.4) the above integral is not one of the easiest to calculate. Now that we have decomposed the potential into its partial waves, the corresponding l-wave Schrödinger equation should be found. For this we expand the momentum wavefunctions into the complete set of spherical harmonics

$$\begin{aligned} \phi(\vec{p}) &= \phi(p, \varphi, \vartheta) = \sum_{l=0}^{\infty} \sum_{m=-l}^l \phi_{lm}(p) Y_{lm}(\varphi, \vartheta) \\ \phi(\vec{p}') &= \phi(p', \varphi', \vartheta') = \sum_{l=0}^{\infty} \sum_{m=-l}^l \phi_{lm}(p') Y_{lm}(\varphi', \vartheta'). \end{aligned} \quad (\text{E.7})$$

E. Numerics in Momentum Space

Inserting (E.5) and (E.7) into the Schrödinger equation (E.3) and using the identity

$$P_l(\cos \theta) = \frac{4\pi}{2l+1} \sum_{m=-l}^l Y_{lm}(\varphi, \vartheta) Y_{lm}^*(\varphi', \vartheta'), \quad (\text{E.8})$$

and keeping the orthogonality and completeness relations of the spherical harmonics in mind, will finally give the one dimensional radial Schrödinger equation in momentum space

$$\frac{p^2}{2m} \phi_l(p) + \int_0^\infty dp' p'^2 V_l(p, p') \phi_l(p') = E \phi_l(p), \quad (\text{E.9})$$

which is now subject to numerical investigations. Since we restricted ourselves to spherical symmetric potentials, the wavefunctions will show no dependence on the quantum number m .

For solving the eigenvalue equation (E.9) numerically, we need to know the l-wave component of the momentum space potential (E.6). This integral can be calculated numerically — the only problem is to have possible fundamental singularities at the end-points of the integrand. When using Gaussian integration methods these points are never reached within a discrete space, but at the expense of having extremely bad convergences. Anyhow our special potential (E.4) allows for an analytical treatment of this integral, which offers a lot of insight into these fundamental momentum space singularities. Since the Rodrigues formula, which writes all Legendre polynomials into one compact notation, can also be written as

$$P_l(x) = \frac{1}{2^l l!} \frac{d^l}{dx^l} (x^2 - 1)^l \equiv \sum_{k=0}^l \frac{1}{2^k} \binom{l}{k} \binom{l+k}{k} (x-1)^k, \quad (\text{E.10})$$

the integral (E.6) is of the form

$$V_l(p, p') = \sum_{k=0}^l \frac{1}{2^k} \binom{l}{k} \binom{l+k}{k} \cdot \mathcal{D}_\mu^{n+1} \int_{-1}^1 dx \frac{(x-1)^k}{a^2 - b^2 \cdot x}, \quad (\text{E.11})$$

where the constants in the integrand are given by $a^2 = \mu^2 + p^2 + p'^2$ and $b^2 = 2pp'$.

Doing the following manipulation in the integrand

$$\frac{(x-1)^k}{a^2 - b^2 \cdot x} = -\frac{(x-1)^k}{b^2 \cdot (x-1) - (a^2 - b^2)} \equiv -\frac{1}{b^2} \left[\frac{y^k}{(x-1) - y} + \frac{(x-1)^k - y^k}{(x-1) - y} \right] \quad (\text{E.12})$$

where $y = a^2/b^2 - 1$, the first term can be integrated easily and the second term has no contribution for $k = 0$, so (E.11) can be written as

$$\begin{aligned} V_l(p, p') &= -\frac{1}{b^2} \mathcal{D}_\mu^{n+1} P_l(a^2/b^2) \ln \frac{a^2 - b^2}{a^2 + b^2} \\ &\quad - \frac{1}{b^2} \sum_{k=1}^l \frac{1}{2^k} \binom{l}{k} \binom{l+k}{k} \cdot \mathcal{D}_\mu^{n+1} \int_{-1}^1 dx \frac{(x-1)^k - y^k}{(x-1) - y} \\ &\equiv -\frac{1}{b^2} [I_l(p, p') + R_l(p, p')]. \end{aligned} \quad (\text{E.13})$$

E. Numerics in Momentum Space

In the last form we can clearly see that when $p = p'$ in the limit $\mu \rightarrow 0$, i.e. $a = b$ and $y = 0$, this special potential consists of two parts. The first term I_l is the irregular term, which will give singularities due to a logarithmic behaviour of the integral. This holds for all angular momenta, since $P_l(1) = 1$. The second term R_l is the regular term, since the integral gives well defined $(x - 1)$ -polynomials with coefficients proportional to y , which can be calculated explicitly by doing a polynomial division.

Before implementing the radial Schrödinger equation (E.9) numerically, we have to treat the singularity of I_l , i.e. we need to control the logarithmic singularity and its derivatives at $p = p'$ in the limit $\mu \rightarrow 0$. The procedure which now follows is called the Nystrom method. Its main task is to convert the integral equation into an equivalent one which cancels the singularity through a subtraction. The first step is to think about which power in the integration variable p' makes the integral over the logarithmic part convergent. A possible candidate is for example

$$\int_0^\infty dp' \frac{1}{p'} \ln \frac{\mu^2 + (p' - p)^2}{\mu^2 + (p' + p)^2} = -2\pi \cdot \arctan \frac{p}{\mu} \underset{\mu \rightarrow 0^+}{=} -\pi^2 \quad (\text{E.14})$$

In comparison with other possible integrals, the above integral is privileged, since it has the big advantage of being independent of any further parameters. To note is that for higher powers in $1/p'$ the integral is divergent because the singularity at the origin $p' = 0$ becomes to strong. Putting this relation as a zero into the singular part I_l of (E.13), the Schrödinger equation (E.9) can be written as

$$\begin{aligned} E\phi_l(p) &= \frac{p^2}{2m}\phi_l(p) + \pi p \phi_l(p) \cdot \mathcal{D}_\mu^{n+1} \left[P_l(c^2) \cdot \arctan \frac{p}{\mu} \right] - \int_0^\infty dp' \frac{R_l(p, p')}{2pp'} p'^2 \phi_l(p') \\ &\quad - \frac{1}{2p} \cdot \mathcal{D}_\mu^{n+1} \int_0^\infty \frac{dp'}{p'} \ln \frac{\mu^2 + (p' - p)^2}{\mu^2 + (p' + p)^2} \left[P_l(a^2/b^2) \cdot p'^2 \phi_l(p') - P_l(c^2) \cdot p^2 \phi_l(p) \right] \end{aligned} \quad (\text{E.15})$$

where $c^2 = 1 + \mu^2/4p^2$. To note again, for parameter values $\mu \neq 0$ it is not necessary to include these numerical counter terms, since all integrands in the above equation are well defined for all p and p' . They are only relevant in the limiting process $\mu \rightarrow 0$.

With this new form (E.15), it seems that when $p = p'$, i.e. $a^2/b^2 = c^2$, the integrand of the logarithmic singular part I_l is identically zero irrespective of the value μ , even in the limit $\mu \rightarrow 0$, and therefore not contributing to the integral. For $\mu \neq 0$ this certainly is true, but for $\mu \rightarrow 0$ its only true for the Coulomb potential, while for the Linear potential this argumentation is no longer valid. To see this, we will discuss for the sake of simplicity only the s-wave equation — for higher l-waves the arguments are identical. For the Coulomb potential, where no derivatives need to be taken, the relevant part of the singular integrand in the limit $\mu \rightarrow 0$ can be written as

$$\ln \frac{(p' - p)^2}{(p' + p)^2} \left[F(p'^2) - F(p^2) \right] = (p'^2 - p^2) \ln \frac{(p' - p)^2}{(p' + p)^2} \left[\frac{F(p'^2) - F(p^2)}{p'^2 - p^2} \right], \quad (\text{E.16})$$

where F is proportional to the wavefunction ϕ . In this case we clearly see how the above integrand in the limit $p' \rightarrow p$ goes to zero, since the term in the square bracket is proportional to the *derivative* of the wavefunction, which must be a well defined expression for all momenta.

E. Numerics in Momentum Space

However, for the Linear potential, where second order derivatives must be taken, the same integrand in the limit $\mu \rightarrow 0$ has the structure

$$\frac{1}{(p'^2 - p^2)^2} [F(p'^2) - F(p^2)] = \frac{1}{p'^2 - p^2} \left[\frac{F(p'^2) - F(p^2)}{p'^2 - p^2} \right], \quad (\text{E.17})$$

which makes it impossible to take the limit $p' \rightarrow p$. Therefore the $p' = p$ term can not be neglected, it will give a contribution which is proportional to the derivative of the function $F \sim \phi$. To calculate this contribution, we have to know the wavefunction ϕ , but our original aim was to solve for ϕ . Thus for the Linear potential the subtraction method (E.15) does not work. The subtraction zero is too weak for the double-pole singularity of the Linear potential — even after the subtraction a single-pole singularity is still left. It is not wrong to start implementing the Linear potential for $\mu \neq 0$, where the $p' = p$ term certainly is a zero contribution, and then taking the limit $\mu \rightarrow 0$ numerically, but the result is an extremely slow converging code and therefore numerically inefficient. For a proper numerical calculation of the Linear potential in momentum space, we have to seek for alternative ways than the Nystrom method. In this sense we continue treating the Linear potential with the Nystrom method, but we will see it as an approximation.

Every integral equation of the type

$$\lambda f(x) = G(x)f(x) + \int dx' K(x, x')f(x'), \quad (\text{E.18})$$

when embedding into a discrete space $x, x' \rightarrow x_i, x_j$, with $i, j = 1 \dots N$, can be approximated by a matrix equation

$$\lambda f_i = \sum_{j=1}^N [\delta_{ij}G_j + \Delta x_j K_{ij}] f_j \equiv \sum_{j=1}^N A_{ij} f_j \iff \mathbf{A} \cdot \mathbf{f} = \lambda \mathbf{f}, \quad (\text{E.19})$$

which now represents a finite dimensional eigenvalue problem.

As a discretization process for equation (E.15) we will choose the Gaussian integration method via Legendre polynomials. As an intermediate step the infinite interval $[0, \infty[$ must be mapped into the Legendre interval of $[-1, 1]$. There are several mapping functions, each of which will give a different distribution of the integration points. The most commonly used are

$$y_1(x) = 1 - 2e^{-x/z} ; \quad y_2(x) = -\frac{1 - x/z}{1 + x/z} ; \quad y_3(x) = \frac{4}{\pi} \arctan(x/z) - 1, \quad (\text{E.20})$$

where the parameter z is used as numerical stability factor within a special mapping function, i.e. it can be chosen in such a way until the distribution of the integration points perfectly suits the problem. Whereas if one wants to work with a fixed $z \sim 1$, the mapping function y_3 is a good choice. Its distribution of integration points has a wide range, being dense in the inner region and more sparse in the asymptotic region. This makes it ideal even for integrands with a relatively slow asymptotic fall-off.

E. Numerics in Momentum Space

Writing (E.15) in a discretized form, and keeping in mind that neglecting the $p = p'$ term in the singular part I_l is exact for the Coulomb while approximative for the Linear potential, will give

$$\begin{aligned}
E\phi_l^i &= \frac{p_i^2}{2m}\phi_l^i + \pi p_i \phi_l^i \cdot \mathcal{D}_\mu^{n+1} \left[P_l(c_i^2) \cdot \arctan \frac{p_i}{\mu} \right] - \frac{1}{2} \sum_{j=1}^N \frac{\omega_j}{p_i p_j} R_l(p_i, p_j) p_j^2 \phi_l^j \\
&\quad - \frac{1}{2} \mathcal{D}_\mu^{n+1} \sum_{j=1; j \neq i}^N \frac{\omega_j}{p_i p_j} \ln \frac{\mu^2 + (p_i - p_j)^2}{\mu^2 + (p_i + p_j)^2} \left[P_l(a_{ij}^2/b_{ij}^2) \cdot p_j^2 \phi_l^j - P_l(c_i^2) \cdot p_i^2 \phi_l^i \right]
\end{aligned} \tag{E.21}$$

where ω_i and p_i are the already transformed weights and abscissas of the Gauss-Legendre integration in the ordered interval $[-1, 1]$. Since our numerical diagonalization code can only treat symmetrical matrices, it is important to have symmetrical off-diagonal matrix elements. Although R_l^{ij} , a_{ij} and b_{ij} are symmetrical in $i \leftrightarrow j$, the above matrix equation still needs to be symmetrized in the off-diagonal terms, due of not having symmetrical weightings. If multiplying the whole equation with $\sqrt{\omega_i} \cdot p_i$, and defining new eigenvectors $u_l^i = \sqrt{\omega_i} \cdot p_i \cdot \phi_l^i$, as well as using the notation of (E.19), the diagonal and symmetric off-diagonal matrix elements are given as

$$\begin{aligned}
\mathbf{A}_{ii} &= \frac{p_i^2}{2m} + \pi p_i \cdot \mathcal{D}_\mu^{n+1} \left[P_l(c_i^2) \cdot \arctan \frac{p_i}{\mu} \right] - \frac{\omega_i}{2} R_l(p_i, p_i) \\
&\quad + \frac{1}{2} \mathcal{D}_\mu^{n+1} \sum_{j=1; j \neq i}^N \omega_j \frac{p_i}{p_j} P_l(c_i^2) \ln \frac{\mu^2 + (p_i - p_j)^2}{\mu^2 + (p_i + p_j)^2} \\
\mathbf{A}_{ij} &= -\frac{1}{2} \sqrt{\omega_i \omega_j} \left[R_l(p_i, p_j) + \mathcal{D}_\mu^{n+1} P_l(a_{ij}^2/b_{ij}^2) \ln \frac{\mu^2 + (p_i - p_j)^2}{\mu^2 + (p_i + p_j)^2} \right].
\end{aligned} \tag{E.22}$$

For calculating the matrix elements for small μ or even for $\mu \rightarrow 0$ it is helpful to make use of the following behaviour of the Legendre polynomials up to first order, which can be derived from (E.10)

$$P_l(c_i^2) = P_l(1 + \mu^2/2p_i^2) \underset{\mu \rightarrow 0}{=} 1 + l(l+1) \frac{\mu^2}{4p_i^2}. \tag{E.23}$$

For calculating the explicit matrix elements for the Yukawa, Coulomb and Linear potential, we have to proceed as given in (E.1). Being reasonable only the s-wave components, i.e. with no contributions of the regular term R_l will be determined explicitly for all three potentials.

E. Numerics in Momentum Space

The simplest one is certainly the Yukawa potential for which no numerical counter terms and no derivatives need to be taken. The s-wave matrix elements are

$$\begin{aligned}\mathbf{A}_{ii}^Y &= \frac{p_i^2}{2m} \\ \mathbf{A}_{ij}^Y &= \frac{\alpha_Y}{2\pi} \sqrt{\omega_i \omega_j} \ln \frac{\mu^2 + (p_i - p_j)^2}{\mu^2 + (p_i + p_j)^2}.\end{aligned}\quad (\text{E.24})$$

The s-wave Coulomb matrix elements are exactly given as

$$\begin{aligned}\mathbf{A}_{ii}^C &= \frac{p_i^2}{2m} - \frac{\alpha_C \pi}{2} p_i - \frac{\alpha_C}{2\pi} \sum_{j=1; j \neq i}^N \omega_j \frac{p_i}{p_j} \ln \frac{(p_i - p_j)^2}{(p_i + p_j)^2} \\ \mathbf{A}_{ij}^C &= \frac{\alpha_C}{2\pi} \sqrt{\omega_i \omega_j} \ln \frac{(p_i - p_j)^2}{(p_i + p_j)^2}.\end{aligned}\quad (\text{E.25})$$

Finally the s-wave Linear matrix elements, with $\alpha_L \leq 0$ have the Nystrom approximation of

$$\begin{aligned}\mathbf{A}_{ii}^L &\sim \frac{p_i^2}{2m} - \frac{\alpha_L}{2\pi} \sum_{j=1; j \neq i}^N \omega_j \frac{p_i}{p_j} \frac{8p_i p_j}{(p_i^2 - p_j^2)^2} \\ \mathbf{A}_{ij}^L &\sim \frac{\alpha_L}{2\pi} \sqrt{\omega_i \omega_j} \frac{8p_i p_j}{(p_i^2 - p_j^2)^2}.\end{aligned}\quad (\text{E.26})$$

E.2 Scattering domain

A scattering problem is regarded as solved if the phase shift and the corresponding scattering wavefunction have been determined. This section will not investigate the wavefunction itself, but will rather work out a numerical method for calculating scattering phases, which are directly linked to cross sections. The basic ideas given here are based on the original paper of Haftel & Tabakin on Nucleon-Nucleon potentials [39]. If we only focus on potentials V which have a finite range in coordinate space, then the T -operator equation (D.27) is a well defined equation in momentum space. If G_0 is the kinetic Greens function, which is diagonal in the momentum eigenstates, the outgoing T -matrix equation turns into the following integral equation

$$\langle \vec{k}' | T | \vec{k} \rangle = \langle \vec{k}' | V | \vec{k} \rangle + \int d^3 k'' \langle \vec{k}' | V | \vec{k}'' \rangle \langle \vec{k}'' | \frac{1}{E - k''^2/2m + i\epsilon} T | \vec{k} \rangle, \quad (\text{E.27})$$

where $E = k^2/2m$ and $\langle \vec{k}' | V | \vec{k} \rangle$ is the momentum space potential, which is also given as a Fourier transformation of the coordinate space potential

$$\langle \vec{k}' | V | \vec{k} \rangle \equiv V(|\vec{k}' - \vec{k}|) = V(q) = \frac{1}{(2\pi)^3} \int d^3 r e^{i\vec{q} \cdot \vec{r}} \cdot V(r). \quad (\text{E.28})$$

E. Numerics in Momentum Space

According to the partial wave analysis of $\langle \vec{k}' | T | \vec{k} \rangle$ in (D.34) and of $\langle \vec{k}' | V | \vec{k} \rangle$ in (E.5), and when using the identity (E.8) as well as the orthogonality and completeness relations of the spherical harmonics, the integration over the angles will give for every angular momentum l the one dimensional integral equation

$$T_l(k', k) = V_l(k', k) + \int_0^\infty dk'' k''^2 V_l(k', k'') \frac{1}{E - k''^2/2m + i\epsilon} T_l(k'', k), \quad (\text{E.29})$$

where a redefinition of T_l has been performed: $-T_l(k', k)/\pi m k \rightarrow T_l(k', k)$. Thus the diagonal element of T_l is given as

$$T_l(k, k) = -\frac{1}{\pi m k} e^{i\delta_l(k)} \sin \delta_l(k). \quad (\text{E.30})$$

In order to calculate the phase shift function we need to know the diagonal element of equation (E.29). Since the momentum space potentials are well defined, the only numerical difficulty that we will encounter is the singularity of the Greens function. But before dealing with this singularity, we notice that the slight imaginary shift will force (E.29) into a complex equation. But using the following relation helps to separate real and imaginary parts:

$$\int_0^\infty dx \frac{f(x)}{c + i\epsilon - x} = \mathcal{P} \int_0^\infty dx \frac{f(x)}{c - x} - i\pi f(c) \quad ; \quad c \geq 0, \quad (\text{E.31})$$

which follows from the residue theorem and some contour distortions, if f can be continued analytically into a complex half-plane, is everywhere regular and vanishes asymptotically in that half-plane. The symbol \mathcal{P} stands for the Cauchy principal-value prescription. Making a change of variables will give the equivalent relation

$$\int_0^\infty dx \frac{F(x)}{c^2 - x^2 + i\epsilon} = \mathcal{P} \int_0^\infty dx \frac{F(x)}{c^2 - x^2} - i\pi \frac{F(c)}{2c}. \quad (\text{E.32})$$

This allows us now to define a *real* R -matrix, which satisfies the relation

$$R_l(k', k) = V_l(k', k) + \mathcal{P} \int_0^\infty dk'' k''^2 V_l(k', k'') \frac{1}{E - k''^2/2m} R_l(k'', k). \quad (\text{E.33})$$

A short calculation shows that the complex T -matrix can be determined from the real R -matrix as

$$T_l(k', k) = \frac{R_l(k', k)}{1 + i\pi m k R_l(k', k)}. \quad (\text{E.34})$$

Thus the scattering phase can now be determined directly from the diagonal elements of the R -matrix

$$\delta_l(k) = -\arctan [\pi m k R_l(k, k)] + \pi \cdot n(k). \quad (\text{E.35})$$

To solve (E.33) numerically we have to do a numerical principal value limit, which is impossible to take in a stable way due to the limited precision of computers.

E. Numerics in Momentum Space

A better prescription for computers follows by introducing again a numerical counter term, which has its origin in the definition of \mathcal{P} itself

$$\mathcal{P} \int_{-\infty}^{\infty} \frac{dx}{c-x} = 0 \iff \mathcal{P} \int_0^{\infty} \frac{dx}{c^2-x^2} = 0. \quad (\text{E.36})$$

Adding this zero to (E.33) the singularity can be removed explicitly

$$R_l(k', k) = V_l(k', k) + \int_0^{\infty} dk'' \frac{2m}{k^2 - k''^2} \left[k''^2 V_l(k', k'') R_l(k'', k) - k^2 V_l(k', k) R_l(k, k) \right]. \quad (\text{E.37})$$

Important to note, is that the $k = k''$ term in the above integrand gives a contribution, which is proportional to derivative of the function in the square bracket, and thus can not be neglected. The integral equation is now ready to be calculated numerically by using finite dimensional matrix methods. As a discretization process we will again choose the Gaussian integration method via Legendre polynomials

$$R_l(k', k) = V_l(k', k) + \sum_{n=1}^N \omega_n \frac{2m}{k^2 - k_n^2} \left[k_n^2 V_l(k', k_n) R_l(k_n, k) - k^2 V_l(k', k) R_l(k, k) \right], \quad (\text{E.38})$$

where ω_n and k_n are the already transformed weights and abscissas of the Gauss-Legendre integration in the ordered interval $[-1, 1]$. The above equation represents one linear equation with $N+1$ unknowns: $R_l(k_n, k)$ for $n = 1 \dots N$, and $R_l(k, k)$.

To get a workable equation, we continue the discretization process by turning this one equation into $N+1$ simultaneously linear equations by evaluating it for $N+1$ momentum values on a grid consisting of the observable and integration points

$$k' = k_i = \begin{cases} \text{quadrature points } k_i \text{ for } i = 1 \dots N \\ \text{observable point } k \text{ for } i = N+1. \end{cases} \quad (\text{E.39})$$

The momentum variable k , which fixes the energy of the scattering system, is not discretized, since it serves as an observable parameter and must be given from the outset. This fact allows us now to circumvent the unknown but finite contribution of the singularity, since the continuous k can always be chosen such that $k \neq k_n$.

There are now $N+1$ unknowns $R_l(k_i, k) = R_l^i$, and $N+1$ linear equations which now can be solved uniquely

$$R_l^i = V_l^i + \sum_{j=1}^N \omega_j \frac{2m}{k^2 - k_j^2} k_j^2 \cdot V_l^{ij} R_l^j - V_l^i R_l^{N+1} \sum_{n=1}^N \omega_n \frac{2m}{k^2 - k_n^2} k^2 \quad ; \quad i = 1 \dots N+1. \quad (\text{E.40})$$

E. Numerics in Momentum Space

If we now combine the denominators and weights into a single vector u_j

$$u_j = \begin{cases} \omega_j \frac{2m}{k^2 - k_j^2} k_j^2 & \text{for } j = 1 \dots N \\ \sum_{n=1}^N \omega_n \frac{2m}{k^2 - k_n^2} k^2 & \text{for } j = N+1, \end{cases} \quad (\text{E.41})$$

equation (E.40) can be expressed as the following matrix equation

$$R_l^i = V_l^i + \sum_{j=1}^{N+1} u_j V_l^{ij} R_l^j \iff \mathbf{A} \cdot \mathbf{R} = \mathbf{V}, \quad (\text{E.42})$$

where the matrix elements of \mathbf{A} are given as $\mathbf{A}_{ij} = \delta_{ij} - u_j V_l^{ij}$, and the partial wave components of the potential V_l^{ij} are calculated by (E.6). The unknown vector \mathbf{R} can now be solved by the usual inverse matrix routines. The last element of this vector will then give the scattering phase (E.35) at the energy $E \sim k^2$.

F. Meson Summary Tables

F Meson Summary Tables

The following table serves as a reminder for the physical nomenclature of mesons. Pseudo-scalar mesons are given on the left, vector mesons on the right of each sector.

| | \bar{d} | \bar{u} | \bar{s} | \bar{c} | \bar{b} | \bar{t} |
|-----|--|--|---------------------------------|-----------------------------|----------------------|---------------------------------|
| d | $\pi^0, \eta, \eta' \rho^0, \omega, \phi$ | $\pi^- \rho^-$ | $K^0 K^{*0}$ | $D^- D^{*-}$ | $B^0 B^{*0}$ | $T^- T^{*-}$ |
| u | $\pi^+ \rho^+$ | $\pi^0, \eta, \eta' \rho^0, \omega, \phi$ | $K^+ K^{*+}$ | $\bar{D}^0 \bar{D}^{*0}$ | $B^+ B^{*+}$ | $\bar{T}^0 \bar{T}^{*0}$ |
| s | $\bar{K}^0 \bar{K}^{*0}$ | $K^- K^{*-}$ | $\eta, \eta' \omega, \phi$ | $D_s^- D_s^{*-}$ | $B_s^0 B_s^{*0}$ | $T_s^- T_s^{*-}$ |
| c | $D^+ D^{*+}$ | $D^0 D^{*0}$ | $D_s^+ D_s^{*+}$ | $\eta_c J/\Psi$ | $B_c^+ B_c^{*+}$ | $\bar{T}_c^0 \bar{T}_c^{*0}$ |
| b | $\bar{B}^0 \bar{B}^{*0}$ | $B^- B^{*-}$ | $\bar{B}_s^0 \bar{B}_s^{*0}$ | $B_c^- B_c^{*-}$ | $\eta_b \Upsilon$ | $T_b^- T_b^{*-}$ |
| t | $T^+ T^{*+}$ | $T^0 T^{*0}$ | $T_s^+ T_s^{*+}$ | $T_c^0 T_c^{*0}$ | $T_b^+ T_b^{*+}$ | $\eta_t \theta$ |

Next we want to look closer into flavor off-diagonal mesons, since only they are subject of this thesis. It is sufficient to sort these mesons as follows: if the orbital angular momentum of a $q\bar{q}$ system is L , the parity P of its wave function is $(-1)^{L+1}$. Furthermore, it also is an eigenstate of charge conjugation, with $C = (-1)^{L+S}$, where the spin S can be 0 or 1. Finally we will make use of the total angular momentum J , which can take on the values $J = |L - S|, \dots, |L + S|$.

States with $S = 0$ and $J^P = 0^-$ are called the pseudo-scalars, while $S = 1$ and $J^P = 1^-$ are the vectors. Important to note is that pseudo-scalar mesons can only have $L = 0$, in other words all pseudo-scalars are singlet s-wave mesons. On the other hand, the vectors can be triplet s-wave or triplet d-wave mesons. Every possible quark model that is able to describe mesons should decide on its own, whether a specific vector meson is to be seen as an $L = 0$ or an $L = 2$ state.

| Sector | $J^{PC} = 0^{-+}$ | $J^{PC} = 1^{--}$ |
|--------|--|--|
| (u;d) | π^\pm : 139.6 $\pi(\mathbf{1300})$: 1300 ± 100 $\pi(\mathbf{1800})$: 1812 ± 14 | $\rho(\mathbf{770})$: 775 ± 1 $\rho(\mathbf{1450})$: 1465 ± 25 $\rho(\mathbf{1700})$: 1700 ± 20 $\rho(\mathbf{1900})^\dagger$: 1900 ± 40 $\rho(\mathbf{2150})^\dagger$: 2149 ± 17 |

F. Meson Summary Tables

| Sector | $J^P = 0^-$ | $J^P = 1^-$ |
|---------|---|--|
| (u,d;s) | K^\pm : 493.7 $K(1460)^\dagger$: 1460 ± 60 $K(1630)^{\dagger\dagger}$: 1629 ± 7 $K(1830)^\dagger$: 1830 | $K^*(892)$: 891.6 $K^*(1410)$: 1414 ± 15 $K^*(1680)$: 1717 ± 27 |
| (u,d;c) | D^\pm : 1869 ± 1 | $D^*(2010)$: 2010 ± 1 $D^*(2640)^{\dagger\dagger}$: 2637 ± 6 |
| (s;c) | D_s^\pm : 1968 ± 1 $D_s(2573)^{\dagger\dagger}$: 2572 ± 2 | $D_s^{*\dagger\dagger}$: 2112 ± 1 |
| (u,d;b) | B^\pm : 5279 ± 1 | B^* : 5325 ± 1 |
| (s;b) | B_s : 5370 ± 3 | B_s^* : 5417 ± 4 |
| (c;b) | B_c : 6400 ± 400 | |

The above table collects all pseudo-scalar and vector mesons that have been experimentally measured up to now, taken from the Particle Data Group [3]. The value next to the meson represents its mass given in MeV.

The particles assigned with the symbol \dagger are regarded as not yet being established. The symbol $\dagger\dagger$ indicates that the value of J^P is still unknown.

REFERENCES

References

- [1] P.A.M. Dirac, *Forms of Relativistic Dynamics*,
Rev.Mod.Phys. **21** 392, 1949.
- [2] H. Leutwyler, J. Stern, *Relativistic Dynamics on a Null Plane*,
Ann.Phys. **112** 94, 1978.
- [3] H. Hagiwara et.al., *Particle Data Group — 2003 update*,
Phys.Rev. **D66** 010001, 2002.
- [4] S. Godfrey, N. Isgur,
Mesons in a relativized quark model with chromodynamics,
Phys.Rev. **D32** 189, 1985.
- [5] H.C. Pauli, *Successful renormalization of a QCD-inspired Hamiltonian*,
Internal Reports, November 2002 - September 2003.
- [6] H.C. Pauli, *On the effective light-cone QCD-Hamiltonian:
Application to the pion and other mesons*,
Nucl.Phys.B. (Proc.Suppl.) **90** 154, 2000.
- [7] H.C. Pauli, *On confinement in a light-cone Hamiltonian for QCD*,
Eur.Phys.J. **C7** 289, 1998.
- [8] T. Frederico, H.C. Pauli, and S.G. Zhou,
*Universal description of S-wave meson spectra in a renormalized
light-cone QCD-inspired model*,
Phys.Rev. **D66** 116011-8, 2002.
- [9] A.V. Anisovich, V.V. Anisovich, and A.V. Sarantsev,
Systematics of $q\bar{q}$ -states in the (n, M^2) and (J, M^2) planes,
Phys.Rev. **D62** 051502-4, 2000.
- [10] C. Elster, L.C. Liu, and R.M. Thaler,
*A practical calculational method for treating Coulomb scattering
in momentum space*,
J.Phys.G: Nucl.Part.Phys. **19** 2123, 1993.
- [11] W.F. Ford, *Anomalous Behaviour of the Coulomb T Matrix*,
Phys.Rev. **133** 1616, 1963.
- [12] S.J. Brodsky, H.C. Pauli, and S.S. Pinsky
Quantum Chromodynamics and other Field Theories on the Light Cone,
Phys.Rep. **301** 299, 1998.
- [13] U. Trittmann, H.C. Pauli, *On rotations in front-form dynamics*,
Nucl.Phys.B. (Proc.Suppl.) **90** 161, 2000.

REFERENCES

- [14] H.C. Pauli, *Mass and Coupling constant*, Internal Report, July 2003.
- [15] M. Sawicki, *Solution of the light-cone equation for the relativistic bound state*, Phys.Rev. **D32** 2666, 1985.
- [16] T. Frederico, A. Delfino, and L. Tomio, *Renormalization group invariance of quantum mechanics*, Phys.Lett. **B481** 143, 2000.
- [17] H. Omer, *Calculation of resonant states of ρ and π from a confining effective potential*, Internal Report, August 2003.
- [18] W.H. Press, S.A. Teukolsky, W.T. Vetterling, and B.P. Flannery, *Numerical Recipes in C (2nd edition)*, Cambridge University Press, 1992.
- [19] A. Krassnigg, H.C. Pauli, *On helicity and spin on the light-cone*, Nucl.Phys.B. (Proc.Suppl.) **108** 251, 2002.
- [20] H.C. Pauli, *On the form factor of physical mesons and their distribution function*, Nucl.Phys.A. **705** 73, 2002.
- [21] D. Ashery, H.C. Pauli, *Non-Perturbative Pion Wave Functions* Eur.Phys.J. **C28** 329, 2003.
- [22] S. Weinberg, *The Quantum Theory of Fields I*, Cambridge University Press, 1995.
- [23] R.U. Sexl, H.K. Urbantke, *Relativität, Gruppen, Teilchen*, Springer Verlag, 1982.
- [24] J. Schwinger, *The Theory of Quantized Fields* Phys.Rev. **82** 914, 1951.
- [25] H.C. Pauli, *Discretized light-cone quantization and the effective interaction in hadrons*, AIP Conf.Proc. **494** 80, 1999.
- [26] S.M. Dancoff, *Non-Adiabatic Meson Theory of Nuclear Forces*, Phys.Rev. **78** 382, 1950.
- [27] H.C. Pauli, *On the effective Hamiltonian for QCD: An overview and status report*, Nucl.Phys.B. (Proc.Suppl.) **108** 273, 2002.
- [28] J. Raufeisen, *Die Ein-Schleifen-Korrekturen zum Quark-Gluon-Vertex in Hamiltonischer Störungstheorie*, Diplomarbeit Heidelberg, 1997.
- [29] H.C. Pauli, *A Compendium of Light-Cone Quantization*, Nucl.Phys.B. (Proc.Suppl.) **90** 259, 2000.

REFERENCES

- [30] M. Abramowitz, I. Stegun, *Handbook of Mathematical Functions*, Dover Publications, 1970.
- [31] P. Roman, *Advanced Quantum Theory*, Addison-Wesley, 1965.
- [32] A. Messiah, *Quantum Mechanics*, North Holland Publishing, 1970.
- [33] A.G. Sitenko, *Scattering Theory*, Springer-Verlag, 1990.
- [34] G. Gamow, C.L. Critchfield,
Theory of the Atomic Nucleus and Nuclear Energy Sources,
Clarendon Press Oxford, 1950.
- [35] E.P. Wigner,
Lower Limit for the Energy Derivative of the Scattering Phase Shift,
Phys.Rev. **98** 145, 1955.
- [36] V.F. Weisskopf, J.M. Blatt, *Theoretical Nuclear Physics*,
John Wiley and Sons, 1952.
- [37] H.M. Nussenzveig,
The Poles of the S-Matrix of a Rectangular Potential Well or Barrier,
Nucl.Phys. **11** 499, 1959.
- [38] H.A. Bethe,
Theory of the Effective Range in Nuclear Scattering,
Phys.Rev. **76** 38, 1949.
- [39] M.I. Haftel, F. Tabakin,
Nuclear Saturation and Smoothness of Nucleon-Nucleon Potentials,
Nucl.Phys. **A158** 1, 1970.